This is to certify that the
dissertation entitled

Motional and Excitation Transport Dynamics in Restricted Environments

presented by

Sarah Ann Stevenson

has been accepted towards fulfillment
of the requirements for the

Ph.D. degree in Chemistry

Major Professor's Signature

7/18/06

Date

DATE DUE	DATE DUE	DATE DUE

MOTIONAL AND EXCITATION TRANSPORT DYNAMICS IN RESTRICTED ENVIRONMENTS

By

Sarah Ann Stevenson

A DISSERTATION

Submitted to
Michigan State University
in partial fulfillment of the requirements
for the degree of

DOCTOR OF PHILOSOPHY

Department of Chemistry

2006

ABSTRACT

MOTIONAL AND EXCITATION TRANSPORT DYNAMICS IN RESTRICTED ENVIRONMENTS

By

Sarah Ann Stevenson

Micelles and vesicles are of interest due to their potential application as simplistic model biological systems. We are particularly interested in the interfacial region between the micelle or vesicle polar region and the bulk solution because this portion of the system mediates exchange processes and partitioning. To examine the interfacial region of micelle systems, we sequester a nonpolar optical donor within a micelle and monitor energy transfer from this molecule to an ionic optical acceptor present in the aqueous phase of the solution. The time constant for this energy transfer is monitored using time-correlated single photon counting measurements. Our data indicate that interactions between the polar head group molecules mediate the efficiency of energy transfer, and we relate this finding to the presence of the micellar electrical double layer. The alteration of the ionic strength of the solution will change the balance of forces that operate within the palisades layer and, depending on the details of the interactions, the micelle structure may be altered as a result. We then expand our discussion to the differences between the interfacial regions of micelle and vesicle systems. These two systems, although similar, are difficult to compare directly due to the difference in the constituents

which form the structures. We use the molecule decanoic acid and its conjugate base sodium decanoate, which form micelles or vesicles depending on solution parameters such as pH, to make this comparison. Our data indicate that, although these systems share a common constituent, there are measurable differences between the micellar and vesicular environments. Our findings show that the environment(s) experienced by chromophores sequestered in the nonpolar regions of the micelle and vesicle structures are characterized by significantly different motional constraints because of the different molecular organization of micelles and vesicles.

To my parents

ACKNOWLEDGMENTS

My first thanks must go to my husband Matt, for his support, understanding, and willingness to move back to Michigan. My parents, Don and Nancy Remus, have also been instrumental in teaching me the value of a good education, as I'm sure was conveyed to them through their own parents. Without their support throughout my entire education I wouldn't be where I am today. My entire family, especially my little brother Jim, has been vital in keeping me in touch with, or at least offering glimpses of, the "real world".

There are many other people who contributed to this dissertation in many ways. I am particularly indebted to my advisor, Gary Blanchard, for his willingness to help me conquer the steep edge of the learning curve as well as his encouragement and insight. I would also like to thank my committee members, Professors Marcos Dantus, Jim McCusker, and David Weliky. Finally, I would like to offer appreciation for all of my other MSU colleagues and Blanchard group members past and present for their scientific insight and comic relief. MSU wouldn't have been the same without any of you!

TABLE OF CONTENTS

Chapter 6 – Conclusions and Future Work

LIST OF TABLES

LIST OF FIGURES

LIST OF ABBREVIATIONS

TCSPC.....Time Correlated Single Photon Counting

CFD..... Constant fraction discriminator

TAC.....Time to amplitude converter

MCP.....Microchannel plate

PMT.....Photomultiplier tube

MCA.....Multichannel analyzer

BBD.....4-Benzylamino-7-nitrobenzofurazan

DSF.....Disodium Fluorescein

R110.....Rhodamine 110 Chloride

TEM.....Transmission Electron Microscope

Cryo-TEM.....Cryogenic Transmission Electron Microscope

Chapter 1

INTRODUCTION

Understanding the dynamics of intermolecular interactions in solutions has been of considerable interest because of the importance of these properties in mediating a number of different phenomena. Solution phase interactions play an essential role in chemical separations, catalysis, and several biologically important processes. In order to gain a better understanding of these processes, a more complete understanding of the dynamic interactions between the solute and solvent molecules is necessary. The common underlying issue that has been most difficult to address is the existence, persistence length and characteristic time-scale of local heterogeneity.

Amphiphilic molecules are examples of heterogeneous systems that exhibit self-assembly behavior. Depending on their structural details, these molecules form bilayer structures, which are the basic component of cell membranes, and also find use in other applications such as detergents, chemical separations, and drug delivery. Two subsets of amphiphilic systems that manifest self-assembly behavior in certain concentration regimes are micelles and vesicles. Micelles have attracted substantial attention from the chemical community due mainly to their utility as interfaces between polar and nonpolar phases. This property has also manifested itself in the use of micelles as encapsulating and biomimetic systems.[1-4] Since most of the utility of these biomimetic structures rests in their ability to exchange species between the

hydrophobic and hydrophilic regions of the systems, it is the interfacial region which mediates these processes that is of interest.

For ionic micelles, the interfacial region between the micelle and the aqueous phase is known as the Stern layer. This region contains the ionic headgroups as well as the majority of the counterions present in the solution, which causes the micellar surface to resemble an electric double layer.[5] As shown in Figure 1, the Stern layer contains most of the counterions, which are electrostatically bound to the micelle surface.[6] After the Stern layer, a diffuse layer is present in which electrostatic interactions between solution phase ions and the micellar surface cause most of the remaining counterions to accumulate in this region. Following the Stern and diffuse layers is the bulk solution. The role that the electrostatic double layer plays in mediating interactions between the polar and nonpolar regions of the micellar systems is not known, and more insight is needed in order to gain a better understanding of the exchange processes between micelles and the solution phase.

Like micelles, vesicles are also commonly used as biomimetic systems and for applications such as drug delivery and immunological studies. Vesicles are usually prepared from phospholipids, however more simplistic amphiphilic compounds have also been shown to form vesicular structures.[7-14] Monnard *et al.* have recently addressed issues of stability, permeability, and encapsulation of macromolecules in vesicles prepared from these simplistic fatty acid amphiphilic molecules.[9] These amphiphiles offer advantages over phospholipids, such as their structural simplicity, dynamic behavior,[11,13,15-17] ability to grow upon

addition of more fatty acid,[13,18] and autocatalytic or self reproducing formation,[12,19] making them well suited to fundamental examinations aimed at understanding organization in these dynamic structures. Recent works by Morigaki *et al.* and Namani *et al.* have investigated the sodium decanoate/decanoic acid fatty acid system and have shown that the same amphiphilic structures will form micelles or vesicles depending on the pH of the solution.[10,20] Since the same constituents form both single and double layer structures, a direct comparision between micelles and vesicles is possible. We are particularly interested in the interfacial regions of these structures and any differences that might exist in their molecular organization.

To elucidate the exchange processes in these model biological systems, various methods have been used to study micelles, such as small-angle neutron scattering, NMR, fluorescence spectroscopy, EPR, X-ray scattering, and an assortment of other techniques.[3,4,21-23] Fluorescence spectroscopy finds wide use because of its characteristically high sensitivity combined with the range of chemical properties available with the fluorophores used. For measurements in heterogeneous systems, it is possible to use fluorescent compounds that will partition selectively into a given phase, or will reside at the interface between two phases. This capability, when combined with fluorescence resonance energy transfer (FRET) measurements, has been used in the study of heterogeneous systems such as micelles, vesicles, and lipid bilayers.[24-45] The transfer of energy

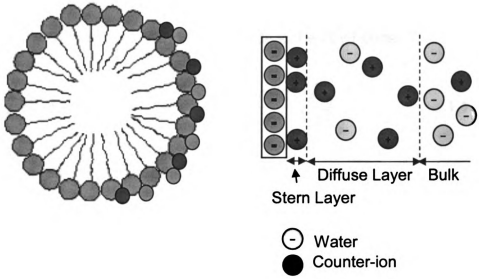

Figure 1.1- Micellar Structure and Double Layer

between molecules can occur by a number of means, ranging from dipolar coupling to collisional quenching. We are concerned in this work with dipolar coupling because of the characteristic length scale over which it operates. The transfer of energy by dipolar coupling has been described by Förster[46],

$$k_{DA} = \frac{\kappa^2 k_r^D}{n^4 R^6} \cdot 8.8x10^{17} \int \frac{\varepsilon_A(\bar{\nu}) f_D(\bar{\nu})}{\bar{\nu}^4} d\bar{\nu} = \frac{\kappa^2 k_r^D}{n^4} \left(\frac{R_0}{R} \right)^6 \qquad 1.1$$

where k_{DA} is the rate constant for the transfer of energy between donor and acceptor. The κ term is a function of the relative orientation of the donor and acceptor transition dipole moments, and for our experimental conditions, $\langle \kappa^2 \rangle = 2/3$. The term k_r^D is the donor radiative decay rate constant in the absence of optical acceptor, n is the refractive index and R is the intermolecular D-A distance. The integral term is a measure of the spectral overlap between the emission spectrum of the optical donor and the absorption spectrum of the optical acceptor. The spectral overlap term, combined with the several constants on the right hand side of Equation 1.1 is typically referred to as the critical or Förster radius, R_0, a quantity which serves as an effective gauge of the operating distance of this dipolar coupling process. While the term R_0 will vary for each donor-acceptor pair, for most organic chromophore pairs, $R_0 \sim 50$ Å.[47,48]

The topology of these systems can significantly influence the efficiency of energy transfer since the dipolar coupling process that mediates energy transfer depends on both the average distance and orientation of the molecules involved. Energy transfer measurements can be used as a "spectroscopic ruler" to

estimate average distances between optical donor and acceptor, and thus we can gain information on the extent to which micelle and acceptor interact. Micellar and vesicular systems are ideal candidates for energy transfer experiments, and previous work with micelles has examined energy transfer between two molecules sequestered inside a micelle, between a molecule inside the micelle and a molecule that is part of the surfactant, and between two molecules on the surface of the micelle.[26,32,35,49] Most of these studies have focused on energy transfer between molecules in the same region of the micelle. We are particularly interested in the interfacial region of micelles, and understanding the intermolecular dynamics in micellar systems will hopefully shed some light on more complex biomimetic systems. Previous work with vesicle systems has explored different aspects of vesicle structure and behavior. Earlier work by Fung and Stryer monitored membrane fusion between vesicles labeled with fluorescent probes and unlabeled vesicles.[50] For simpler single chain amphiphilic vesicles, Chen utilized FRET, or Fluorescence Resonance Energy Transfer, to examine the kinetics of fatty acid vesicle growth.[13] Several researchers, such as Dobretsov *et al.* and van Zandvoort *et al.* have used FRET measurements to determine the location of various fluorescent probes in lipid membranes.[51,52] While all of these studies have lead to greater understanding of vesicle systems, a direct comparison between micellar and vesicular structures remains to be made.

To probe the local environments of the micelle and vesicle systems, we use fluorescence lifetime and depolarization measurements. The picosecond

time-correlated single photon counting laser spectrometer used for all of the fluorescence lifetime and depolarization experiments has been described previously[53] and we recap a brief outline of its performance features here. A graphical depiction of the instrument is offered in Figure 1.2. The source laser is a mode locked CW Nd:YAG laser (Coherent Antares 76s), that produces 100 ps 1064 nm pulses at a 76 MHz repetition rate. The 1064-nm pulse train is frequency tripled to produce ~1.3 W average power at 354.7 nm for all experiments. The third harmonic (354.7 nm light) of the Nd:YAG laser is used to excite a Coherent 702-2 cavity dumped dye laser. The dye laser is cavity dumped at a repetition rate of 4 MHz and can generate pulses ranging from ~ 550 -1000 nm depending on the optics used. For these experiments, we produced output using Stilbene 420 laser dye (Exciton) to produce 420 nm light for experiments involving perylene and 460 nm light for 4-bezylamino-7-nitrobenzofurazan (BBD) experiments. Excitation power at the sample was ≤ 1 mW average power for all measurements. The output from the dye laser is divided and half of the light is sent through the reference channel while the other half travels to the sample holder. The reference channel was delayed optically and detected using an in-house built fiber optic delay line. Fluorescence was collected at at 0°, 54.7° and 90° with respect to the vertically polarized excitation pulse with the polarization being selected by a Glan-Taylor prism. The polarization of this selected light is then scrambled and a subtractive double monochromator (American Holographic DB10-S) is used for wavelength selection. A subtractive double monochromator is utilized to reduce the effects of

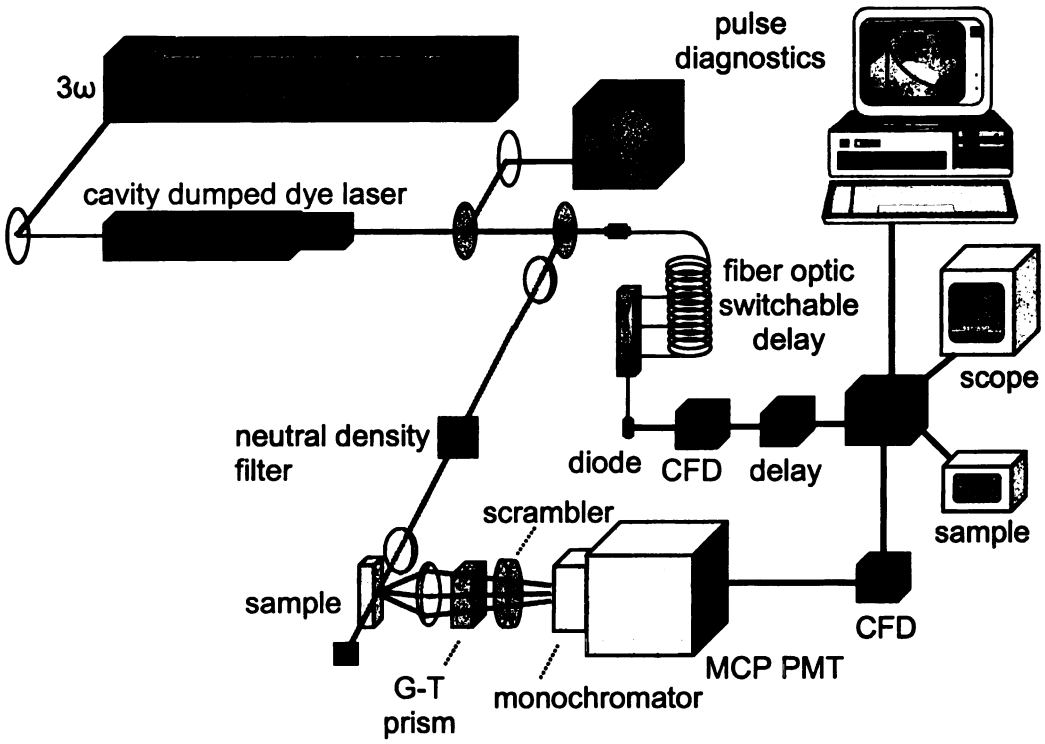

Figure 1.2 – Schematic of time-correlated single photon counting laser spectrometer.

dispersion-induced time broadening of the collected light.[54] Fluorescence signals were detected using a Hamamatsu R3809U microchannel plate photomultiplier tube that has a rise time of 156 ps and a transit time spread of 42 ps FWHM. The signal was then sent to a Tennelec 454 quad constant fraction discriminator where a Tennelec 864 time-to-amplitude converter and biased amplifier is used for signal processing. For most TCSPC measurements, the systems are typically operated in reverse mode to avoid temporal distortions caused by electronic dead time limitations.[53,55] The remaining half of the dye laser output is coupled into an optical fiber and then routed to a custom made fiber optic delay line[53], which allows a range of lifetimes from microseconds to picoseconds. A Hamamatsu S2381 avalanche photodiode collects the optically delayed laser output and is input to the CFD. The signal from the reference channel is delayed electronically (Tennele 412A) and travels to the stop channel of the TAC. TAC output counts are observed using a Tektronix 100-MHz oscilloscope and are sent to a Tennelec PCA-11 multichannel analyzer for collection. The fluorescence collected at 54.7° polarization provides fluorescence lifetime data by eliminating molecular contributions to the signal while 0° and 90° polarizations are of interest for rotational diffusion measurements. Data were acquired and the collection wavelength and polarization selector were computer controlled using a program written with LabVIEW® v. 7.1 and a Newport PMC200-P programmable motion controller. Lifetimes range from ~800 ps to ~6000 ps, while an instrument

response function of typically 35 ps fwhm is observed for this system. We did not deconvolute the instrument response function from the fluorescence transients.

To observe the interactions of solvent molecules in the solution phase we utilize two complementary techniques; fluorescence lifetime and depolarization measurements. Fluorescence lifetime data provide information about the local environment of the probe molecule as well as the extent of fluorescence resonance energy transfer while fluorescence depolarization measurements offer insight into the microenvironments that exist within the heterogeneous systems. Lifetime measurements give us a qualitative picture of the interfacial region while reorientation data provide us with quantitative information regarding the local viscosity of the nonpolar regions of micelle and vesicle systems.

In rotational diffusion measurements, the probe molecule rotates in solution and sweeps out a particular volume. The volume that the probe sweeps out depends on the size and shape of the probe molecule as well as the properties of the surrounding solvent. By examining the rotational dynamics of a probe molecule in solution, we can gain insight into the local environment of the probe molecule. Reorientation dynamics have been used extensively to investigate local organization in solutions because of the well developed theoretical framework for interpretation of the data and the relatively high information content of the experimental signals.[56-60] Using vertically polarized light we can preferentially excite those probe molecules whose transition dipole moments are parallel to the excitation. This induced anisotropy decays over time,

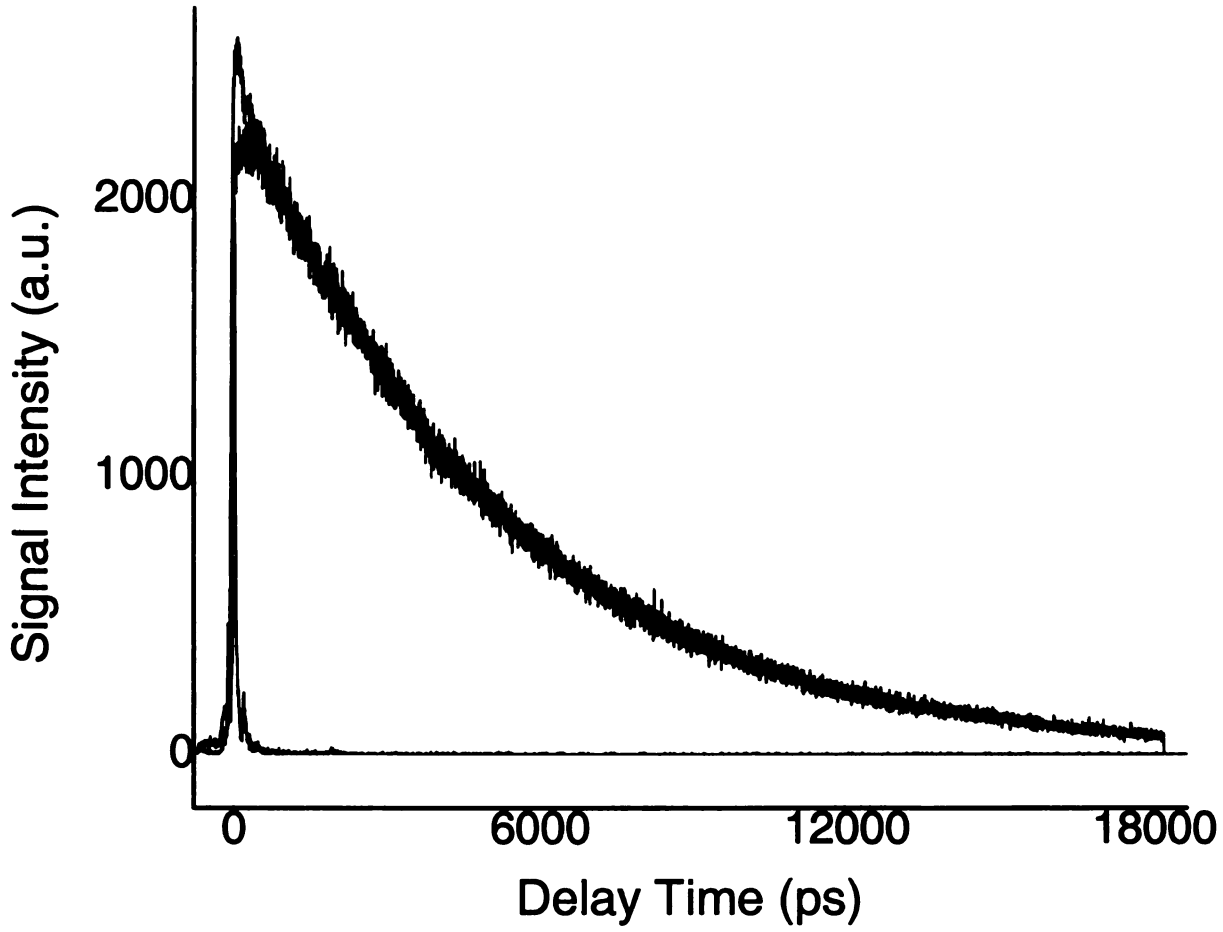

Figure 1.3 – Experimental $I_{\parallel}$ and $I_{\perp}$ scans for perylene in CTAB, along with the instrumental response function. These data are typical of those recorded for reorientation measurements.

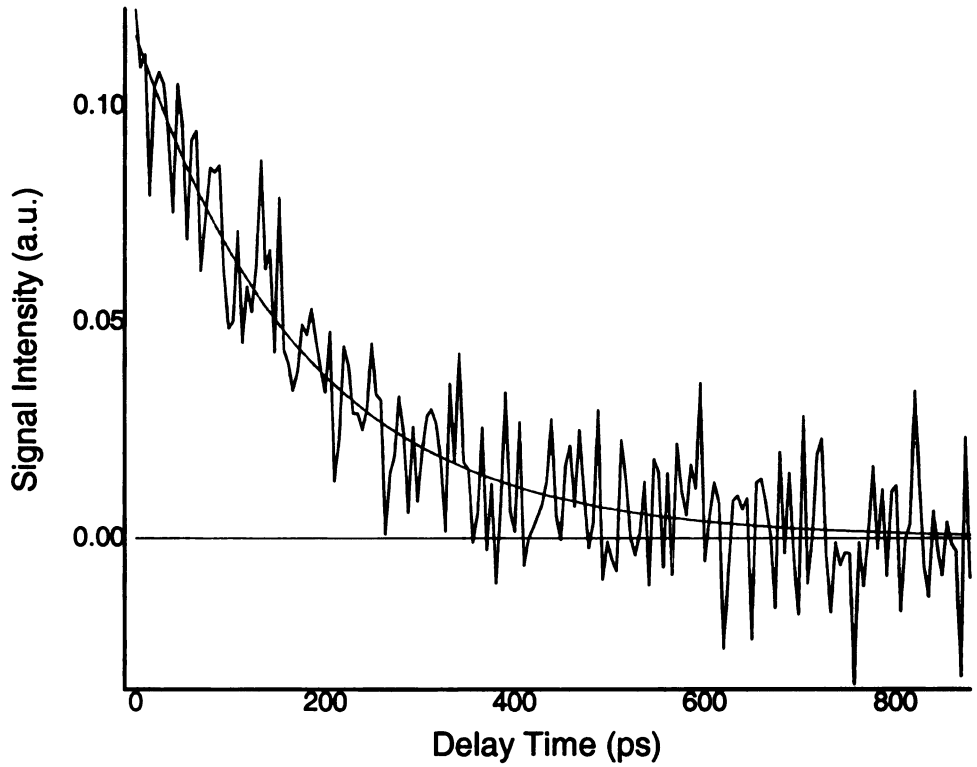

Figure 1.4 – Anisotropy function, R(t), for the data shown in Figure 1.3. The decay is fit to the function $R(t) = R(0)\exp(-t/\tau)$

providing information on the rotational diffusion dynamics. The induced orientational anisotropy function, R(t), is shown in equation 1.2 and is obtained by combining the data collected parallel and perpendicular to the excitation polarization,

$$R(t) = \frac{I_{\parallel}(t) - I_{\perp}(t)}{I_{\parallel}(t) + 2I_{\perp}(t)} \qquad 1.2$$

where $I_{\parallel}(t)$ and $I_{\perp}(t)$ are the polarized emission intensities. A representative sample data set is presented in Figure 1.3. The chemical information contained in these data is in the decay time constant(s) of R(t), and its zero-time value, R(0). The theory has been well established by Chuang and Eisenthal, who calculate that R(t) can decay with up to five exponential terms.[56] For most chromophores, one or two exponentials are typically observed and the functionality of the decay depends on the orientation of the chromophore transition dipole moments relative to the rotational motion axes and the shape of the ellipsoid swept out by the rotating moiety. Several physical models have been presented to interpret the experimental data. The choice of model will determine the physical and chemical significance of the decay time constant(s) extracted from the R(t) data. For chromophores tethered to a substantially larger entity, such as a protein, or imbedded in a mono- or bilayer structure, the hindered rotor model is suitable. In this model the chromophore is attached to the larger assembly at one point within the system, and its motion is considered in the context of the conic volume it sweeps out. For chromophores that are able to rotate freely in solution, the modified Debye-Stokes-Einstein (DSE) equation is

the preferred model. The modified Debye-Stokes-Einstein (DSE) equation is given by Eq. 1.2,[61]

$$\tau_{or} = \frac{\eta V f}{k_B T S} \qquad 1.3$$

where η is the solvent viscosity, V is the solute hydrodynamic volume, T is the temperature, k_B is the Boltzmann constant, *f* is the frictional interaction term,[59] and *S* is the solute molecular shape factor.[62] The DSE model is limited in the sense that it does not account for the molecular nature of the solvent, yet for many systems it provides remarkably close agreement with experimental data. We make use of this model throughout this dissertation to help in understanding the behavior of chromophores sequestered within the micelle and vesicle structures we consider here.

These fluorescence measurements can be used to gain insight about the model biological systems that we have choosen to investigate. To utilize these measurements, we use fluorescent probe molecules to observe changes in local environments. Perylene is an extensively studied hydrophobic chromophore that is known to position itself in nonpolar environments. For the heterogeneous micellar and vesicular systems that we would like to observe, we are able to sequester perylene in the nonpolar regions of these systems.

Chapter 2 of this dissertation examines the micelle-solution interface using fluorescence resonance energy transfer. We have found that the presence of counterions in ionic surfactants mediate the excitation transport between a probe

sequestered inside a micelle and one present in the aqueous phase of the solution.

Chapter 3 deals with the dynamics of 4-benzylamino-7-nitrobenzofurazan in the 1-propanol-water binary solvent system. It is clear that in the 1-propanol/water solvent system there is discernible microscopic solvent heterogeneity, with the details of this transient solution phase structure depending sensitively on the composition of the solvent system.

Chapters 4 and 5 examine the differences between micelles and vesicles. We look at the different local environments of decanoate/decanoic acid micelles and vesicles in Chapter 4. In Chapter 5, we look at the communication between a probe molecule sequestered in the nonpolar region of the micelle or vesicle structure and a probe in the solution phase.

Chapter 6 provides some final conclusions as well as possible suggestions for future experiments to further examine the sodium decanoate/decanoic acid system.

Literature Cited

(1) Inada, A.; Nakamura, Y.; Morita, Y. *Chemical & Pharmaceutical Bulletin* **1988**, *36*, 462.

(2) Ikura, T.; Go, N.; Inagaki, F. *Proteins: Structure, Function, and Genetics* **1991**, *9*, 81.

(3) Hwang, P. M.; Vogel, H. J. *Biochemistry and Cell Biology* **1998**, *76*, 235.

(4) Henry, G. D.; Sykes, B. D. *Methods in enzymology FIELD Publication Date:1994*, *239*, 515.

(5) Rangel-Yagui, C. O.; Pessoa, A., Jr.; Tavares, L. C. *Journal of Pharmacy & Pharmaceutical Sciences* **2005**, *8*, 147.

(6) Israelachvili, J. *Intermolecular & Surface Forces*, second edition ed.; Academic Press: San Diego, 1992.

(7) Gebicki, J. M.; Hicks, M. *Nature (London, United Kingdom)* **1973**, *243*, 232.

(8) Hargreaves, W. R.; Deamer, D. W. *Biochemistry* **1978**, *17*, 3759.

(9) Monnard, P.-A.; Deamer, D. W. *Methods in Enzymology* **2003**, *372*, 133.

(10) Morigaki, K.; Walde, P.; Misran, M.; Robinson, B. H. *Colloids and Surfaces, A: Physicochemical and Engineering Aspects* **2003**, *213*, 37.

(11) Sacerdote, M. G.; Szostak, J. W. *Proceedings of the National Academy of Sciences of the United States of America* **2005**, *102*, 6004.

(12) Walde, P.; Wick, R.; Fresta, M.; Mangone, A.; Luisi, P. L. *Journal of the American Chemical Society* **1994**, *116*, 11649.

(13) Chen, I. A.; Szostak, J. W. *Biophysical Journal* **2004**, *87*, 988.

(14) Cistola, D. P.; Hamilton, J. A.; Jackson, D.; Small, D. M. *Biochemistry* **1988**, *27*, 1881.

(15) Kamp, F.; Zakim, D.; Zhang, F.; Noy, N.; Hamilton, J. A. *Biochemistry* **1995**, *34*, 11928.

(16) Zhang, F.; Kamp, F.; Hamilton, J. A. *Biochemistry* **1996**, *35*, 16055.

(17) Kleinfeld, A. M.; Chu, P.; Romero, C. *Biochemistry* **1997**, *36*, 14146.

(18) Hanczyc, M. M.; Fujikawa, S. M.; Szostak, J. W. *Science (Washington, DC, United States)* **2003**, *302*, 618.

(19) Oberholzer, T.; Wick, R.; Luisi, P. L.; Biebricher, C. K. *Biochemical and Biophysical Research Communications* **1995**, *207*, 250.

(20) Namani, T.; Walde, P. *Langmuir* **2005**, *21*, 6210.

(21) Griffiths, P. C.; Cheung, A. Y. F.; Finney, G. J.; Farley, C.; Pitt, A. R.; Howe, A. M.; King, S. M.; Heenan, R. K.; Bales, B. L. *Langmuir* **2002**, *18*, 1065.

(22) Itri, R.; Amaral, L. Q. *Journal of Physical Chemistry* **1991**, *95*, 423.

(23) Paradies, H. H. *Colloids and Surfaces* **1983**, *6*, 405.

(24) Barzykin, A. V.; Tachiya, M. *Journal of Chemical Physics* **1995**, *102*, 3146.

(25) Birch, D. J. S.; Suhling, K.; Holmes, A. S.; Salthammer, T.; Imhof, R. E. *Pure and Applied Chemistry* **1993**, *65*, 1687.

(26) Choi, K. J.; Turkevich, L. A.; Loza, R. *Journal of Physical Chemistry* **1988**, *92*, 2248.

(27) de Oliveira, H. P. M.; Gehlen, M. H. *Chemical Physics* **2003**, *290*, 85.

(28) DelaCruz, J. L.; Blanchard, G. J. *Journal of Physical Chemistry B* **2003**, *107*, 7102.

(29) Dutt, G. B. *Journal of Physical Chemistry B* **2002**, *106*, 7398.

(30) Ediger, M. D.; Domingue, R. P.; Fayer, M. D. *Journal of Chemical Physics* **1984**, *80*, 1246.

(31) Ediger, M. D.; Fayer, M. D. *Journal of Chemical Physics* **1983**, *78*, 2518.

(32) Johansson, L. B. A.; Niemi, A. *Journal of Physical Chemistry* **1987**, *91*, 3020.

(33) Kelepouris, L.; Blanchard, G. J. *Journal of Physical Chemistry B* **2002**, *106*, 6600.

(34) Kelepouris, L.; Blanchard, G. J. *Journal of Physical Chemistry B* **2003**, *107*, 1079.

(35) Kenney-Wallace, G. A.; Flint, J. H.; Wallace, S. C. *Chemical Physics Letters* **1975**, *32*, 71.

(36) Klein, U. K. A.; Haar, H. P. *Chemical Physics Letters* **1978**, *58*, 531.

(37) Maiti, N. C.; Krishna, M. M. G.; Britto, P. J.; Periasamy, N. *Journal of Physical Chemistry B* **1997**, *101*, 11051.

(38) Maiti, N. C.; Mazumdar, S.; Periasamy, N. *Journal of Physical Chemistry* **1995**, *99*, 10708.

(39) Mattjus, P.; Molotkovsky, J. G.; Smaby, J. M.; Brown, R. E. *Analytical Biochemistry* **1999**, *268*, 297.

(40) Menger, F. M. *Accounts of Chemical Research* **1979**, *12*, 111.

(41) Quitevis, E. L.; Marcus, A. H.; Fayer, M. D. *Journal of Physical Chemistry* **1993**, *97*, 5762.

(42) Rao, U. R. K.; Manohar, C.; Valaulikar, B. S.; Iyer, R. M. *Journal of Physical Chemistry* **1987**, *91*, 3286.

(43) Saha, D. C.; Ray, K.; Misra, T. N. *Spectrochimica Acta, Part A: Molecular and Biomolecular Spectroscopy* **2000**, *56A*, 797.

(44) Stryer, L. *Annual Review of Biochemistry* **1978**, *47*, 819.

(45) Wistrom, C. A.; Jones, G. M.; Tobias, P. S.; Sklar, L. A. *Biophysical Journal* **1996**, *70*, 988.

(46) Forster, T. *Ann. Physik.* **1948**, *2*, 55.

(47) Ishii, Y.; Yoshida, T.; Funatsu, T.; Wazawa, T.; Yanagida, T. *Chemical Physics* **1999**, *247*, 163.

(48) Hiller David, A.; Fogg Jonathan, M.; Martin Amy, M.; Beechem Joseph, M.; Reich Norbert, O.; Perona John, J. *Biochemistry FIELD Publication Date:2003*, *42*, 14375.

(49) Marcus, A. H.; Diachun, N. A.; Fayer, M. D. *Journal of Physical Chemistry* **1992**, *96*, 8930.

(50) Fung, B. K.-K.; Stryer, L. *Biochemistry* **1978**, *17*, 5241.

(51) Dobretsov, G. E.; Kurek, N. K.; Makhov, V. N.; Syreishchikova, T. I.; Yakimenko, M. N. *Journal of Biochemical and Biophysical Methods* **1989**, *19*, 259.

(52) van Zandvoort, M. A. M. J.; Gerritsen, H. C.; van Ginkel, G.; Levine, Y. K.; Tarroni, R.; Zannoni, C. *Journal of Physical Chemistry B* **1997**, *101*, 4149.

(53) DeWitt, L.; Blanchard, G. J.; LeGoff, E.; Benz, M. E.; Liao, J. H.; Kanatzidis, M. G. *Journal of the American Chemical Society* **1993**, *115*, 12158.

(54) Holtom, G. R. *Proc. SPIE* **1990**, *1204*, 2.

(55) Haugen, G. R.; Wallin, B. W.; Lytle, F. E. *Rev. Sci. Instrum.* **1979**, *50*, 64.

(56) Chuang, T. J.; Eisenthal, K. B. *Journal of Chemical Physics* **1972**, *57*, 5094.

(57) Klein, U. K. A.; Haar, H. P. *Chemical Physics Letters* **1979**, *63*, 40.

(58) Labhart, H.; Pantke, E. R. *Chemical Physics Letters* **1973**, *23*, 482.

(59) Hu, C.-M.; Zwanzig, R. *Journal of Chemical Physics* **1974**, *60*, 4354.

(60) Youngren, G. K.; Acrivos, A. *Journal of Chemical Physics* **1975**, *63*, 3846.

(61) Debye, P. Polar Molecules. In *Chemical Catalog Co.* New York, 1929.

(62) Perrin, F. *Journal de Physique et le Radium* **1936**, *7*, 1.

Chapter 2

DYNAMICS OF 4-BENZYLAMINO-7-NITROBENZOFURAZAN IN THE 1-PROPANOL-WATER BINARY SOLVENT SYSTEM. EVIDENCE FOR COMPOSITION-DEPENDENT SOLVENT ORGANIZATION

Introduction

The interactions between dissimilar molecules in the solution phase have been the subject of a great deal of study because of the importance of such interactions in processes that include chemical separations, synthesis and heterogeneous and homogeneous catalysis. In all of this work, the common underlying issue that has been most difficult to address is the existence, persistence length and characteristic time-scale of local heterogeneity. We have been investigating micellar systems [1-5] and have found that the composition of the solutions from which the micelles are formed can have an influence on the resulting micelles. In an effort to understand these effects and in a larger sense to determine whether or not solution phase heterogeneity plays a role in the solutions we use, we have studied the lifetime and motional dynamics of a chromophore dissolved in a series of 1-propanol/water binary solvent systems.

A variety of spectroscopic methods have been utilized to probe solution phase systems, including vibrational relaxation,[6-16] fluorescence lifetime, and molecular reorientation measurements.[5,17-34]. In this study, we have chosen to use time-resolved fluorescence lifetime and anisotropy measurements of 4-Benzylamino-7-Nitrobenzofurazan (BBD) because of the properties of this chromophore and the wide use of its structural derivatives in the study of micellar and lipid bilayer structures. We use rotational diffusion due to the relatively high

information content of the signal and the established theoretical framework that is available for interpretation of the experimental data.[35-39] While the interpretation of fluorescence lifetime data is less straightforward and more system-dependent, for the chromophore we use here, there is an established dependence of its fluorescence lifetime on the "polarity" of the local environment. The chromophore that we have chosen for this work (BBD, Figure 10) is a member of a family of chromophores with the 7-nitrobenz-2-oxa-1,3-diazol-4-yl (NBD) group. These chromophores are known to exhibit absorption and emission band positions that are sensitive to solvent polarity, causing them to be used widely as fluorescent probes in biological and model membrane systems.[40-43] Shorter fluorescence lifetimes are observed with more polar solvents, making these probes well suited for studies of binary solvent systems. We have investigated the 1-propanol/water solvent system to understand whether or not there is discernible local heterogeneity in this system. Our data show that there is indeed local heterogeneity in this binary solvent system, and that the characteristic persistence time of this transient organization lies in the time window between the chromophore reorientation time (ca. 100 ps) and its fluorescence lifetime (several ns). Our reorientation data do not follow the simple viscosity-dependence predicted by the Debye-Stokes-Einstein (DSE) model (*vide infra*) and the composition of the solvent system modulates the strength of solvent-solute interactions measurably. We find that for the 1-propanol/water binary system, there is a range of propanol concentrations for which the solvent-solvent interactions are strong enough to alter the chromophore interactions with the

solvent system. The range of 1-propanol concentrations for which this occurs coincides with the concentration range for which 1-propanol and water are known to form an azeotrope. These findings shed new light on the heterogeneity of the local environment in binary solvent systems.

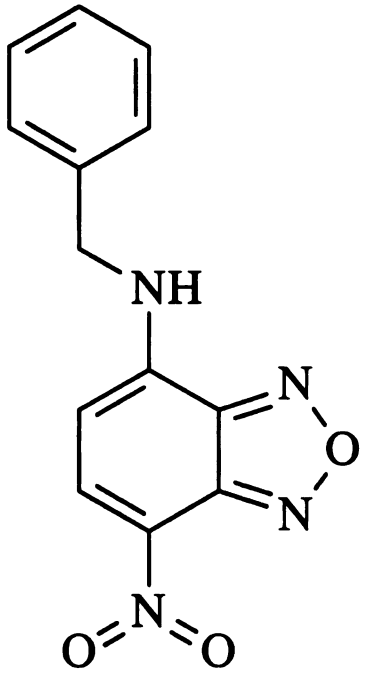

Figure 2.1 – The structure of 4-Benzylamino-7-Nitrobenzylfurazan (BBD).

Experimental

Materials. 4-Bezylamino-7-nitrobenzofurazan (BBD) was obtained from Sigma-Aldrich, inc. and used as received. 1-Propanol was acquired from CCI, Inc., and used as received. Water was distilled in-house. The BBD concentration for all solutions was 10 μM. Solution temperatures were maintained at 298 ±0.5 K (Neslab EX100-DD) for all time-resolved fluorescence lifetime and anisotropy measurements.

Time-Correlated Single Photon Counting Measurements. Fluorescence lifetime and anisotropy measurements of BBD in a series of 1-propanol/water solutions were made using a time-correlated single photon counting (TCSPC) instrument that has been described in detail previously,[44] and a more detailed description can be seen in Chapter One. The excitation for the BBD experiments is 460 nm, and fluorescence is collected at 490 nm.

Steady-State Spectroscopy. Absorption spectra were recorded with 1 nm spectral resolution using a Cary model 300 double-beam UV-visible absorption spectrometer. Spontaneous emission spectra were acquired with a Spex Fluorolog 3 spectrometer, with both excitation and emission monochromators set to 3 nm resolution.

Semi-empirical calculations. The permanent dipole moment of BBD was calculated for the ground state (S_0) and first excited electronic state (S_1) using Hyperchem® v. 6.0, with PM-3 parameterization.[45]

Results and Discussion

We have been involved in the study of micellar systems using optical spectroscopic methods. Such studies require the incorporation of fluorescent molecules into micelles, a task which is not always straightforward. Owing to the typically limited solubility of fluorescent probe molecules in aqueous solutions, concentrated chromophore solutions made with an alcohol cosolvent are sometimes used. Even with the presence of a small amount of an alcohol in the micellar solution, there is a question of how the micelles are altered by its presence, and this is an issue that we have addressed experimentally.[4] In this work we are concerned with the intrinsic solution phase heterogeneity that attends binary 1-propanol/water solvent systems. If there is, in fact, detectable solution phase heterogeneity in alcohol/water binary systems, such transient solution phase organization could give rise to unexpected partitioning phenomena in multi-component solutions in which micelles are formed. Our fluorescence lifetime and anisotropy measurements point to local heterogeneity in 1-propanol/water solutions, with a characteristic persistence time on the sub-nanosecond timescale. We find that the 1-propanol/water system interacts with the chromophore BBD in a manner that depends sensitively on the composition of the solvent system, with the nominally weakest BBD-solvent interactions occurring for solvent ratios close to those for which 1-propanol and water form azeotropes.

Steady State Spectroscopy. As a first step in the characterization of BBD in 1-propanol/water solvent systems, we consider the solvent-dependence of the

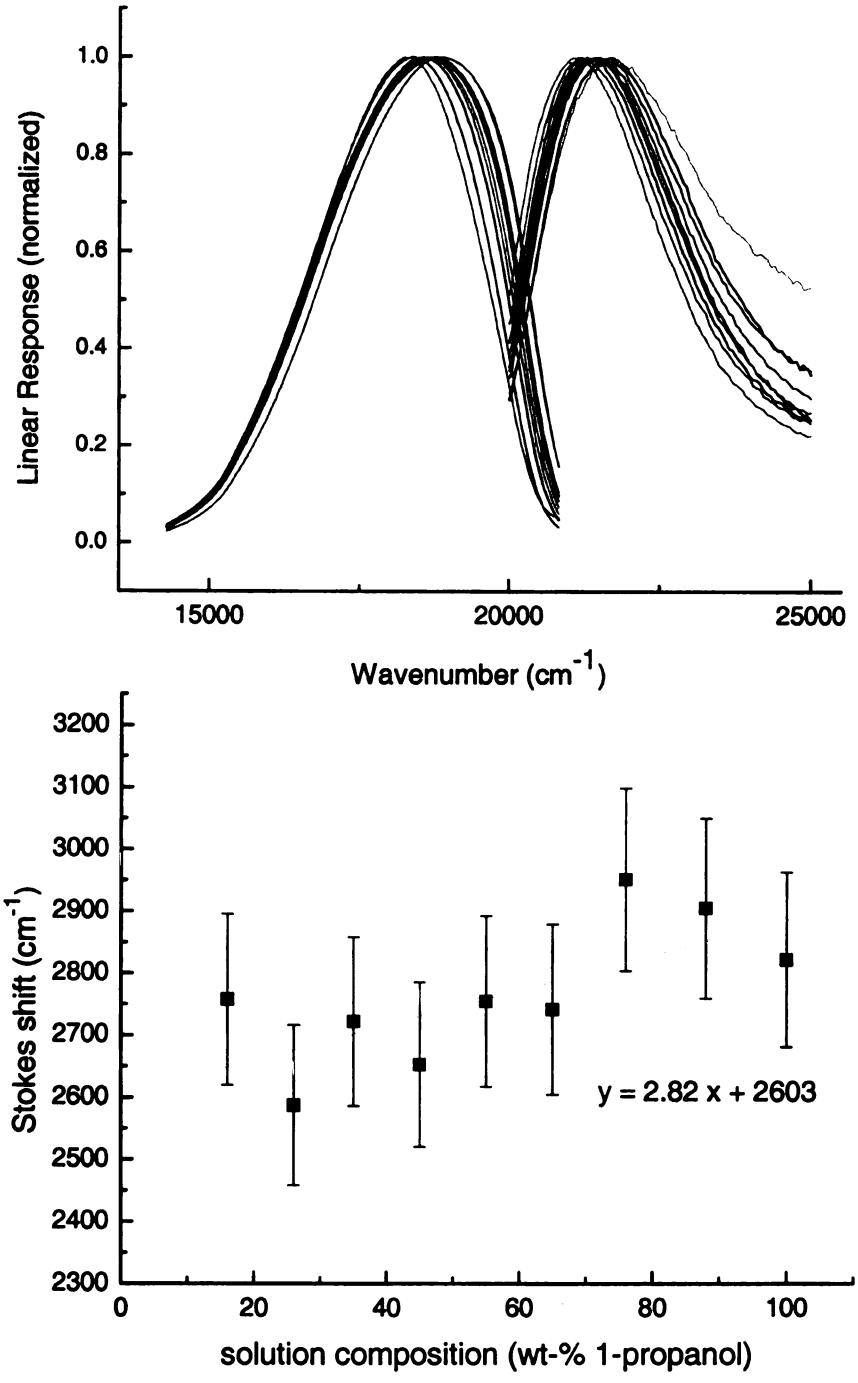

Figure 2.2 - (a) Absorption and emission spectra of BBD as a function of 1-propanol/water solvent system composition. The absorption and emission spectra shift to shorter wavelength with increasing 1-propanol concentration. (b) The Stokes shift of BBD as a function of 1-propanol/water solvent system composition (5% error).

chromophore steady state absorption and emission spectra (Figure 2.2). The absorption maximum of BBD is shifted to shorter wavelengths with increasing 1-propanol concentration. This is an expected result since it is known that as the polarity of the solution increases the absorption maximum shifts to the red. While the physical origin of the spectral band position dependence on solvent polarity remains to be elucidated for this chromophore, these steady state data demonstrate that, on average, as the 1-propanol content of the solvent system is increased, the chromophore senses this change in a proportional manner. This is not a surprising result, owing to the expected transient nature of local organization in the solution phase, and these data are consistent with the fluorescence lifetime data (*vide infra*). Since the ground and excited state dipole moments are not being perturbed, the steady state data can be thought of in the context of simple energy level shifts.

Fluorescence lifetime measurements. Fluorescence lifetime data are useful for a variety of reasons. For some chromophores, such as BBD, the fluorescence lifetime is related to the polarity of the medium, analogous to the relationship seen for the BBD steady state spectra and solvent polarity. To the best of our knowledge, there is not a fundamental explanation for the relationship between solvent properties and BBD spectroscopic response, but there are still several interesting points that can be discerned from these data.

For many solvatochromic chromophores, the Stokes shift and emission band positions are related to the ability of the solvent medium to stabilize the chromophore excited electronic state. We observe for BBD that both the

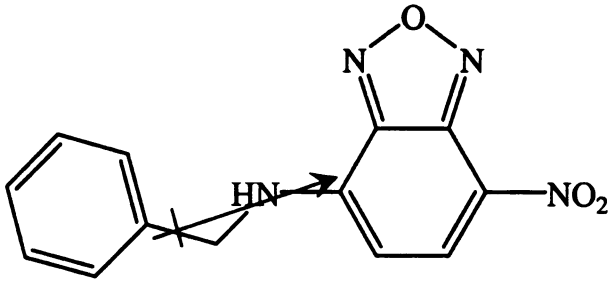

S_0

μ=8.9 D

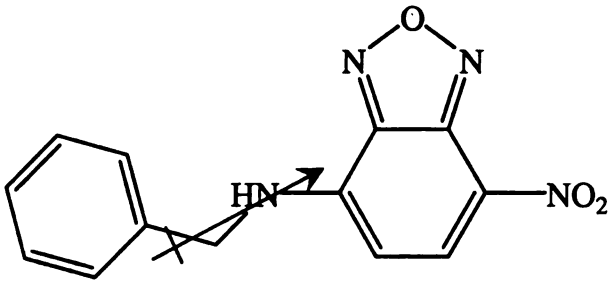

S_1

μ=10.9 D

Figure 2.3 - Permanent dipole moment magnitude and orientation for S_0 (top) and S_1 (bottom) BBD. These calculations were performed at the semi-empirical level using a PM-3 parameterization. Note that the orientation of the permanent dipole moment changes little on excitation.

absorption and emission bands blue-shift as the polarity of the solvent system is reduced, while the Stokes shift remains constant (Figs. 2.2). These data suggest that both the S_0 and S_1 electronic states of this chromophore are relatively polar, with the S_1 state being more polar than the S_0. Specifically, there appears not to be any site-specific solvent-solute interaction that gives rise to the preferential stabilization of either the S_1 or S_0 electronic states. This interpretation is supported by semi-empirical calculations of BBD (Figure 2.3) indicating the S_0 dipole moment to be 8.9 D and the S_1 dipole moment to be 10.9 D. Interestingly, the S_1 lifetime increases as the polarity of the solvent decreases, but in all cases decays as a single exponential (Figure 2.4). The S_1 lifetime for any chromophore can be modulated by a number of factors, including the ability of the solvent medium to allow a relatively rigid (planar) chromophore. Clearly the data we present here do not provide sufficient information to elucidate the basis for the dependence of the fluorescence lifetime on the solvent system polarity, but we do note that, even if there is discernible heterogeneity in the solvent system, this structural heterogeneity is effectively averaged over the lifetime of the S_1 state of BBD, thereby placing an upper bound on the persistence time of any solvent system transient organization (*vide infra*). With this information in hand, we turn to a discussion of the fluorescence anisotropy data.

Molecular Reorientation. For the systems under study here, fluorescence anisotropy data are accounted for in the context of molecular rotational motion. We obtain fluorescence depolarization data experimentally by exciting BBD with a vertically polarized light pulse and collecting the emission decay transients

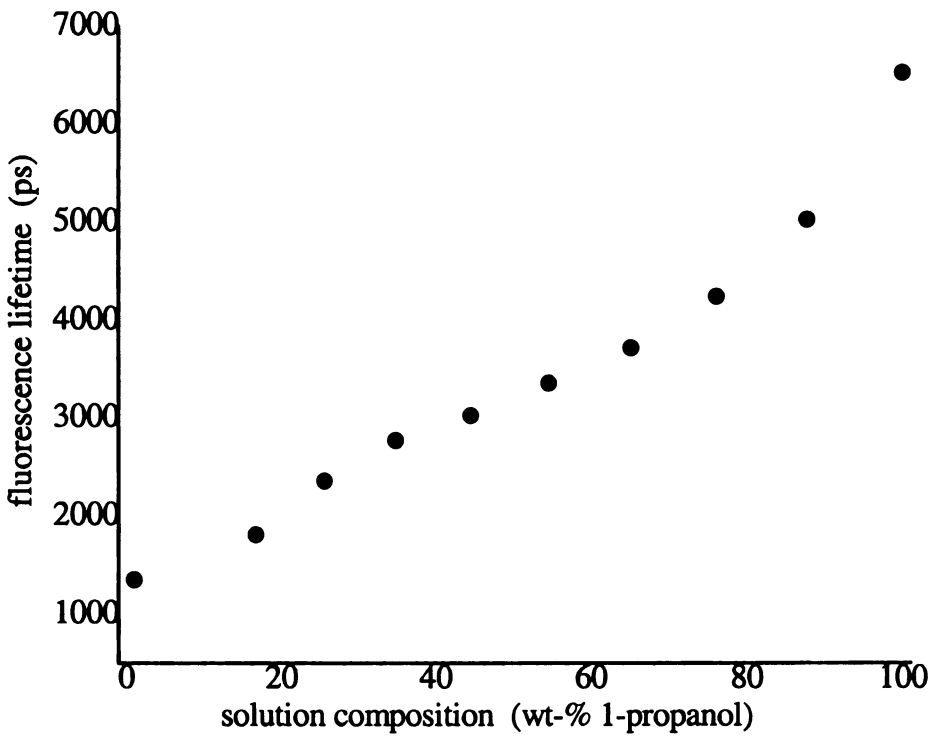

Figure 2.4 - Fluroescence lifetime of BBD as a function of 1-propanol concentration.

polarized parallel and perpendicular to the excitation polarization. These data are combined to produce the induced orientational anisotropy function, R(t)

$$R(t) = \frac{I_{\parallel}(t) - I_{\perp}(t)}{I_{\parallel}(t) + 2I_{\perp}(t)} \quad (1)$$

where $I_{\parallel}(t)$ and $I_{\perp}(t)$ are the polarized emission intensities. The chemical information contained in these data resides in the decay time constant(s) of R(t), and its zero-time value, R(0). There is a well established body of theory for the interpretation of R(t)[35-39]. In principle, R(t) can decay with up to five exponential terms, but for most chromophores Chuang and Eisenthal's theory[35] reduces to either one or two exponential decay components, depending on the shape of the ellipsoid swept out by the rotating moiety and the orientation of the chromophore transition dipole moments relative to the rotational motion axes. Experimentally, the most common result is the recovery of a single exponential decay component in R(t), and that is the functional form of the data we have acquired for BBD in 1-propanol/water. The functional form of R(t) allows the interpretation of our data within the framework of the modified Debye-Stokes-Einstein model.

The modified Debye-Stokes-Einstein (DSE) equation is given by Eq. 2[36,37]

$$\tau_{or} = \frac{\eta V f}{k_B T S} \quad (2)$$

where η is the solvent viscosity, V is the solute hydrodynamic volume[46], T is the temperature, k_B is the Boltzmann constant, f is the frictional interaction term[38], and S is the solute molecular shape factor[37]. The DSE model is limited in the sense that it does not account for the molecular nature of the solvent, yet for

many systems it provides remarkably close agreement with experimental data. The success of this model lies in the fact that the recovered time constant averages over the many fast molecular interactions that are collectively responsible for solvation. It is only when the characteristic time constant for the molecular solvent-solute interactions becomes on the order of the reorientation time constant that one observes a substantial contribution from discrete intermolecular interactions. When experimental values diverge from the modified DSE model predictions, the discrepancy between experiment and model is typically attributed to deviations in the solvent viscosity, solute hydrodynamic volume, frictional boundary condition, or solute shape factor. Given the experimental information available in most cases, it is not possible to clearly distinguish which of these quantities accounts for experimental behavior. Solvent-solute interactions dominated by frictional interactions or a discrepancy between the microscopic and bulk solvent viscosity usually are taken to account for deviations in the trends predicted by DSE, whereas non-monotonic variations in τ_{OR} with solvent system properties such as composition or bulk viscosity typically imply an important role for molecular-scale processes. The shape of the probe molecule is, in general, predicted to be ellipsoidal, with the shape of the volume swept out during reorientation being described by Perrin's equations[37]. In many cases, especially where single exponential anisotropy decays are recovered experimentally, the actual volume swept out by the reorienting moiety is not simply that of the probe molecule. The hydrodynamic volume of the reorienting moiety can deviate from model predictions due to preferential,

relatively long-lived solvent-solute interactions (*e.g.* H-bonding), and there have been several accounts of such behavior in binary solvent systems.[47-51]

We recover single exponential anisotropy decays for BBD in all 1-propanol/water solvent systems. Our data are consistent with BBD reorienting as a prolate rotor, assuming the $S_1 \leftarrow S_0$ transition moment lies in the chromophore π-system plane along the long axis. We recognize that the orientation of the transition dipole moment may deviate slightly from this geometric axis due to the asymmetric substitution of the chromophore 6-membered ring, but such an effect does not bear on the substance of our findings. We calculate the hydrodynamic volume of BBD to be 215 A^3,[46] T=300 K, and f=1 (stick limit). We have not reported a value for S because of the uncertainty in the volume swept out by the reorienting chromophore because of the bulky amino-methylphenyl substituent. Based on these quantities and using Eq. 2, we calculate τ_{OR}/η = 51.9 ps/cP in the stick limit. We show in Figure 14a the dependence of the experimental reorientation time on the solvent system composition. These data do not follow a trend that is monotonic with respect to the solvent system bulk composition, and it is this point which requires a more detailed treatment.

As noted above, trends in reorientation data that scale linearly with solution viscosity can indicate molecular motion being mediated by processes that are averaged over a large number of molecular-scale events. To address whether or not the reorientation data we report here do, in fact, vary monotonically with solvent viscosity, we must understand how the viscosity of the 1-propanol/water system depends on composition. These data have been

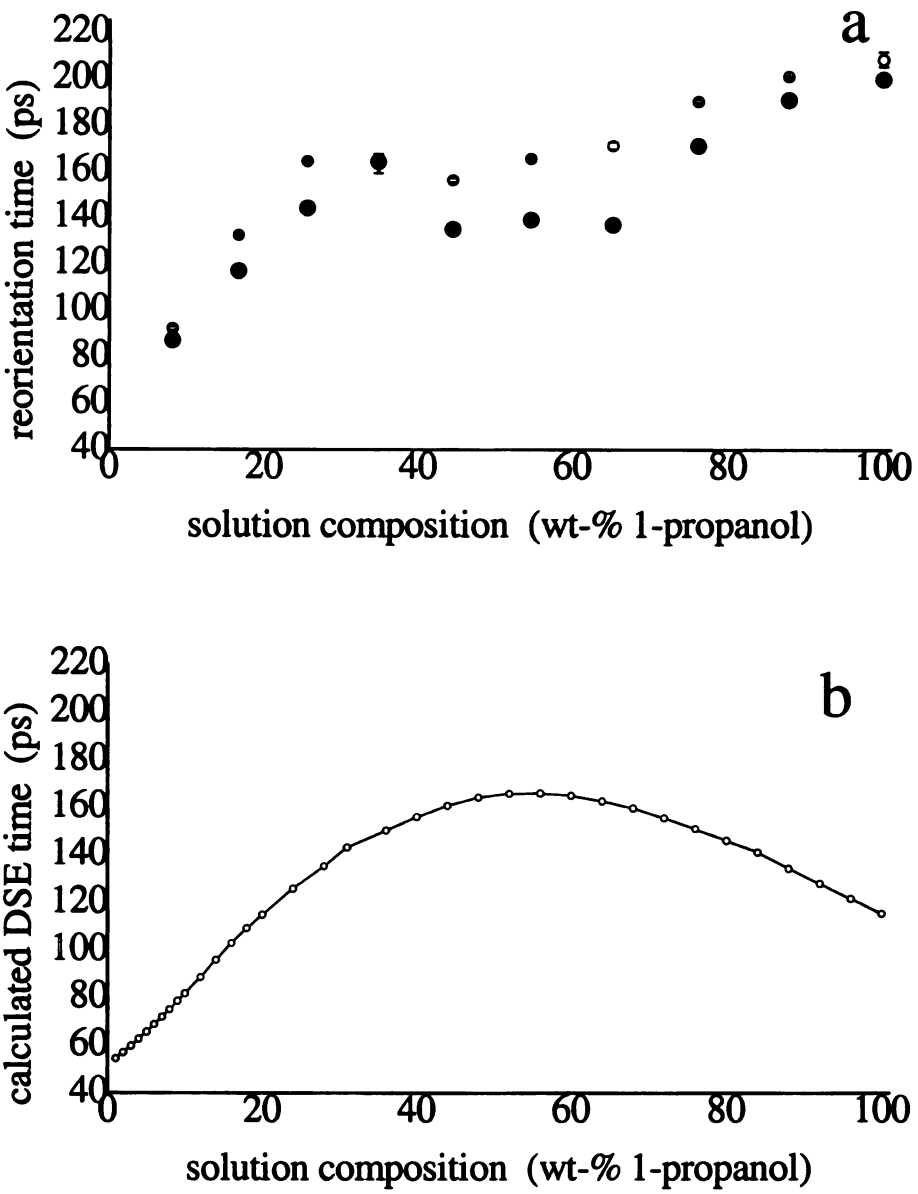

Figure 2.5 - (a) Fluroescence anisotropy decay times as a function of solution 1-propanol concentration. The calculated model times from Table 1 are plotted for comparison to the experimental data. Error bars are indicated on individual data points and are the result of at least six individual determinations of each point. (b) Solution bulk viscosity of the 1-propanol/water solvent system as a function of 1-propanol concentration. These data were adapted from ref [52-54].

tabulated in the literature,[52-54] and there is a nonlinear dependence of solution viscosity on solution composition. Using the DSE model parameters given above and the literature data on 1-propanol/water viscosity, we show the calculated τ_{OR} times in Figure 2.5b. Clearly the calculated results do not agree well with the experimental data. At high 1-propanol concentrations, the experimental τ_{OR} values are much larger than the calculated values, and for 1-propanol concentrations in the region of 30%, there is an anomalous spike in the experimental reorientation data which is not reflected in the calculations. The experimental reorientation data cannot be understood wholly in the context of solvent properties, and the physicochemical phenomena that give rise to these data operate on a time scale commensurate with the measured anisotropy decay time(s).

The hydrodynamic volume of BBD is 215 $Å^3$ using Edward's model. This model is well established and yields results that are consistent with the reorientation dynamics of many chromophores in neat solvents. The experimental, non-monotonic deviations from the DSE model predictions are not associated the calculated volume of BBD, but the total volume of the reorienting moiety can vary with solution composition. It is possible that one or more solvent molecules (presumably propanol) are associated with the probe molecule, yielding a reorienting species that has a larger hydrodynamic volume than that of the chromophore alone. In this case we describe $V = V_{BBD} + nV_{solvent}$, where V is the total hydrodynamic volume of the reorienting entity, $V_{BBD} = 215$ $Å^3$, $V_{solvent}$ is the hydrodynamic volume of a solvent (1-propanol) molecule, and n is the

number of solvent molecules that are closely associated with BBD. Using Edward's method, we calculate $V_{solvent}$ = 70 Å^3 for 1-propanol, and within the context of this explanation, the added solvent volume required for consistency of the model with the data is n = 1 for low 1-propanol concentrations, reducing to no added solvent volume for solution compositions where 1-propanol and water are known to form an azeotrope, then increasing to a high value of n = 3 at high 1-propanol concentrations (see Table 2.1). We note that the agreement between this model and the experimental data is not exact, but rather produces good qualitative agreement. We believe that the discrepancies between model and data lie in the fact that we have assumed simplistically that a solvent is either interacting strongly enough to reorient with the BBD chromophore, or not. This assumption can be re-expressed in terms of the average lifetime of the solvent-solute interactions, where we assume that the 1-propanol-BBD interaction persists for a time interval that is longer, on average, than the anisotropy decay time of the reorienting moiety. If this is not the case, then we would expect in this model to recover solvent-related "additional volume" that would be a fraction of whole solvent molecule(s), and indeed, if we were to invoke this parameter, we could achieve better correspondence between experiment and model. We do not have any experimental information, however, on the lifetime of the 1-propanol-BBD interaction, so we do not feel justified in pushing the model this far.

It is not surprising, in our view, to find that there exist strong solvent-solute interactions between BBD and 1-propanol. What is interesting is that our data

Wt % Propanol	V (calculated from exp. data)	*n*	V ($V_{BBD}+nV_{PrOH}$)	τ_{OR} calculated (ps)	τ_{OR} experimental (ps)
100	388	3	425	200	209 ± 3
88	321	2	355	191	201 ± 1
76	271	1	285	171	190 ± 1
65	227	0	215	137	171 ± 2
55	214	0	215	139	166 ± 1
45	208	0	215	135	156 ± 1
35	236	1	285	164	163 ± 4
26	272	1	285	144	164 ± 1
17	270	1	285	117	132 ± 1
8	261	1	285	87	92 ± 1

Table 2.1 - Solvent association calculations for $V = V_{probe} + nV_{solvent}$. Values of V calculated from experimental t_{OR} times are shown in the second column, and from these data we can estimate the number of 1-propanol molecules that reorient with the BBD chromophore. From this estimate of *n* and experimental viscosity data (from Ref [52-54]), we calculate a model τ_{OR}.

are consistent with the extent of solvent-solute interactions varying in a non-monotonic manner with solvent system composition. This finding implies that, over a significant composition range for the 1-propanol/water system, the interactions between water and 1-propanol are sufficiently strong to preclude 1-propanol interacting strongly with the BBD chromophore. We note that the formation of an azeotrope for a binary solvent system implies significant interactions between the two solvents, and for 1-propanol and water, the azeotrope-forming composition range lies between 28 to 70 weight percent 1-propanol. In this solvent system composition range, it is possible that the most stable solvent configuration(s) are those for which 1-propanol and water are interacting more strongly with themselves than with BBD. In concentration regions away from where an azeotrope forms, the individual solvent molecules could, in principle, interact more strongly with BBD.

The above explanation provides qualitative agreement with our experimental data, but it cannot provide more detail, based in part on the dearth of molecular-scale information extant on the nature of azeotrope(s) between 1-propanol and water. It appears that the strength of interactions between BBD and the 1-propanol/water system are closely matched with 1-propanol-water interactions, and that in all cases these interactions must persist over a time scale that is consistent with hydrogen bond formation and breakage. Regardless of the inability to provide a detailed picture of the solvation dynamics of BBD in the 1-propanol/water system, it is clear that depending on the amount of alcohol present in solution, there can be significant intermolecular interactions between

chromophores and solvents, and these interactions can, in principle, have some influence on the formation of micelles.

Conclusions

We have examined the fluorescence lifetime and rotational diffusion dynamics of BBD in the 1-propanol/water solvent system. The increase of the fluorescence lifetime of BBD with increasing 1-propanol concentration is fully consistent with the known behavior of chromophores containing an NBD group, and indicates that the persistence time of any local organization is less than nanoseconds. Modeling the reorientation behavior of BBD in the context of the modified DSE model indicates that, for higher concentrations of 1-propanol, the experimental anisotropy decay times are significantly longer than expected. Because of the non-monotonic nature of the reorientation data, we understand this anomalous behavior in the context of strong, associative solvent-solute interactions, with the persistence time of the interactions being on the order of the measured reorientation time. While strong solvent-solute association has been seen before[5,25-27], this is a particularly pronounced example of solvent-composition dependent interactions, and we note that the solvent-solute interactions are weakest in the 1-propanol concentration regime where azeotropes are formed with water. It is clear that in the 1-propanol/water solvent system there is discernible microscopic solvent heterogeneity, with the details of this transient solution phase structure depending sensitively on the composition of the solvent system.

Literature Cited

(1) DelaCruz, J. L.; Blanchard, G. J. *Journal of Physical Chemistry B* **2003**, *107*, 7102.

(2) Kelepouris, L.; Blanchard, G. J. *Journal of Physical Chemistry B* **2002**, *106*, 6600.

(3) Kelepouris, L.; Blanchard, G. J. *Journal of Physical Chemistry B* **2003**, *107*, 1079.

(4) Stevenson, S. A.; Blanchard, G. J. *In Preparation.*

(5) Dela Cruz, J. L.; Blanchard, G. J. *Journal of Physical Chemistry A* **2001**, *105*, 9328.

(6) Goldie, S. N.; Blanchard, G. J. *Journal of Physical Chemistry A* **2001**, *105*, 6785.

(7) Goldie, S. N.; Blanchard, G. J. *Journal of Physical Chemistry A* **1999**, *103*, 999.

(8) Jiang, Y.; Blanchard, G. J. *Journal of Physical Chemistry* **1994**, *98*, 9411.

(9) Jiang, Y.; Blanchard, G. J. *Journal of Physical Chemistry* **1995**, *99*, 7904.

(10) Heilweil, E. J.; Casassa, M. P.; Cavanagh, R. R.; Stephenson, J. C. *Annual Review of Physical Chemistry* **1989**, *40*, 143.

(11) Heilweil, E. J.; Cavanagh, R. R.; Stephenson, J. C. *Chemical Physics Letters* **1987**, *134*, 181.

(12) Casassa, M. P.; Heilweil, E. J.; Stephenson, J. C.; Cavanagh, R. R. *Journal of Chemical Physics* **1986**, *84*, 2361.

(13) Cavanagh, R. R.; Heilweil, E. J.; Stephenson, J. C. *Journal of Electron Spectroscopy and Related Phenomena* **1987**, *45*, 31.

(14) McCarthy, P. K.; Blanchard, G. J. *Journal of Physical Chemistry* **1995**, *99*, 17748.

(15) McCarthy, P. K.; Blanchard, G. J. *Journal of Physical Chemistry* **1996**, *100*, 5182.

(16) McCarthy, P. K.; Blanchard, G. J. *Journal of Physical Chemistry* **1996**, *100*, 14592.

(17) Millar, D. P.; Shah, R.; Zewail, A. H. *Chemical Physics Letters* **1979**, *66*, 435.

(18) Goldie, S. N.; Blanchard, G. J. *Book of Abstracts, 213th ACS National Meeting, San Francisco, April 13-17* **1997**, ANYL.

(19) Fleming, G. R.; Morris, J. M.; Robinson, G. W. *Chemical Physics* **1976**, *17*, 91.

(20) Pauls, S. W.; Hedstrom, J. F.; Johnson, C. K. *Chemical Physics* **1998**, *237*, 205.

(21) Truong, T. V.; Shen, Y. R. *Journal of Chemical Physics* **2005**, *122*, 091104/1.

(22) Balabai, N.; Sukharevsky, A.; Read, I.; Strazisar, B.; Kurnikova, M.; Hartman, R. S.; Coalson, R. D.; Waldeck, D. H. *Journal of Molecular Liquids* **1998**, *77*, 37.

(23) Hartman, R. S.; Konitsky, W. M.; Waldeck, D. H. *Journal of the American Chemical Society* **1993**, *115*, 9692.

(24) Sanders, M. J.; Wirth, M. J. *Chemical Physics Letters* **1983**, *101*, 361.

(25) Mukherjee, A.; Bagchi, B. *PhysChemComm* **2003**, 28.

(26) Von Jena, A.; Lessing, H. E. *Chemical Physics Letters* **1981**, *78*, 187.

(27) Dela Cruz, J. L.; Blanchard, G. J. *Journal of Physical Chemistry A* **2002**, *106*, 10718.

(28) Srinivas, G.; Bhattacharyya, S.; Bagchi, B. *Journal of Chemical Physics* **1999**, *110*, 4477.

(29) Labhart, H.; Pantke, E. R. *Chemical Physics Letters* **1973**, *23*, 482.

(30) Blanchard, G. J. *Journal of Chemical Physics* **1987**, *87*, 6802.

(31) Blanchard, G. J. *Journal of Physical Chemistry* **1988**, *92*, 6303.

(32) Blanchard, G. J. *Analytical Chemistry* **1989**, *61*, 2394.

(33) Blanchard, G. J.; Wirth, M. J. *Journal of Physical Chemistry* **1986**, *90*, 2521.

(34) Templeton, E. F. G.; Quitevis, E. L.; Kenney-Wallace, G. A. *Journal of Physical Chemistry* **1985**, *89*, 3238.

(35) Chuang, T. J.; Eisenthal, K. B. *Journal of Chemical Physics* **1972**, *57*, 5094.

(36) Debye, P. Polar Molecules. In *Chemical Catalog Co.* New York, 1929.

(37) Perrin, F. *Journal de Physique et le Radium* **1936**, *7*, 1.

(38) Hu, C.-M.; Zwanzig, R. *Journal of Chemical Physics* **1974**, *60*, 4354.

(39) Zwanzig, R.; Harrison, A. K. *Journal of Chemical Physics* **1985**, *83*, 5861.

(40) Fery-Forgues, S.; Fayet, J.-P.; Lopez, A. *Journal of Photochemistry and Photobiology, A: Chemistry* **1993**, *70*, 229.

(41) Lin, S.; Struve, W. S. *Photochemistry and Photobiology* **1991**, *54*, 361.

(42) Mukherjee, S.; Chattopadhyay, A. *Journal of Fluorescence* **1995**, *5*, 237.

(43) Mukherjee, S.; Chattopadhyay, A.; Samanta, A.; Soujanya, T. *Journal of Physical Chemistry* **1994**, *98*, 2809.

(44) DeWitt, L.; Blanchard, G. J.; LeGoff, E.; Benz, M. E.; Liao, J. H.; Kanatzidis, M. G. *Journal of the American Chemical Society* **1993**, *115*, 12158.

(45) Froimowitz, M. *BioTechniques FIELD Publication Date:1993*, *14*, 1010.

(46) Edward, J. T. *Journal of Chemical Education* **1970**, *47*, 261.

(47) Bhattacharyya, S.; Bagchi, B. *Journal of Chemical Physics* **2001**, *115*, 9065.

(48) Dutt, G. B.; Doraiswamy; Periasamy, N. *Journal of Chemical Physics* **1991**, *94*, 5360.

(49) Alavi, D. S.; Waldeck, D. H. *Journal of Physical Chemistry* **1991**, *95*, 4848.

(50) Mukherjee, A.; Bagchi, B. *Journal of Physical Chemistry B* **2001**, *105*, 9581.

(51) Beddard, G. S.; Doust, T.; Hudales, J. *Nature (London, United Kingdom)* **1981**, *294*, 145.

(52) *CRC Handbook of Chemistry and Physics*, 1980-1981.

(53) Mikhail, S. Z.; Kimel, W. R. *Journal of Chemical and Engineering Data* **1963**, *8*, 323.

(54) Wensink, E. J. W.; Hoffmann, A. C.; van Maaren, P. J.; van der Spoel, D. *Journal of Chemical Physics* **2003**, *119*, 7308.

Chapter 3

INVESTIGATING THE MICELLE-SOLUTION INTERFACIAL REGION USING FLUORESCENCE RESONANCE ENERGY TRANSFER

Introduction

Surfactants have attracted considerable interest for a number of years due to their many uses, ranging from chemical separations to industrial and home-use detergents. Among the interesting properties of surfactants is their ability to form micelles of various shapes, depending on the specific surfactant and its concentration. Despite the substantial micelle literature extant, a detailed understanding of the structure and dynamics of this family of systems remains to be achieved. We are interested in understanding the intermediate region between micelle head groups and the bulk solvent surrounding them because it is this interface that mediates exchange processes and interactions between the micelles and other species in solution. Depending on the strength of such interactions, it is also possible that the interior of the micelle will be affected, and this is an issue we address experimentally. Because there is no direct means to probe the micelle-solution interface electrochemically, we are interested in determining the utility of fluorescence spectroscopy for that purpose.

Fluorescence spectroscopy finds wide use because of its characteristically high sensitivity combined with the range of chemical properties available with the fluorophores used. For measurements in heterogeneous systems, it is possible to use fluorescent compounds that will partition selectively into a given phase, or will reside at the interface between two phases. This capability, when combined

with fluorescence resonance energy transfer (FRET) measurements, has been used in the study of heterogeneous systems such as micelles, vesicles, and lipid bilayers. [1-23] The topology of these systems can significantly influence the efficiency of energy transfer since the dipolar coupling process that mediates energy transfer depends on both the average distance and orientation of the molecules involved. Energy transfer measurements can be used as a "spectroscopic ruler" to estimate average distances between optical donor and acceptor, and thus we can gain information on the extent to which micelle and acceptor interact. Time-domain reorientation measurements can provide information on the microenvironments that exist within a heterogeneous system. Micellar systems are ideal candidates for energy transfer experiments, and previous work in this area has examined energy transfer between two molecules sequestered inside a micelle, between a molecule inside the micelle and a molecule that is part of the surfactant, and between two molecules on the surface of the micelle. [12,16,19,24] Most of these studies have focused on energy transfer between molecules in the same region of the micelle. We are particularly interested in the interfacial region of micelles, and understanding the intermolecular dynamics in micellar systems will hopefully shed some light on more complex biomimetic systems.

We have sequestered perylene inside sodium dodecyl sulfate (SDS, anionic) and cetyltrimethylammonium bromide (CTAB, cationic) micelles, and have used the steady state and time-resolved fluorescence of this chromophore to obtain information on how different acceptor chromophores in the aqueous

ph
be
se
di
sp
op
for
ac
chi
inte
inte
the
a fu
of t

phase interact with the donor. Perylene is a hydrophobic chromophore that has been studied extensively, making it an obvious choice for a probe to be sequestered within micelles. The two ionic acceptor chromophores, anionic disodium fluorescein (DSF) and cationic rhodamine 110 (R110), have spectroscopic properties well suited to their role as optical acceptors, and their opposite ionic charges make them useful for studying interactions with micelles formed by the two ionic surfactants we use. By varying the concentration of the acceptor chromophores, and the ionic charges present on both the acceptor chromophores and the micelle head groups, we can evaluate the role of ionic interactions in mediating molecular communication across the micelle-solution interface. From these data we can estimate the association constant between the chromophores and the micelles. Reorientation measurements of perylene as a function of optical acceptor concentration point to the role of the palisades layer of the micelles in mediating the properties of the micelle interior regions.

Experimental

Materials. The surfactants sodium dodecyl sulfate (SDS) and cetyltrimethylammonium bromide (CTAB) were obtained from Sigma-Aldrich, Inc. and used as received. Perylene (Aldrich), disodium fluorescein (Aldrich) and rhodamine 110 chloride (Exciton) were checked for fluorescent impurities and used as received. The structures of the chromophores used in this chapter can be seen in Figure 3.1. The perylene concentration for all solutions was 10 μM. The micellar solution temperatures were maintained at 298 ±0.5 K (Neslab EX100-DD) for all time-resolved fluorescence measurements. For the SDS solutions, perylene was dissolved in a 50/50 solution of butanol and methanol ($3x10^{-5}$ M perylene concentration) before addition of surfactant and, similarly, for CTAB solutions the perylene was dissolved in acetonitrile ($3x10^{-5}$ M) before addition of the surfactant. These cosolvents were required to get perylene into the micellar solutions. For the formation of micelles, we used 17 mM SDS, which is twice the critical micelle concentration, and 2 mM CTAB, also corresponding to twice the critical micelle concentration. Cryo-TEM images (*vide infra*) show uniform size and shape of resulting spherical micelles in solution. The ionic strengths of the solutions varied with composition.

Time-Correlated Single Photon Counting Measurements. Fluorescence lifetime and anisotropy measurements of perylene sequestered within SDS and CTAB micelles were made using a time-correlated single photon counting (TCSPC) instrument that has been described in detail previously.[25] The excitation wavelength was 420 nm and the emission was collected at 470 nm.

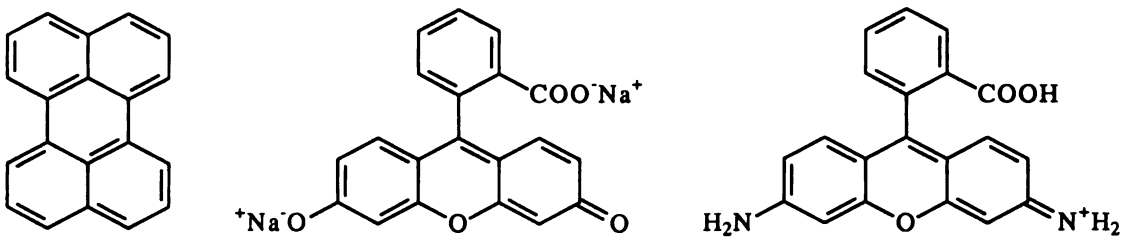

perylene

Disodium fluorescein
DSF

Rhodamine 110
R110

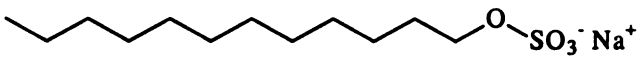

Sodium dodecyl sulfate (SDS)

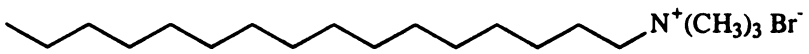

Cetyl trimethylammonium bromide (CTAB)

Figure 3.1 - Structures of the chromophores used in this chapter.

Steady-State Spectroscopy. Absorption spectra were recorded using a Cary model 300 double-beam UV-visible absorption spectrometer, with 1 nm spectral resolution. Spontaneous emission spectra were acquired with a Spex Fluorolog 3 spectrometer, with both excitation and emission monochromators set to 3 nm resolution.

Cryo-TEM imaging. Cryogenic TEM images were acquired on our samples by Dow-Corning Analytical Solutions, Auburn Hills, MI. To prepare the samples, ca. 2.3 mL of the micelle-containing solution was loaded on a holey carbon film coated Cu TEM grid using a micropipette. The excess fluid on the grid surface was removed by blotting the surface with a filter paper make an aqueous thin film for the TEM. The grid was immersed in liquid ethane contained in a small vessel that itself was housed in a larger liquid nitrogen vessel. The water film on the grid was vitrified to avoid water crystallization. The sample was loaded into the TEM (JEOL JEM 2100F) and the morphology was observed below 104 K. The digital images were acquired using a Gatan CCD camera attached at the bottom of the TEM column and Digital Micrograph software. The cryo-TEM images are shown in Figure 3.2.

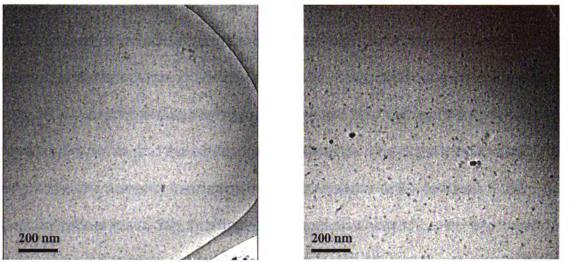

Figure 3.2 - Cryo-TEM images of SDS (a) and CTAB (b) micelles, showing a range of sizes less than 100nm diameter.

Results and Discussion

The objective of this chapter is to better understand the interfacial region between the micelle head groups and the bulk solution. We are concerned with the role of ionic charge in determining the interactions between ionic micelle head groups and constituents in the bulk solution. We probe this region by monitoring the effect that ionic optical acceptor molecules in the aqueous phase have on a fluorophore sequestered within the micelle. Excitation transport between the donor and the solution phase acceptor chromophore provides insight into the extent of interaction between acceptor and micelle, and the motional properties of the chromophore sequestered within the micelle relate to micellar organization and local viscosity. We detail below how our results point to discernible heterogeneity in the micellar solutions and changes in the nonpolar region of the micelle with the addition of an optical acceptor chromophore.

Before discussing our experimental data in detail, a word is in order on what is known about the micelle/solution interface. While it may be tempting to consider the interface between micelles and the bulk solution to be relatively well defined, several issues serve to complicate this picture. The first is surfactant exchange between the solution phase and the micelle. The typical residence time for a surfactant molecule in the micelle assembly will, of course, vary depending on the specific system, but such times are on the order of nanoseconds to microseconds. [26] These interfaces are also not well represented as a single, charged "ball". If this were the case, head group ionic repulsions

would preclude micelle formation. Based on a large body of literature and previous work in the Blanchard group,[4,27] it is clear that the counter ions in solution play a significant screening role and mediate ionic interactions between surfactant head groups. The interface between the micelle and the bulk solution is not abrupt, progressing from a non-polar micelle interior, through an ionically compensated region, through a solvent "layer" that likely exhibits organization analogous to that of the electric double layer, and finally to bulk solution. This intermediate region is termed the "palisades layer", [26,28-30] and it is the details of this intermediate region that are of primary interest to us in this work.

Fluorescence lifetime measurements. Our experiments are designed to understand whether or not the ionic charge of micelle head groups serves as a point of strong interaction with ionic constituents in solution. To make this determination, we use fluorescence lifetime measurements to characterize excitation transport dynamics in micelle-containing solutions. The concentration of optical donor in the micelles is such that we estimate there to be a single perylene chromophore in approximately 1% of the micelles. The optical acceptor concentrations we use are such that in a homogeneous solution, the average distance between donor and acceptor would be 150 Å or more. Under these experimental conditions, very little donor-acceptor excitation transfer will be seen, and we will observe acceptor concentration-dependent changes in the donor fluorescence lifetime only if the optical acceptor interacts preferentially with the micelles.

The transfer of energy between molecules can occur by a number of mechanisms, ranging from collisional quenching to dipolar coupling. We are concerned in this work with the latter phenomenon because of the characteristic length scale over which it operates. The transfer of energy by dipolar coupling has been described by Förster, [31]

$$k_{DA} = \frac{\kappa^2 k_r^D}{n^4 R^6} \cdot 8.8x10^{17} \int \frac{\varepsilon_A(\bar{\nu}) f_D(\bar{\nu})}{\bar{\nu}^4} d\bar{\nu} = \frac{\kappa^2 k_r^D}{n^4} \left(\frac{R_0}{R} \right)^6 \qquad 3.1$$

where k_{DA} is the rate constant for the transfer of energy between donor and acceptor. The κ term is a function of the relative orientation of the donor and acceptor transition dipole moments, and for our experimental conditions, $\langle \kappa^2 \rangle = 2/3$. The term k_r^D is the donor radiative decay rate constant in the absence of optical acceptor, n is the refractive index and R is the intermolecular D-A distance. The integral term is a measure of the spectral overlap between the emission spectrum of the optical donor and the absorption spectrum of the acceptor. The spectral overlap term, combined with the several constants on the right hand side of Eq. 3.1 is typically referred to as the critical radius, R_0, a quantity which serves as an effective gauge of the operating distance of this dipolar coupling process. While the term R_0 will vary for each donor-acceptor pair, for most organic chromophore pairs, $R_0 \sim 50$ Å. [22,23,31,32]

We have used the optical donor perylene and two different acceptor molecules, DSF (anionic) and R110 (cationic). The acceptor molecules were chosen because of their ionic charge and their absorption spectral profiles, which overlap significantly with the emission spectrum of perylene (Figure 3.3). Based

Fig
per

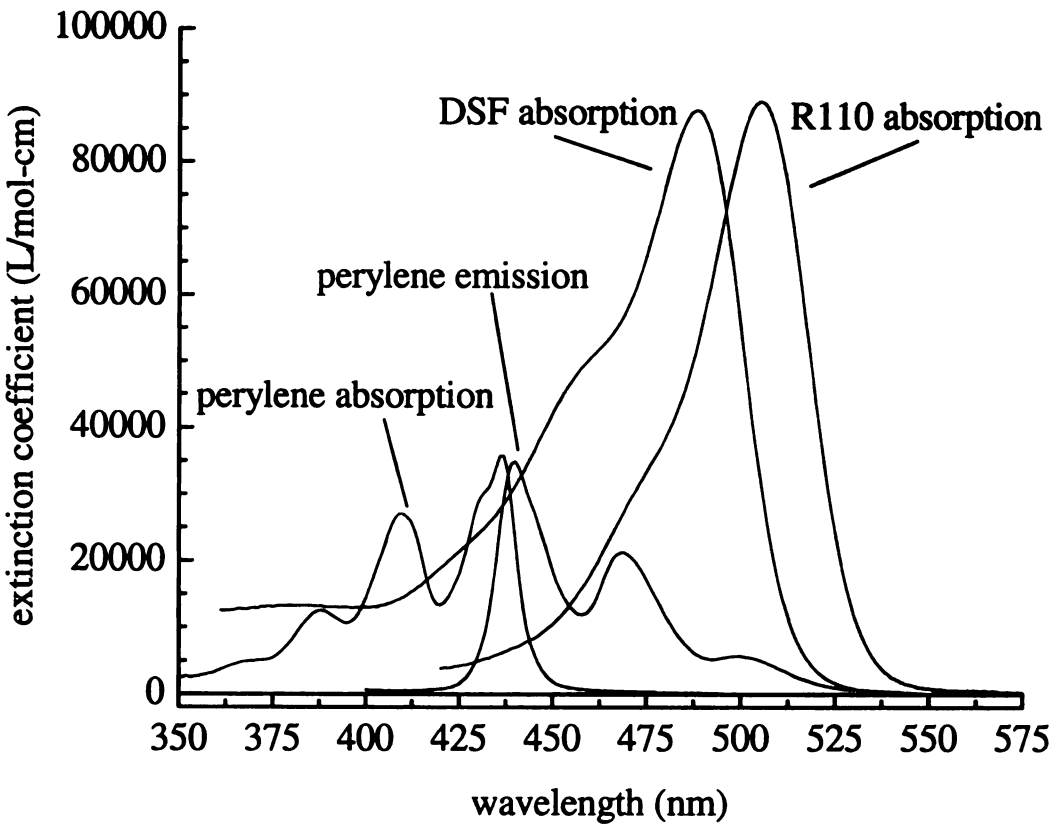

Figure 3.3 - Normalized absorption and spontaneous emission spectra of perylene, and absorption spectra of DSF and R110.

on the spectral overlap, and the extinction and fluorescence quantum yield data on these molecules, we estimate R_0 ~ 54 Å for the perylene/DSF pair and R_0 ~ 51 Å for the perylene/R110 pair. We excite perylene at 420 nm and measure its fluorescence lifetime at ca. 470 nm, without interference from acceptor emission. The measurement of donor lifetime as a function of acceptor concentration is a direct means of evaluating variations in k_{DA}, since this rate constant will operate in an additive manner with the intramolecular decay rate constant(s) that govern the depopulation of the donor excited state. Since the concentration of perylene is held constant at 10^{-5} M, the amount of energy transfer between two donor molecules should be negligible because of the small fraction of micelles that contain a perylene molecule. Even if this process were significant, it would appear as a depolarization of the perylene fluorescence, but not a diminution of its lifetime. [33]

We consider first the interactions between (anionic) DSF in solution and perylene in (anionic) SDS micelles. As shown in Table 3.1, the fluorescence lifetime of perylene decreases with increasing DSF solution concentration. This is an expected result. In addition to the decrease in fluorescence lifetime, the increasing concentration also affects the functionality of the perylene decay. For 10^{-3} M DSF, we observe a two-component perylene fluorescence lifetime. We understand this behavior in the context of interactions between the acceptor chromophore and the micelle, and will return to a discussion of this point after we consider the analogous data for other systems.

Acceptor	Concentration	τ_{fl1} (ps)	τ_{fl2} (ps)
-	-	5696 ± 1	--
DSF	10^{-5}	5491 ± 1	
DSF	10^{-4}	5278 ± 1	
DSF	10^{-3}	888 ± 10	4362 ± 3
R110	10^{-5}	5468 ± 2	
R110	10^{-4}	5197 ± 12	
R110	10^{-3}	953 ± 4	4749± 4

Table 3.1 - Fluorescence lifetime data for perylene sequestered in SDS micelles as a function of optical acceptor concentration. The data reported here are the averages of 6 independent determinations, and the uncertainties reported are ± 1σ.

We compare these data to those for perylene in SDS micelles and (cationic) R110 in solution. These results are qualitatively the same as for the perylene/SDS/DSF system, including the onset of a two-component perylene fluorescence lifetime for 10^{-3} M R110 acceptor. If simple ionic interactions were responsible for these data, we would expect a substantial difference the perylene lifetime with these two acceptors. The similarity of the perylene lifetimes in the presence of either acceptor points to the significant role that counter ions must play in mediating interactions between charged species at the micelle surface.

We have also studied perylene in (cationic) CTAB micelles, in the presence of the two acceptor chromophores. For the solutions containing DSF, the perylene lifetime exhibits qualitatively the same acceptor concentration-dependence as is seen in SDS. For acceptor concentrations less than 10^{-3} M we observe the expected acceptor concentration-dependent single exponential decay, and for 10^{-3} M acceptor we observe a two-component decay. For R110 in solution and perylene in CTAB, we recover essentially the same results as for the other systems, save for 10^{-3} M R110, where two different double exponential lifetimes are observed (Table 3.2). The fact that two different decay functionalities can be obtained reproducibly and interchangeably suggest that we are near some phase transition for this system. In both cases a double exponential is observed, consistent with two different environments for the perylene, but the lifetime data in and of themselves are not sufficient to provide any structural detail on these environments. We consider the result for 10^{-3} M R110 with perylene in CTAB to be a variant of the results we have obtained for

Acceptor	Concentration	τ_{fl1} (ps)	τ_{fl2} (ps)
-	-	5529 ± 1	
DSF	10^{-5}	5374 ± 1	
DSF	10^{-4}	5096 ± 1	
DSF	10^{-3}	701 ± 4	3877 ± 3
R110	10^{-5}	5470 ± 1	
R110	10^{-4}	5243 ± 1	
R110	10^{-3}	1315 ± 25 2040 ± 11	3936 ± 7 5827 ± 16

Table 3.2. Fluorescence lifetime data for perylene sequestered in CTAB micelles as a function of optical acceptor concentration. The data reported here are the averages of 4 independent determinations, and the uncertainties reported are ± 1σ.

the other systems. Overall, the similarity of these excitation transport data for cationic and anionic micelles, and cationic and anionic acceptors points to the significant screening role that counter-ions must play in determining the properties of the palisades region of the micelle/solvent interface.

In addition to qualitative insight into excitation transport between the interior and exterior region of the micelles, these lifetime data can also provide quantitative insight into the interfacial region. We consider that acceptors form a complex with the micelle. In this picture, the acceptors are either in very close spatial proximity to the donor when complexed, or too far distant to transfer energy efficiently when free. This is, of course, an oversimplification, but it allows for the ready use of the Förster equation in the estimation of association constants for these systems.

It is first important to consider the approximate stoichiometry of the donor, acceptor and micelles in our solutions. As noted above, the perylene donor concentration is such that there is one donor per ~100 micelles. As we increase the acceptor concentration from 10^{-5} M to 10^{-3} M, the acceptor-to-micelle stoichiometry changes from one acceptor per ~ 100 micelles to ~ 4 acceptors per micelle for SDS. We base this estimate on the micelle concentration being

$$[micelle] \sim \frac{n * CMC}{\text{surfactant molecules per micelle}} \qquad 3.2$$

Where n is the number of CMC concentrations we use (n=2 here) for SDS (CMC = 8.5 mM), there are ~63 surfactant molecules per micelle, and for CTAB (CMC =

0.8 mM) there are ~90 molecules per micelle.[34,35] This estimate yields [micelle]~ 0.27 mM for SDS and 0.02 mM for CTAB.

Because of the perylene:micelle ratio of 1:100, for a 10^{-5} M acceptor concentration, there is one acceptor per ~100 micelles, so only 0.01% of the micelles will have both a donor sequestered within and an acceptor complexed to them. Under these conditions, there will be essentially no donor-containing micelles that are complexed to more than one acceptor. We can thus approximate safely that for low acceptor concentrations, the equilibrium process we monitor with our donor lifetime measurements corresponds to interactions between single donors and single acceptors. For 10^{-3} M acceptor concentrations, the situation is fundamentally different. There are ~4 acceptor molecules per micelle, making the association between micelles and multiple acceptors the dominant interaction, and this situation is manifested by the change in the donor decay functionality from single exponential to double exponential.

Before considering the information content of these data, we need to evaluate the sizes of the micelles under investigation. The cryo-TEM data on our micelles (Figure 3.2) indicate that the micelles are in the sub-10 nm range, but we are not able to extract precise average diameters. It is important to consider that these micelles have experienced vitrification, so it is not unreasonable to expect that there has been some structural perturbation prior to acquisition of the images. The larger point of these images is that we do indeed have nanoscale micelles present in our solutions, and with their existence established, we will use

the more precise estimates of micelle size that have been reported elsewhere. Specifically, the radius of SDS is taken to be 19 Å and the radius of CTAB is taken to be 25 Å for the purposes of the calculations we present below.[36,37]

We assert that the lifetimes that we measure are actually weighted averages of the fluorescence lifetime of perylene in micelles complexed with one acceptor and the lifetime of perylene in an uncomplexed micelle. We take the experimentally determined fluorescence lifetime as the weighted average of the free form $\tau_{free} = (k_r^D)^{-1}$ and the complexed form, where $\tau_{cplx} = (k_r^D + k_{DA})^{-1}$, with k_{DA} being calculated for R =21 Å (SDS) or R =25 Å (CTAB) and R_0 as given above.

$$\tau_{obs} = n_{free}\tau_{free} + n_{cplx}\tau_{cplx}$$
$$n_{free} = \frac{[M]}{[M]+[MA]}, \qquad n_{cplx} = \frac{[MA]}{[M]+[MA]} \tag{3.3}$$

From these calculations, we recover the fractional contributions from the free and complexed forms of the perylene-containing micelles. For the acceptor association with the micelles, the relevant equilibrium process is:

$$M + A \underset{}{\overset{K}{\rightleftharpoons}} MA \qquad K = \frac{[MA]}{[M][A]} = \frac{n_{cplx}}{n_{free}[A]} \tag{4}$$

We know [M] and [A] from solution composition, and determine the ratio of [MA]/[M] experimentally from the lifetime measurements. We determine the quantities n_{free} and n_{cplx} (Eq. 3.3), and use them to calculate K. We estimate the equilibrium constants for the donor/acceptor systems in both of the micellar solutions (Table 3.3). We find that for either acceptor present at 10^{-5} M in SDS micelles, K ~ 2000 M^{-1}, and in CTAB micelles, K ~ 1300 M^{-1} under these same conditions.

Micelle	Acceptor	Concentration	K_{eq}	n_{free}	n_{cplx}
SDS	DSF	10^{-5}	1833	0.982	0.018
SDS	DSF	10^{-4}	395	0.962	0.038
SDS	R110	10^{-5}	2040	0.980	0.020
SDS	R110	10^{-4}	482	0.954	0.046
CTAB	DSF	10^{-5}	1420	0.986	0.014
CTAB	DSF	10^{-4}	428	0.959	0.041
CTAB	R110	10^{-5}	1215	0.988	0.012
CTAB	R110	10^{-4}	277	0.973	0.027

Table 3.3 - Equilibrium constant calculations for DSF and R110 in SDS and CTAB.

If this same treatment is applied to solutions containing 10^{-4} M DSF and R110, we obtain values of K in the range of 250 M^{-1} to 500 M^{-1}, depending on the system. We do not believe the formation constant(s) for the 10^{-4} M acceptor solutions to be different than those for the 10^{-5} M solutions. Rather, we view the value of K ~ 250 – 500 M^{-1} as the overall equilibrium constant for multiple equilibrium processes. For a multiple equilibrium process,

$$M + A \underset{}{\overset{K_1}{\rightleftharpoons}} MA + A \underset{}{\overset{K_2}{\rightleftharpoons}} MA_2 \qquad K = K_1 K_2 \tag{5}$$

From the experiments with 10^{-5} M acceptor, K_1 ~ 2000, and for the 10^{-4} M acceptor solutions, K_1K_2 ~ 400, leading to a value of K_2 ~ 0.2, its exact value depending on the system. While it is normal for the equilibrium constants to diminish monotonically with the addition of complexing species, the difference between K_1 and K_2 for acceptor/micelle complexation is substantial. It is possible that the size of the acceptors and facile translational motion of the acceptor on the micelle "surface" give rise to a significant contribution from steric effects for the association of multiple acceptors with a given micelle.

The Fayer group's elegant work on excitation transport in micellar media has shown that a Green's function describes the donor population decay dynamics. [9,24,32,33,38,39] It is fair to question whether the data we report here are characterized better by a Green's function or a simple sum of exponentials. We have attempted to fit our data to the appropriate Green's function, and find that a sum of exponentials accounts most accurately for the decay functionality of our systems. This finding indicates that the observed decay is most likely the result of two different perylene populations, *i.e.* those where one acceptor is associated

with the micelle, and one where two acceptors are associated with the micelle. This finding is consistent with multiple micelle-acceptor association equilibria contributing to our experimental findings at high acceptor concentrations. We base this assertion on the comparatively abrupt change in functionality between one and two component decays. To evaluate the possibilities of either a phase transition for these micelles at high acceptor concentrations, or potential changes in organization within the micelles, we have investigated the motional freedom of the perylene molecule sequestered within the micelles as a function of acceptor concentration.

Despite any subtle differences in detail, it is important to note the overall similarity of the results for both micelles, and for both anionic and cationic chromophores. These data demonstrate clearly that it is not direct ionic interactions that dominate in these systems. Rather, the mediating effect that the solution phase counterions play in the interactions between micelles and other moieties in solution dominates the observed behavior.

Rotational diffusion within the micelles. To understand the influence of the acceptor molecules on the motional freedom of the sequestered donor, we have studied the rotational diffusion dynamics of perylene within the micelles as a function of acceptor concentration and micelle identity. Rotational diffusion has been used extensively to interrogate local organization in solutions, because of the well developed theoretical framework for interpretation of the data and the relatively high information content of the experimental signals. [40-44] Our data indicate that the two acceptor molecules influence donor motion differently.

We obtain fluorescence depolarization data by exciting perylene with a vertically polarized light pulse and collecting the emission decay transients polarized parallel and perpendicular to the excitation polarization. These data are combined to produce the induced orientational anisotropy function, R(t),

$$R(t) = \frac{I_{\parallel}(t) - I_{\perp}(t)}{I_{\parallel}(t) + 2I_{\perp}(t)} \qquad (2)$$

where $I_{\parallel}(t)$ and $I_{\perp}(t)$ are the polarized emission intensities. The chemical information contained in these data lies in the decay time constant(s) of R(t), and its zero-time value.

Before discussing these data further, we note that donor-donor excitation transport can give rise to fluorescence depolarization[33], the same physical phenomenon that we use to characterize the molecular motion of perylene sequestered within micelles. The D-A excitation transport data (*vide supra*) point to modest donor-acceptor excitation transport, and given the low perylene concentrations used (~1 perylene per 100 micelles), we believe that fluorescence depolarization resulting from donor-donor transport does not contribute measurably to our data.

Because we are studying heterogeneous systems, it is fair to consider which model is most appropriate for the treatment of the anisotropy data. For chromophores tethered to a substantially larger entity, such as a protein, or imbedded in a mono- or bilayer structure, the hindered rotor model is appropriate.[3,45] In this model the chromophore is bound at one point within the system and its motion is considered in the context of the conic volume it sweeps out. For the micellar systems we are concerned with here, the hindered rotor

model is not appropriate because the chromophore is not bound to a specific point in or on the micelle. Rather, perylene is free to diffuse within the micelle, and we treat this system in the context of perylene reorienting in a quasi-bulk solvent. The model most appropriate for this type of system is the modified Debye-Stokes-Einstein (DSE) equation, [46] which is described in more detail in chapter 1 (equation 1.3).

For perylene the hydrodynamic volume is 225 $Å^3$,[47] T = 300 K, $S = 0.69$ (prolate rotor based on single exponential decay). [48,49] We note that our experimental anisotropy data are all single exponential decays, allowing us to conclude that perylene reorients as a prolate rotor in the micelles we have studied. Perylene has been shown previously to reorient either as a prolate rotor (single exponential anisotropy decay) or as an oblate rotor (double exponential anisotropy decay), depending on its environment. [49,50] While it may seem plausible to invoke a slip boundary condition for our experimental conditions, experimental data for perylene in *n*-alkanes are consistent with behavior intermediate between the stick and slip limits. From the modified DSE model, in the stick limit we calculate the quantity $\tau_{or}/\eta = 78$ ps/cP, and in the slip limit we calculate $\tau_{or}/\eta = 5.8$ ps/cP. Experimentally we know from earlier work on perylene in *n*-alkanes longer than C_8, $\tau_{or}/\eta = 12.7 \pm 1.5$ ps/cP, intermediate between the stick and slip limit, and we use this experimental value to estimate the viscosity of the micellar media.[48-52] For perylene in SDS micelles, in the

Acceptor	Concentration	τ_{OR}	η (cP)
-	-	62 ± 3	4.9 ± 0.9
DSF	10^{-5}	95 ± 3	7.5 ± 1.3
DSF	10^{-4}	127 ± 2	10.0 ± 0.9
DSF	10^{-3}	128 ± 4	10.1 ± 1.7
R110	10^{-5}	123 ± 5	9.7 ± 1.6
R110	10^{-4}	116 ± 3	9.1 ± 1.5
R110	10^{-3}	86 ± 2	6.8 ± 1.1

Table 3.4. Rotational diffusion time constants of perylene sequestered in SDS micelles as a function of optical acceptor concentration. The data reported here are the averages of 6 independent determinations, and the uncertainties reported are ± 1σ.

absence of acceptor chromophores in solution, we estimate the viscosity within the micelle to be $\eta = 4.9 \pm 0.9$ cP, and with the addition of anionic DSF acceptor, the viscosity of the interior of the micelle varies monotonically between 7.5 cP and 10.1 cP (Table 3.4). The viscosity of the aliphatic medium within the micelles is substantially higher than the corresponding length *n*-alkane (~ 3.5 cP). Some of this "excess" viscosity is likely due to the geometric constraints imposed by the micellar structure itself. The increase in apparent viscosity with the addition of acceptor suggests that the solution phase ionic species interact with the micelle in such a way at to make the interior of the micelle less fluid. This finding is consistent with either strong micelle-acceptor interactions mediating the exchange of amphiphiles between solution and micelle, or a change in the lateral mobility of the amphiphiles within the micellar structure. For the case of an anionic acceptor (DSF) and anionic micelle head groups (SDS), we observe an increase in the apparent micelle viscosity with the addition of acceptor, and a plateau effect for 10^{-4} and 10^{-3} M acceptor concentrations. For the perylene in SDS micelles, with the cationic R110 acceptor, we observe a different trend (Table 3.4, Figure 3.4a). As the concentration of R110 is increased from 10^{-5} M to 10^{-3} M, the micelle interior viscosity decreases from 9.7 cP to 6.8 cP. This trend in micelle viscosity is opposite that seen for the anionic acceptor, pointing to a structural role for charge-dependent interactions between the micelle head groups and the solution phase acceptor.

Acceptor	Concentration	τ_{OR}	η (cP)
-	-	100 ± 5	7.9 ± 1.5
DSF	10^{-5}	50 ± 1	3.9 ± 0.7
DSF	10^{-4}	153 ± 3	12.0 ± 1.9
DSF	10^{-3}	84 ± 7	6.6 ± 1.5
R110	10^{-5}	147 ± 7	11.6 ± 2.2
R110	10^{-4}	116 ± 3	9.0 ± 1.6
R110	10^{-3}	180 ± 2	14.2 ± 2.1

Table 3.5. Rotational diffusion time constants of perylene sequestered in CTAB micelles as a function of optical acceptor concentration. The data reported here are the averages of 4 independent determinations, and the uncertainties reported are ± 1σ.

For cationic micelles, we do not observe analogous monotonic trends with increasing donor or acceptor concentration (Figure 3.4). For the native CTAB micelle, in the absence of any optical acceptor, we recover a viscosity of 7.9 cP for the micelle interior (Table 3.4). As anionic DSF acceptor is added to the micelle-containing solution, the micelle interior viscosity ranges from 3.9 cP to 12.0 cP, but this trend does not vary linearly with acceptor concentration. With the addition of the cationic acceptor R110, the micelle interior viscosity varies between 9.0 cP and 14.2 cP, but again, this trend is not monotonic with increasing acceptor concentration (Table 3.5, Figure 3.4). In these experiments, we observe significant variations in the apparent viscosity of the micellar environment with changes in solution phase acceptor concentration. This situation could be the result of a number of phenomena, but it is significant that the trends we observe are not monotonic. If these data were accounted for in the context of variations in a system property such as ionic strength, we would expect monotonic trends in the reorientation and lifetime data. In fact, the reorientation data do not correlate with the fluorescence lifetime data, and the addition of the cationic R110 acceptor causes anomalous, non-monotonic behavior in both cationic and anionic micelles. Given that the reorientation dynamics of perylene within the micelles depend primarily on the viscosity of the

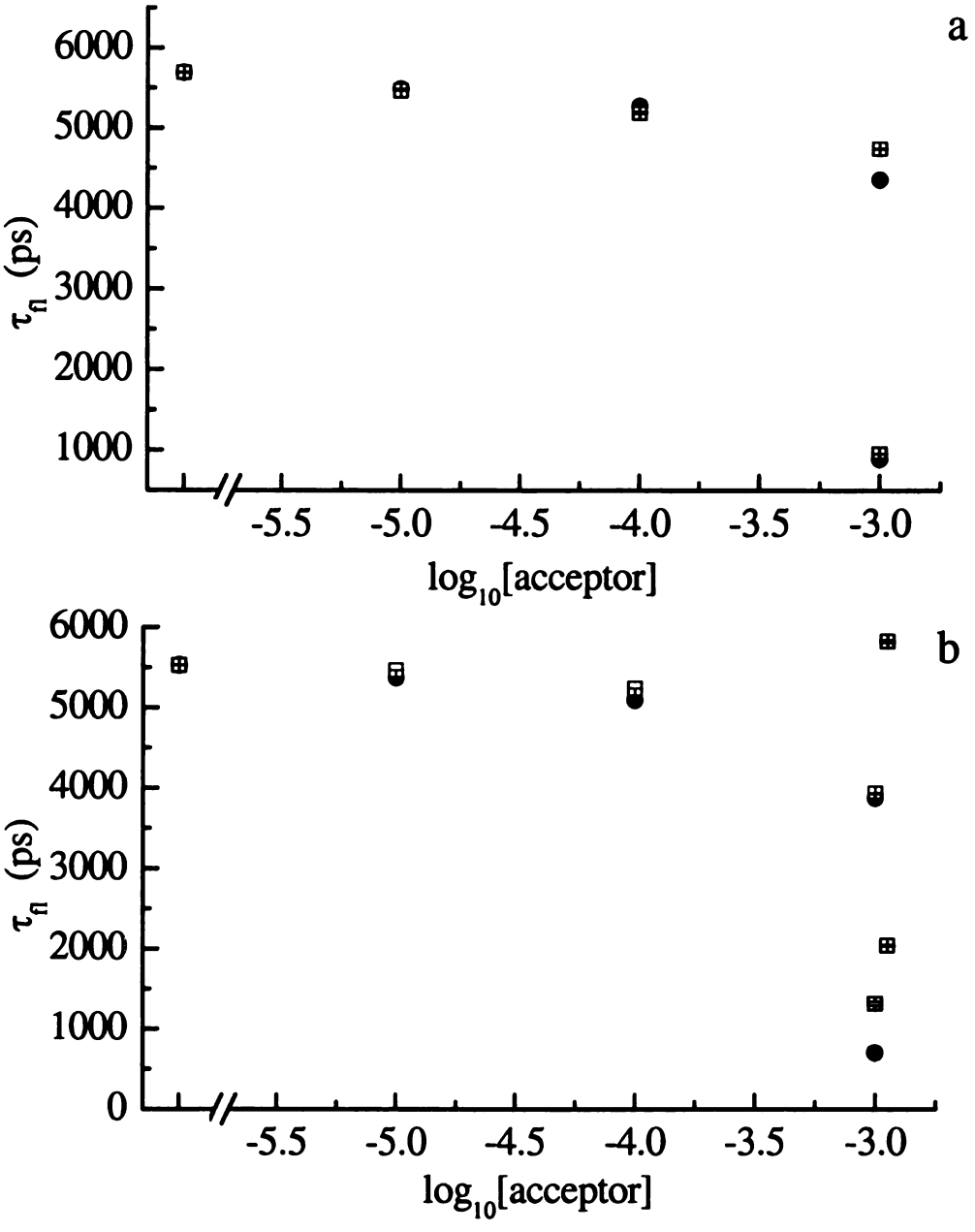

Figure 3.4 - Fluorescence lifetimes of perylene sequestered in micelles as a function of optcal acceptor concentration. (a) SDS micelles, • = DSF, ⊞ = R110. (b) CTAB micelles, • = DSF, ⊞ = R110.

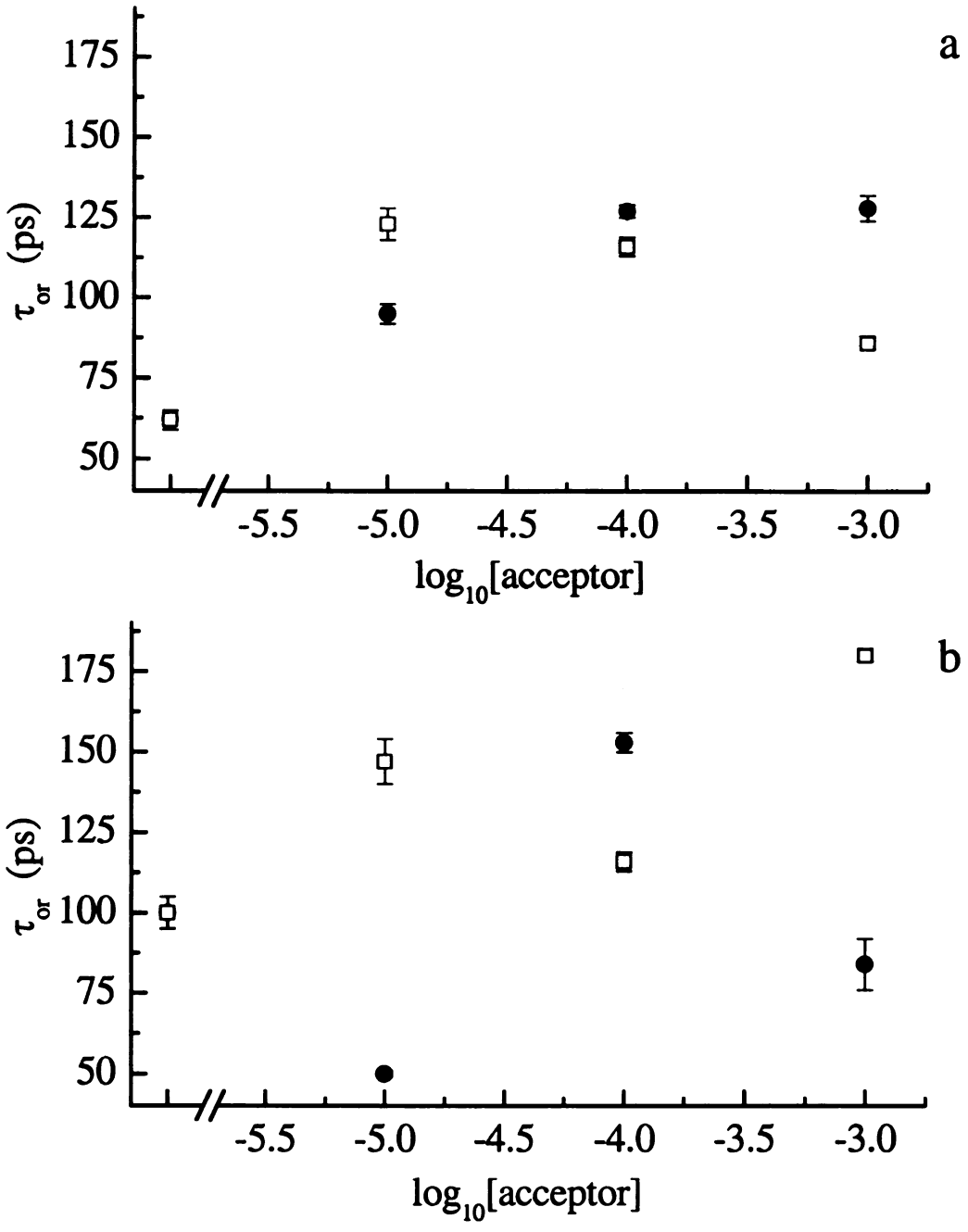

Figure 3.5 - Rotational diffusion time constants of perylene sequestered in micelles as a function of optcal acceptor concentration. (a) SDS micelles, • = DSF, = R110. (b) CTAB micelles, • = DSF, = R110.

micelle interior, our findings suggest a micelle structural rearrangement occurs with the addition of R110. This rearrangement could either be structural, such as a transformation from a spherical micelle to some other shape or attachment of multiple R110 molecules to the micelle, or it could be compositional. We have added a small amount of butanol cosolvent to the system, approximately 20% by volume, to dissolve the perylene chromophore and thereby allow its incorporation into the micelles. If the presence of butanol plays a role in the structure of the micelle, the addition of acceptor molecules would alter the ionic strength of the micelle-containing solution, thus changing the extent to which the butanol cosolvent would partition into the micelles. Such an effect would scale with the solution ionic strength, and thus a monotonic change in τ_{or} would be expected, and that trend should be qualitatively the same for both acceptor chromophores.

The fact that the reorientation dynamics of perylene vary with the presence of the two acceptors suggests an energetically significant interaction between the acceptors and some constituent(s) of the micelles. This finding is consistent with the substantial first association constants we measure for micelle-acceptor interactions. The amphiphiles SDS and CTAB may undergo hydrogen bonding with the solvent, but their ionic charge would likely cause them to be in close association with their counter ions. The acceptor chromophores could, in principle, participate in hydrogen bonding with butanol, and such an interaction would be different for the two acceptors. Any interaction such as this, however, should scale linearly with acceptor concentration (at least to the point of

saturation), and this expectation is counter to the experimental data we have for R110. We are thus in need of acquiring further information to understand the perylene/acceptor/CTAB data fully, but there is a substantial literature on the modification of micelle properties with *n*-alkanols, the usual result being a reduction in the viscosity of the micelle with increasing alkanol concentration.[48] It is possible that the presence of butanol in the solution and/or micelles gives rise to structural variations akin to a phase transition within the micelle, and this is a point which will require further investigation to resolve.

Regardless of the details of the interactions responsible for the anomalous reorientation of perylene in CTAB micelles, we find in all cases that the observed viscosity within the micelles is significantly higher than that of the corresponding length alkane solvent. The microviscosities of micellar environments have been investigated before, and our values are fully consistent with other literature reports. [53-55] The fact that the viscosity within micelles is higher than that seen for the corresponding alkane, and more on a par with that seen for the corresponding *n*-alkanol, underscores the role that the solution-head group interactions in the palisades layer region play in mediating the behavior of the hydrophobic micelle inner region. For bulk liquid phase alkanols, hydrogen bonding between the hydroxyl groups functions in concert with van der Waals interactions of the aliphatic tails to determine the viscosity of the medium. In the case of micelles, the palisades layer must be sufficiently charge compensating to prevent repulsive Coulombic forces from interfering with micelle formation. This balance of ionic and H-bonding forces in the palisades layer will function in

concert with van der Waals forces within the micelle interior to yield a relatively viscous environment. The alteration of the ionic strength of the solution will change the balance of forces that operate within the palisades layer and, depending on the details of the interactions, the micelle structure may be altered as a result.

Conclusions

We have studied the fluorescence lifetime and reorientation dynamics of perylene in the aqueous micellar systems SDS and CTAB in the presence of varying concentrations of cationic (R110) and anionic (DSF) optical acceptor molecules. The decrease in the lifetime of perylene in the presence of the acceptors is fully consistent with dipolar excitation transport and from these data we can infer the association constant(s) for micelle-acceptor interactions. Comparing data for cationic and anionic micelles and both cationic and anionic acceptors, we find that direct ionic interactions play little role in our data. In homogeneous solutions, the average intermolecular distance is such that excitation transport would be expected not to play a significant role, and our observation of this effect in micellar solutions is an indication of interactions between the charged optical acceptors and the palisades layer of the micelles. The similarity of the behavior seen for all micelle/acceptor combinations points to the important role that spectator ion charge compensation plays in micelle formation and dynamics.

Rotational diffusion measurements of perylene sequestered within SDS and CTAB micelles show that the viscosities within these confined environments is higher than that of the corresponding alkane, and closer to that of the corresponding length alkanol. This result is fully consistent with the literature and chemical intuition, underscoring the balance of forces between ionic/polar interactions within the palisades layer and van der Waals interactions within the

micelle interior. This balance of forces is sensitive to the composition of the aqueous solution phase and the addition of optical acceptors to the micelle solutions alters the balance of forces at the solution/micelle interface to the extent of substantially altering the internal microviscosity of the micelles. Clearly there is also a role played by the presence of *n*-butanol, a cosolvent used to allow the introduction of perylene into the micellar solutions, and such effects have been seen for similar *n*-alkanol additives previously. [48] Future investigations will focus on the detailed reasons for the non-monotonic variation in micelle microviscosity with increasing optical acceptor concentration. We anticipate that the microscopic variations in micelle structure that result from the balance between polar and dispersive forces in these systems will account for our findings.

Literature Cited

(1) DelaCruz, J. L.; Blanchard, G. J. *Journal of Physical Chemistry B* **2003**, *107*, 7102.

(2) Dutt, G. B. *Journal of Physical Chemistry B* **2002**, *106*, 7398.

(3) Kelepouris, L.; Blanchard, G. J. *Journal of Physical Chemistry B* **2002**, *106*, 6600.

(4) Kelepouris, L.; Blanchard, G. J. *Journal of Physical Chemistry B* **2003**, *107*, 1079.

(5) Klein, U. K. A.; Haar, H. P. *Chemical Physics Letters* **1978**, *58*, 531.

(6) Maiti, N. C.; Krishna, M. M. G.; Britto, P. J.; Periasamy, N. *Journal of Physical Chemistry B* **1997**, *101*, 11051.

(7) Maiti, N. C.; Mazumdar, S.; Periasamy, N. *Journal of Physical Chemistry* **1995**, *99*, 10708.

(8) Menger, F. M. *Accounts of Chemical Research* **1979**, *12*, 111.

(9) Quitevis, E. L.; Marcus, A. H.; Fayer, M. D. *Journal of Physical Chemistry* **1993**, *97*, 5762.

(10) Rao, U. R. K.; Manohar, C.; Valaulikar, B. S.; Iyer, R. M. *Journal of Physical Chemistry* **1987**, *91*, 3286.

(11) Barzykin, A. V.; Tachiya, M. *Journal of Chemical Physics* **1995**, *102*, 3146.

(12) Choi, K. J.; Turkevich, L. A.; Loza, R. *Journal of Physical Chemistry* **1988**, *92*, 2248.

(13) de Oliveira, H. P. M.; Gehlen, M. H. *Chemical Physics* **2003**, *290*, 85.

(14) De, S.; Girigoswami, A.; Mandal, A. K. *Spectrochimica Acta, Part A: Molecular and Biomolecular Spectroscopy* **2003**, *59A*, 2487.

(15) Ediger, M. D.; Domingue, R. P.; Fayer, M. D. *Journal of Chemical Physics* **1984**, *80*, 1246.

(16) Kenney-Wallace, G. A.; Flint, J. H.; Wallace, S. C. *Chemical Physics Letters* **1975**, *32*, 71.

(17) Saha, D. C.; Ray, K.; Misra, T. N. *Spectrochimica Acta, Part A: Molecular and Biomolecular Spectroscopy* **2000**, *56A*, 797.

(18) Wistrom, C. A.; Jones, G. M.; Tobias, P. S.; Sklar, L. A. *Biophysical Journal* **1996**, *70*, 988.

(19) Johansson, L. B. A.; Niemi, A. *Journal of Physical Chemistry* **1987**, *91*, 3020.

(20) Mattjus, P.; Molotkovsky, J. G.; Smaby, J. M.; Brown, R. E. *Analytical Biochemistry* **1999**, *268*, 297.

(21) Stryer, L. *Annual Review of Biochemistry* **1978**, *47*, 819.

(22) Birch, D. J. S.; Suhling, K.; Holmes, A. S.; Salthammer, T.; Imhof, R. E. *Pure and Applied Chemistry* **1993**, *65*, 1687.

(23) Ediger, M. D.; Fayer, M. D. *Journal of Chemical Physics* **1983**, *78*, 2518.

(24) Marcus, A. H.; Diachun, N. A.; Fayer, M. D. *Journal of Physical Chemistry* **1992**, *96*, 8930.

(25) DeWitt, L.; Blanchard, G. J.; LeGoff, E.; Benz, M. E.; Liao, J. H.; Kanatzidis, M. G. *Journal of the American Chemical Society* **1993**, *115*, 12158.

(26) Jha, B. K.; Patist, A.; Shah, D. O. *Langmuir* **1999**, *15*, 3042.

(27) Dela Cruz, J. L.; Blanchard, G. J. *Journal of Physical Chemistry A* **2001**, *105*, 9328.

(28) Berr, S. S.; Caponetti, E.; Johnson, J. S., Jr.; Jones, R. R. M.; Magid, L. J. *Journal of Physical Chemistry* **1986**, *90*, 5766.

(29) Berr, S. S.; Coleman, M. J.; Jones, R. R. M.; Johnson, J. S., Jr. *Journal of Physical Chemistry* **1986**, *90*, 6492.

(30) Berr, S. S. *Journal of Physical Chemistry* **1987**, *91*, 4760.

(31) Forster, T. *Ann. Physik.* **1948**, *2*, 55.

(32) Jones, G. M.; Wofsy, C.; Aurell, C.; Sklar, L. A. *Biophysical Journal* **1999**, *76*, 517.

(33) Keller, L.; Hussey, D. M.; Fayer, M. D. *Journal of Physical Chemistry* **1996**, *100*, 10257.

(34) Benrraou, M.; Bales, B. L.; Zana, R. *Journal of Physical Chemistry B* **2003**, *107*, 13432.

(35) Perche, T.; Auvray, X.; Petipas, C.; Anthore, R.; Rico, I.; Lattes, A.; Bellissent, M. C. *Journal de Physique I* **1992**, *2*, 923.

(36) Dutt, G. B. *Langmuir* **2005**, *21*, 10391.

(37) Wu, C.; Ma, R.; Zhou, B.; Shen, J.; Chan, K. K.; Woo, K. F. *Macromolecules* **1996**, *29*, 228.

(38) Finger, K. U.; Marcus, A. H.; Fayer, M. D. *Journal of Chemical Physics* **1994**, *100*, 271.

(39) Gochanour, C. R.; Fayer, M. D. *Journal of Physical Chemistry* **1981**, *85*, 1989.

(40) Chuang, T. J.; Eisenthal, K. B. *Journal of Chemical Physics* **1972**, *57*, 5094.

(41) Klein, U. K. A.; Haar, H. P. *Chemical Physics Letters* **1979**, *63*, 40.

(42) Labhart, H.; Pantke, E. R. *Chemical Physics Letters* **1973**, *23*, 482.

(43) Hu, C.-M.; Zwanzig, R. *Journal of Chemical Physics* **1974**, *60*, 4354.

(44) Youngren, G. K.; Acrivos, A. *Journal of Chemical Physics* **1975**, *63*, 3846.

(45) Lipari, G.; Szabo, A. *Biophysical Journal* **1980**, *30*, 489.

(46) Debye, P. Polar Molecules. In *Chemical Catalog Co.* New York, 1929.

(47) Edward, J. T. *Journal of Chemical Education* **1970**, *47*, 261.

(48) Goldie, S. N.; Blanchard, G. J. *Journal of Physical Chemistry A* **1999**, *103*, 999.

(49) Jiang, Y.; Blanchard, G. J. *Journal of Physical Chemistry* **1994**, *98*, 6436.

(50) Jiang, Y.; Blanchard, G. J. *Journal of Physical Chemistry* **1995**, *99*, 7904.

(51) Palma, S.; Manzo, R. H.; Allemandi, D.; Fratoni, L.; Lo Nostro, P. *Colloids and Surfaces, A: Physicochemical and Engineering Aspects* **2003**, *212*, 163.

(52) Zinsli, P. E. *Chemical Physics* **1977**, *20*, 299.

(53) Shinitzky, M.; Dianoux, A. C.; Gitler, C.; Weber, G. *Biochemistry* **1971**, *10*, 2106.

(54) Emert, J.; Behrens, C.; Goldenberg, M. *Journal of the American Chemical Society* **1979**, *101*, 771.

(55) Dutt, G. B. *Journal of Physical Chemistry B* **2004**, *108*, 3651.

Chapter 4

INVESTIGATING INTERNAL STRUCTURAL DIFFERENCES BETWEEN MICELLES AND UNILAMELLAR VESICLES OF DECANOIC ACID/SODIUM DECANOATE

Introduction

Micelles and bilayer vesicle structures bear a loose structural resemblance, but differ in fundamental ways in the details of their structure. Differences in the molecular organization of these structures are difficult to compare directly because, in most cases, the molecules used to construct these systems are different.

Micelles have been investigated extensively because they are capable of encapsulating compounds in solution and because of their ability to mimic biological systems. Properties such as micelle size, shape and permeability have been found to depend sensitively on amphiphile identity and concentration. A particularly useful tool for this work has been the interrogation of probe molecules by fluorescence spectroscopy, where the dynamics of the probe molecule have been related to system pressure, solvent viscosity, and the solubility of the probe.[1-18]

Unilamellar vesicle structures have found significance in immunological studies, understanding cellular membrane structure and function, and drug delivery. By far the most commonly used compounds for the formation of unilamellar vesicles are phospholipids, a family of natural compounds that are

the principal constituents of plasma membranes. Vesicle structures can also be formed by simpler amphiphilic compounds, such as octanoate, oleate and decanoate.[19-27] Decanoate micelles have been used for drug solubilization[12] and vesicles show potential for enzyme-catalyzed polymerizations.[28] These amphiphiles offer advantages over phospholipids, such as their dynamic behavior,[21,22,29-31] ability to grow upon addition of more fatty acid,[22,24,32] autocatalytic formation,[27,33] and structural simplicity, making them well suited to fundamental investigations aimed at understanding organization in these dynamic structures.

A further advantage that alkanoate amphiphiles offer is the ability to alter the system morphology through adjustment of the solution pH. Sodium decanoate solutions will form micelles at alkaline pH, provided the concentration is above the CMC, and will form bilayers (vesicular) structures at intermediate pH, provided the concentration is above the critical formation concentration,[28] analogous to the phase transition reported in the more extensively studied caprylic acid (octanoate) [20,23,27,34] or oleic acid[20,26,27,35] systems. The pH range for vesicle formation has been reported as 6.8 – 7.8, with solutions of higher pH existing in the micellar phase and solutions of lower pH resulting in phase separation, with the formation of a precipitate.[23,28] If these spontaneously assembled vesicles are extruded through a small-pore (100nm) filter, stable vesicles of comparatively well defined size can be generated.[19,32,36]

The fact that the same components form different structures allows for an important comparison to be made directly. This is an issue of fundamental

significance, not only because of the passing structural similarity of micelles and unilamellar vesicles, but because of the characteristic dimensions of these structures. Micelles are expected to have a diameter on the order of 5 nm, depending on the amphiphile used, while the unilamellar vesicles we use have diameters on the order of 100 nm. It is important to consider the different radii of curvature for the two types of structures and to understand from an experimental standpoint the implications of the curvature of these systems on the internal organization of the aliphatic regions. Indeed, the issue of curvature has been discussed extensively in the context of phospholipid bilayer structures, but we are not aware of any direct comparisons of internal organization and dynamics between micelles and unilamellar vesicles comprised of the same amphiphiles.

We have sequestered perylene inside the sodium decanoate micelles and unilamellar vesicles and have used fluorescence lifetime and anisotropy measurements to obtain information on how the local environments differ between these one and two layered systems. Perylene is a hydrophobic chromophore that has been studied extensively,[37-40] making it an excellent choice for sequestration in a micelle or vesicle structure. We have investigated the decanoate micelle and vesicle systems to understand whether or not there is a discernible difference in the local organization of the nonpolar regions of these structures. Our data show that these structures do indeed produce different local environments, with the unilamellar vesicle being of slightly lower effective viscosity than the micelle.

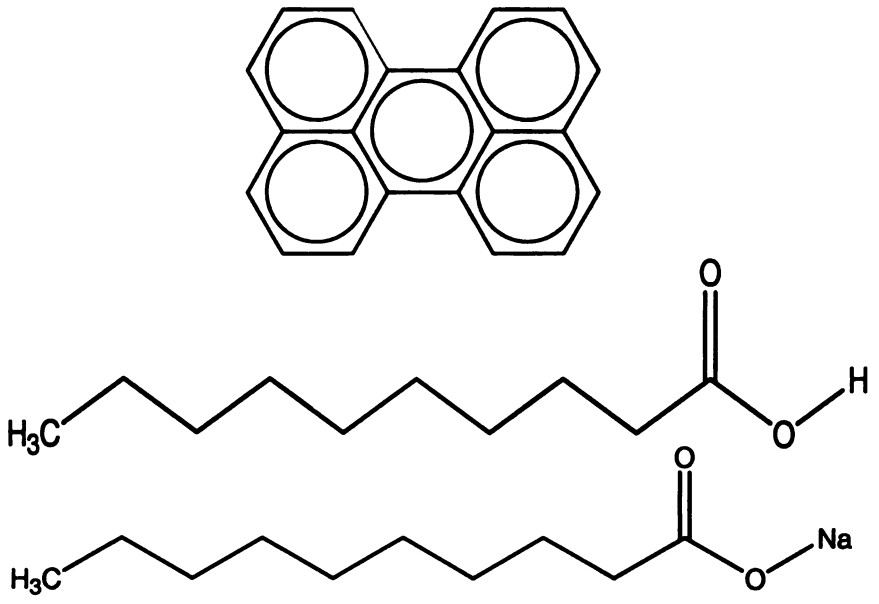

Figure 4.1 – The structures of perylene, sodium decanoate, and decanoic acid

Experimental Section

Materials. Decanoic acid sodium salt (sodium decanoate, 98%) was purchased from Fluka and used as received. Perylene was obtained from Sigma-Aldrich, Inc. and used as received. These chemical structures can be seen in Figure 4.1. Sodium phosphate, ethanol, and hydrochloric acid were purchased from Fisher. The perylene concentration for all solutions was 10 μM. For all decanoate solutions, perylene was first dissolved in an ethanol solution,(10^{-4} M) then added to the decanoate solutions for solubility reasons. Solution temperatures were maintained at 298 ±0.5 K (Neslab EX100-DD) for all time-resolved fluorescence measurements. Micelle solutions were maintained at a pH of ca. 9.3 (Orion Research digital ionanalyzer/501) using 150 mM phosphate buffer, while vesicle solutions were lowered to a pH of ca. 6.8 by adding 0.1 M HCl. All solutions were 100 mM in sodium decanoate, approximately twice the critical micelle[28,41] and critical bilayer[23,25,28] forming concentration.

Vesicle Formation. Vesicles were formed using the extrusion method.[42] First, the solutions containing decanoate at the appropriate pH were subjected to five freeze-thaw-vortex cycles. For each cycle the solution was immersed in liquid nitrogen for five minutes, thawed in a hot water bath ca. 60°C for five minutes, then vortexed for two minutes. The resulting solution was then passed through polycarbonate filters with 100 nm diameter pores eleven times using a Mini-Extruder system (Avanti Polar Lipids). The resulting unilamellar vesicles were used within two days of extrusion.

Time-Correlated Single Photon Counting Measurements. Fluorescence lifetime and anisotropy measurements of perylene in decanoate micelles and decanoic acid/decanoate vesicles were made using a time-correlated single photon counting (TCSPC) instrument that has been described in detail previously.[43] The instrument description can be seen in Chapter 1. For the experiments performed in this chapter, the excitation wavelength was set to 420 nm while the emission was collected at 470 nm.

Steady-State Spectroscopy. Absorption spectra were recorded using a Cary model 300 double-beam UV-visible absorption spectrometer, with 1 nm spectral resolution. Spontaneous emission spectra were acquired with a Spex Fluorolog 3 spectrometer, with both excitation and emission monochromators set to 3 nm resolution.

TEM Imaging. Unilamellar vesicle samples were stained with uranyl acetate. A 5 μL drop was placed on formvar and carbon coated grids, allowed to sit for several minutes, and the excess was removed with a filter paper. The microscope was a JEOL 100CX (Japan) operated at an accelerating voltage of 100 kV. A representative image of decanoate vesicles is shown in Figure 4.2a.

Cryo-TEM imaging. Cryogenic TEM images were acquired on our micelle samples by Dow-Corning Analytical Solutions, Auburn Hills, MI. To prepare the samples, ca. 2.3 mL of the micelle-containing solution was loaded on a holey carbon film coated Cu TEM grid using a micropipette. The excess fluid on the grid surface was removed by blotting the surface with a filter paper make an aqueous thin film for the TEM. The grid was immersed in liquid ethane contained

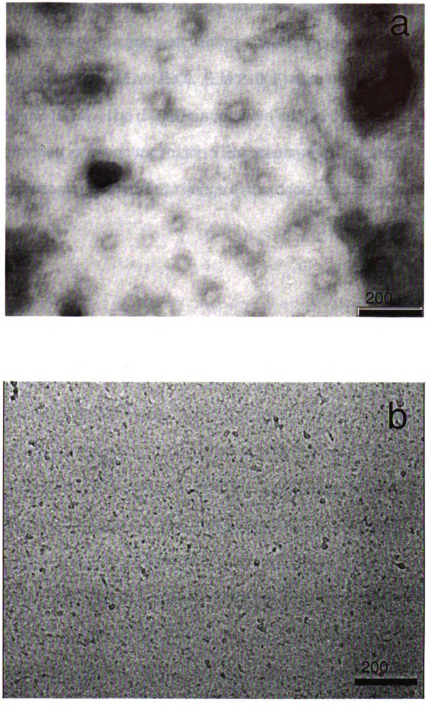

Figure 4.2 – (a) TEM image of decanoic acid/decanoate unilamellar vesicles. The average size is ca. 100 nm diameter. (b) Cryo-TEM image of decanoate micelles indicating a characteristic diameter of ca. 10 nm.

in a small vessel that itself was housed in a larger liquid nitrogen vessel. The water film on the grid was vitrified to avoid water crystallization. The sample was loaded into the TEM (JEOL JEM 2100F) and the morphology was observed below 104 K. The digital images were acquired using a Gatan CCD camera attached at the bottom of the TEM column and Digital Micrograph software. A representative cryo-TEM image of the decanoate micelle is shown in Figure 4.2b.

Results and Discussion

The objective of this work is to better understand the differences between the nonpolar regions of micelles and vesicles. Although micelles and vesicles bear some structural resemblance, there are issues of curvature and the characteristic length scale of any organization within these structures. To this point, our ability to address these issues has been limited by the systems that are capable of forming both types of structures. A recent report by Namani and Walde has shown the decanoic acid/sodium decanoate system to be capable of forming either micelles or unilamellar vesicles, depending on solution properties such as pH. They have reported that the pH range for vesicle formation in this system is 6.4 to 7.8.[28] The bilayer phase is stable when the pH of the system is similar to the pK_a of the acid (decanoic acid pK_a ~ 4.83),[44] due to hydrogen bonding interactions between the protonated and deprotonated acid head groups.[22,24,27,35] The difference between the pK_a of the acid and the actual pH at which bilyer formation occurs has been discussed before,[19,26,28,35,45,46] and deals with the variations between the pH of a polyanionic surface and the pH of the bulk solution. Because both the micellar and vesicular systems are composed of the same alkanoic acid, we can compare the dynamics of the perylene molecule sequestered within each of these structural entities directly. The difference between the lifetime and reorientation of the sequestered chromophore in the micelle and vesicle structures will provide insight into the structural differences in the aliphatic regions of these two structural forms. We consider the fluorescence lifetime data first, to provide general information on the local environment(s) of

the perylene chromophores, then consider the fluorescence anisotropy data in detail.

Fluorescence lifetime data. Fluorescence lifetime measurements of perylene are useful in providing a qualitative picture of the local environment. Perylene is less sensitive to either environmental polarity or the presence of quenchers than some other polycyclic aromatic hydrocarbons (*e.g.* pyrene),[47] but the information obtained from the data we report here on perylene still indicates that the environments formed within the micelles and vesicles of decanoic acid/decanoate are discernibly different. We recover a perylene fluorescence lifetime of 5815 ns for the chromophore in decanoate/decanoic acid micelles, and 5942 ns for the chromophore in decanoate/decanoic acid unilamellar vesicles. We note that for both systems we recover a single exponential decay population decay, indicating rapid exchange between the distribution of environments that are characteristic of each medium. The fact that the fluorescence lifetime is shorter in the micelle than in the vesicle suggests that the environment in the micelle is slightly more polar. This situation could result either from perturbations to the micelle associated with amphiphile exchange with the solution or from the location of perylene within the micelle. More likely is the difference in the dielectric response of the interior of the micelle and vesicle structures. In the micelle the influence of the surrounding solution dielectric is spatially uniform, whereas it is anisotropic in the vesicle. There is a known relationship between chromophore fluorescence lifetime and the presence of a dielectric gradient,[48-51] and it is possible that this physical effect is responsible for our perylene lifetime

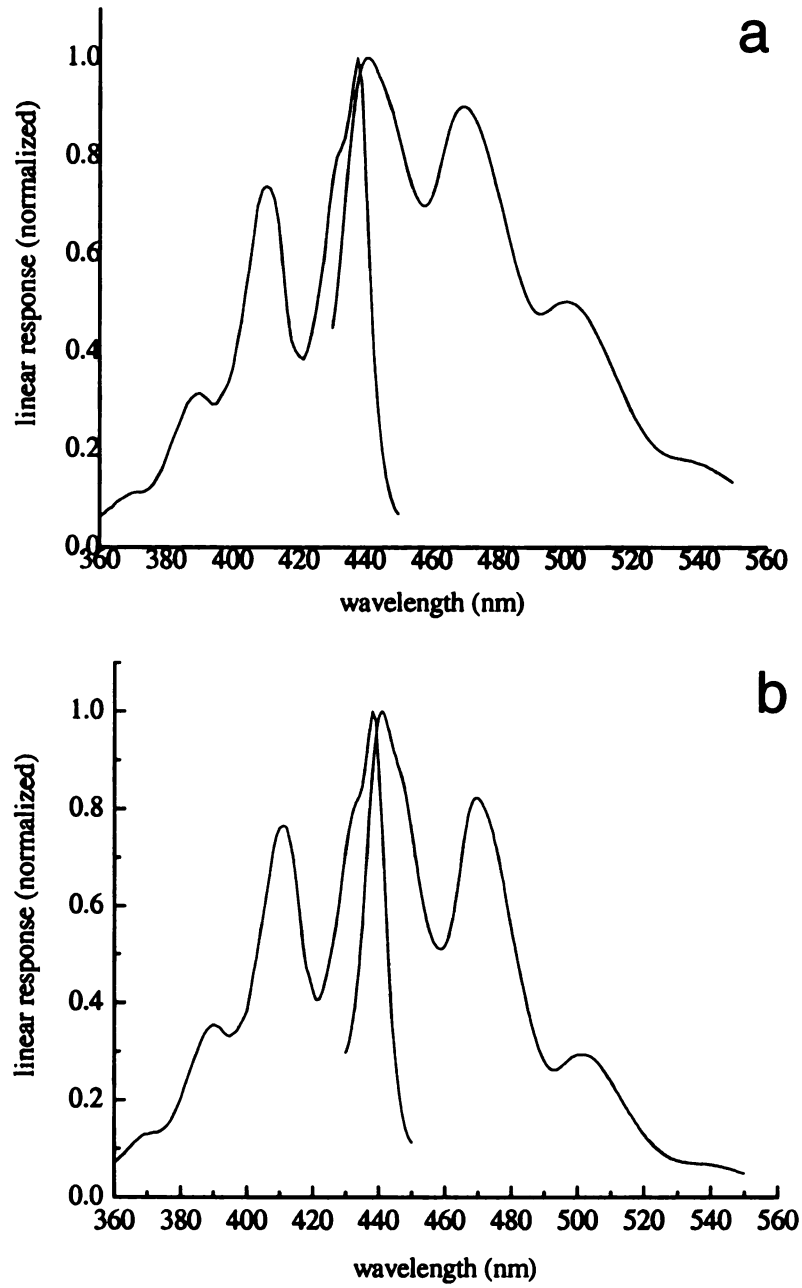

Figure 4.3 - (a) Normalized absorption and emission spectra of perylene in 100 mM decanoate/decanoic acid micelles (b) Normalized absorption and emission spectra of perylene in 100 mM decanoate/decanoic acid vesicles.

data. This result may appear to be slightly at odds with the steady state spectroscopic data (see Figure 4.3) showing essentially identical results for micelles and vesicles. Given that the steady state spectra of perylene exhibit such a weak dependence on solvent polarity, the steady state and lifetime results are consistent with one another.

Fluorescence anisotropy measurements. In an effort to understand in some level of detail the local environment of the probe molecule, we have measured the fluorescence anisotropy dynamics of perylene. For the systems we report on here, where the concentration of perylene within the micelles and vesicles is low, with one perylene chromophore for every 100 to 200 micelles, depending on the fraction of surfactant sequestered in the micelles.[28] The fluorescence anisotropy decay of the chromophore is associated with rotational diffusion within the nonpolar region(s) of the micelles and vesicles. Rotational diffusion is a well understood phenomenon and has been used extensively to interrogate local organization in a variety of systems.[38,40,52-55] There is a well established theoretical framework for the interpretation of reorientation data,[16,56-59] and we consider several aspects of these data separately.

We obtain fluorescence depolarization data by exciting perylene with a vertically polarized light pulse and collecting the emission decay transients polarized parallel and perpendicular to the excitation polarization. These data are combined to produce the induced orientational anisotropy function, a description of which can be seen in Chapter 1.

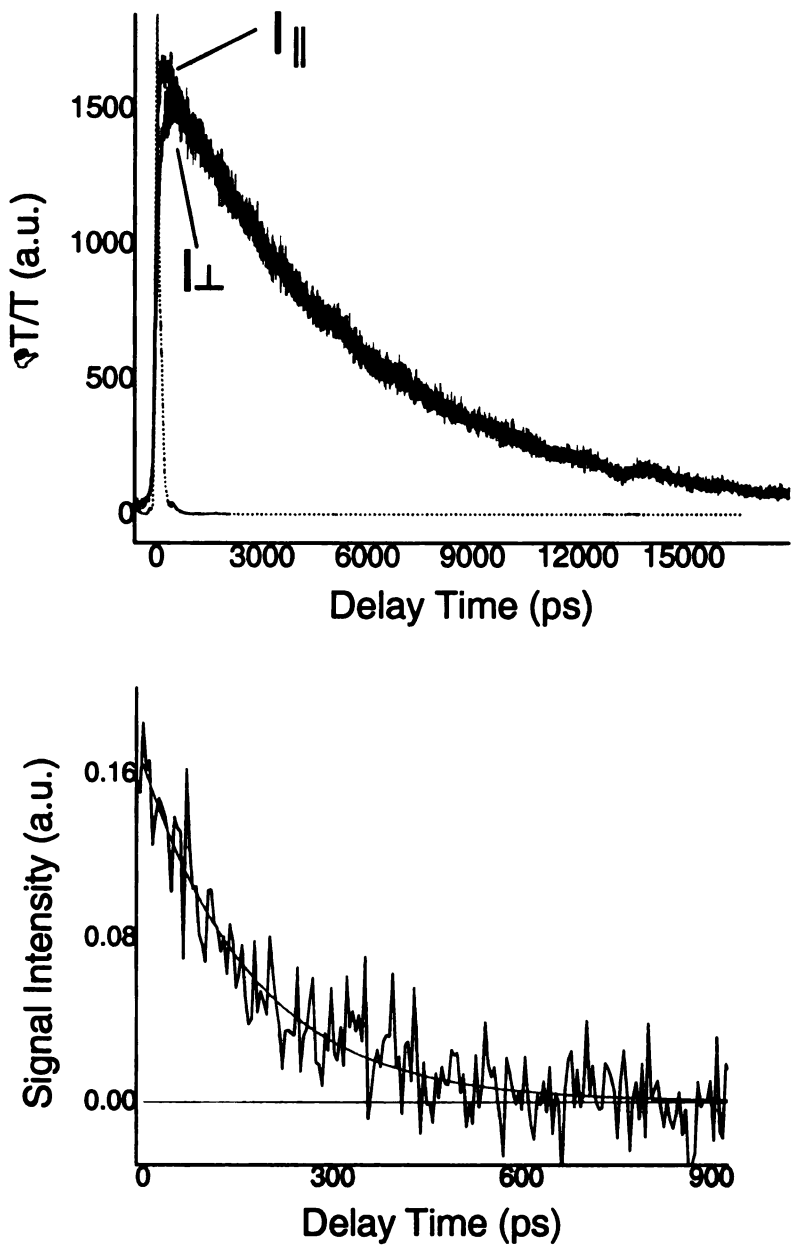

Figure 4.4 - (a) Experimental $I_{\parallel}(t)$ and $I_{\perp}(t)$ scans for perylene in decanoate micelles, along with the instrumental response funcation. These data are typical of those obtained for reorientation measurements. (b) Anisotropy function, R(t), generated from the data shown in (a). The decay is single exponential and is fit to the function $R(t) = R(0) \exp(-t/\tau)$.

Because we are studying systems where the chromophore resides in a confined environment, we need to consider the physical model that is best suited to interpreting the experimental data. The choice of model will determine the physical and chemical significance of the decay time constant(s) extracted from the R(t) data. For chromophores tethered to a substantially larger entity, such as a protein, or imbedded in a mono- or bilayer structure, the hindered rotor model is appropriate. In this model the chromophore is attached to the larger assembly at one point within the system, and its motion is considered in the context of the conic volume it sweeps out. For the micelles and vesicles we consider here, the hindered rotor model is not appropriate because the chromophore is not bound to a specific point in or on the micelle or vesicle structure. Rather, perylene is able to diffuse within the micelle or vesicle, and we thus treat this system in the context of perylene reorienting in a quasi-bulk solvent. The model most appropriate for this type of system is the modified Debye-Stokes-Einstein (DSE) equation,[56,58] which is covered in more detail in Chapter 1.

As noted above, perylene has been investigated extensively[37-40,60,61], and much about its reorientation dynamics are known. For perylene the hydrodynamic volume is 225 Å^3,[62] and $S = 0.69$. Because perylene is a symmetric molecule, its transition dipole moments and rotational diffusion Cartesian axes are coincident, and the $S_1 \leftarrow S_0$ transition is known to be polarized along its long in-plane axis, which is typically assigned as the x-axis. For these experimental conditions, it has been established previously that a

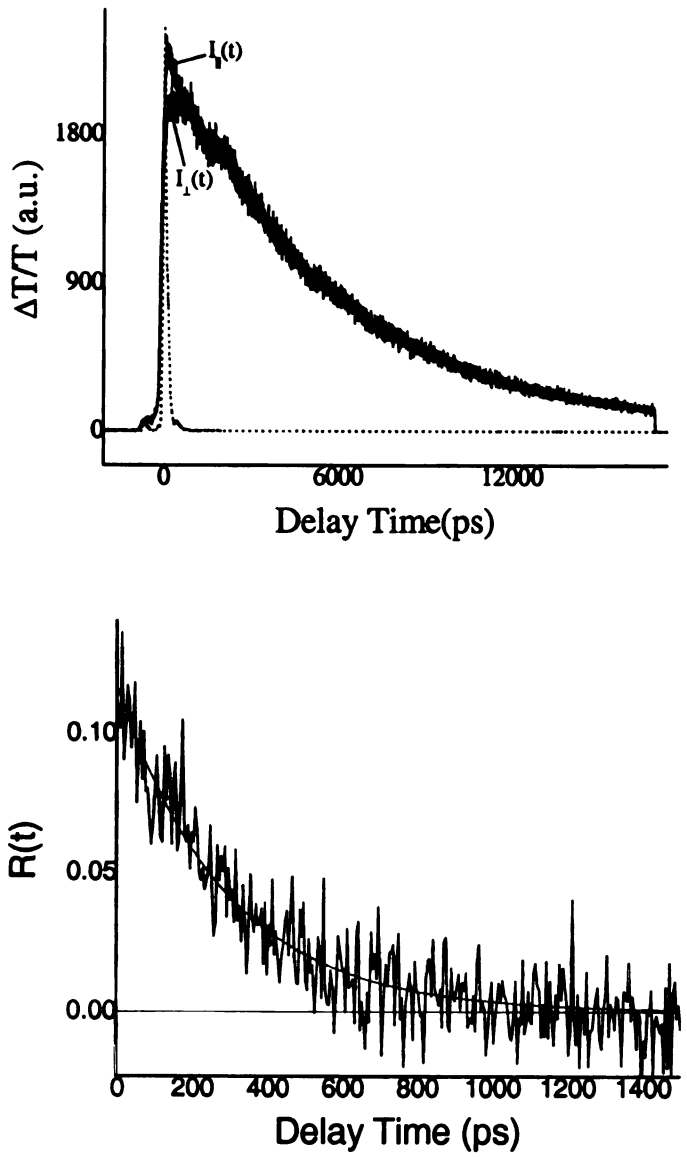

Figure 4.5 - (a) Experimental $I_{\parallel}(t)$ and $I_{\perp}(t)$ scans for perylene in decanoate vesicles, along with the instrumental response funcation. These data are typical of those obtained for reorientation measurements. (b) Anisotropy function, R(t), generated from the data shown in (a). The decay is single exponential and is fit to the function $R(t) = R(0) \exp(-t/\tau)$.

single exponential anisotropy decay corresponds to perylene reorienting as a prolate rotor, with the time constant $\tau_{or} = 1/6D_z$.[37,38,60] For the systems we have examined here, we observe exclusively single exponential anisotropy decays, indicating that perylene reorients as a prolate rotor in both micelles and vesicles made of decanoic acid/decanoate. This is a significant finding when placed in the context of previous work on perylene. This chromophore is known to exhibit either a single or double exponential anisotropy decay, depending on environment.[38,63] The consistent finding of a single exponential decay in the experiments we report here indicates that we can compare the data for perylene in micelles and vesicles directly.

We consider next the appropriate treatment of the quantity *f*, which reflects the frictional interactions between perylene and the constituents within the nonpolar region of the micelles or vesicles. Intuition may seem to suggest a "slip" boundary condition for these systems because of their non-polar character, but our earlier work on the reorientation of perylene in *n*-alkanes indicates that a slip boundary condition is not appropriate.[38] The experimental data for perylene in *n*-alkanes, reorienting as a prolate rotor, are consistent with behavior intermediate between the stick and slip limits. Experimentally, in the *n*-alkanes perylene exhibits a viscosity dependence of 40 ± 3 ps/cP for *n*-alkanes $C_5 - C_8$, and for $C_9 - C_{16}$, the viscosity dependence is measured as 12.7 ± 1.5 ps/cP. We believe that our data for micelles and vesicles can be treated in the context of a 12.7 ps/cP viscosity dependence owing to the length of the amphiphile aliphatic chains. We measure experimentally τ_{or} = 268 ± 3 ps for perylene in micelles,

corresponding to a viscosity of η = 21 (+3.1, -2.4) cP. For perylene reorienting in decanoate vesicles, we measure τ_{or} = 194 ± 10 ps, yielding η = 15 (+2.9, -2.3) cP.

While there are few other data to compare with our results, the viscosity values we infer are of some physical significance. First, we note that the viscosity of the micelle is higher, outside of the experimental uncertainty, than that of the vesicle. We anticipate that the extent of disorder and fraction of gauche chain conformers in the micelle to be higher than that seen in the vesicle, owing to the curvature of the micelle surface being greater than that of the vesicle. TEM data (see Figure 4.2a) show that the decanoate unilamellar vesicles are generally spherical in shape and are approximately 100 nm in diameter. The larger diameter (micelles are ca. 10 nm diameter, Figure 4.2b) should result in a decreased curvature. There exists a great deal of uncertainty in the viscosity of micelle interiors as well as phospholipid bilayers. Previous studies of micelle interiors proposed that the interiors were more rigid, with viscosities on the order of 100 cP[64] while others suggest that micelle interiors are quite fluid, with viscosities on the order of 10 - 20 cP.[5,65,66] Early work on phospholipid bilayer structures likewise suggested a viscosity on the order of 100 cP,[67,68] but this estimate has been shown to be relatively high and also quite dependent on the constituents of the phospholipid bilayer.[69] Koan and Blanchard have recentlyexamined this issue and estimate the viscosity of a C_{14} phospholipid bilayer to be in the range of 15 cP,[69] a value similar to that we recover here for a decanoate bilayer structure. We recognize that decanoate and a phospholipid

are very different compounds, both in terms of structure and polarity, but the result we obtain for the decanoate bilayer structure is not inconsistent with these findings.

Conclusions

We have studied the steady state and time resolved properties of the chromophore perylene in both the micellar and vesicular structures of the decanoate/decanoic acid/water system. The increase in the perylene fluorescence lifetime in the decanoic acid/decanoate vesicle system is fully consistent with the known behavior of the chromophore, and indicates that the persistence time of any local organization is less than nanoseconds. The fluorescence lifetime of perylene in the micelle is longer than in the vesicle, a finding that may be related either to environmental polarity, disorder or to the intrinsic differences in the dielectric environment of the micelle. We use anisotropy decay data of the sequestered perylene to infer the viscosities of the micelles (ca. 21 cP) and vesicles (ca. 15 cP). These findings are consistent with other measurements of vesicle viscosity and suggest that the spatial confinement imposed by the micelle curvature gives rise to less motional freedom within these smaller structures than exists within the quasi-2D environment of the unilamellar vesicles.

Literature Cited

(1) Jarzeba, W.; Walker, G. C.; Johnson, A. E.; Kahlow, M. A.; Barbara, P. F., *J. Phys. Chem.*, **1988**, *92*, 7039.

(2) Visser, A. J. W. G.; Vos, K.; van Hoek, A.; Santema, J. S., *J. Phys. Chem.*, **1988**, *92*, 759.

(3) Marcus, A. H.; Dichun, N. A.; Fayer, M. D., *J. Phys. Chem.*, **1992**, *96*, 8930.

(4) Templeton, E. F. G.; Quitevis, E. L.; Kenney-Wallace, G. A., *Journal of Physical Chemistry*, **1985**, *89*, 3238.

(5) Wirth, M. J.; Chou, S. H.; Piasecki, D. A., *Analytical Chemistry*, **1991**, *63*, 146.

(6) Streletzky, K.; Phillies, G. D. J., *Langmuir*, **1995**, *11*, 42.

(7) Nandi, N.; Bagchi, B., *J. Phys. Chem.*, **1996**, *100*, 13914.

(8) Maiti, N. C.; Krishna, M. M. G.; Britto, P. J.; Periasamy, N., *J. Phys. Chem. B*, **1997**, *101*, 11051.

(9) Matzinger, S.; Hussey, D. H.; Fayer, M. D., *J. Phys. Chem. B*, **1998**, *102*, 7216.

(10) Riter, R. E.; Willard, D. M.; Levinger, N. E., *J. Phys. Chem. B*, **1998**, *102*, 2705.

(11) Willard, D. M.; Riter, R. E.; Levinger, N. E., *J. Am. Chem. Soc.*, **1998**, *120*, 4151.

(12) Palma, S.; Manzo, R. H.; Allemandi, D.; Fratoni, L.; Lo Nostro, P., *Colloids and Surfaces, A: Physicochemical and Engineering Aspects*, **2003**, *212*, 163.

(13) Bhattacharyya, K.; Bagchi, B., *J. Phys. Chem. A*, **2000**, *104*, 10603.

(14) Cang, H.; Brace, D. D.; Fayer, M. D., *J. Phys. Chem. B*, **2001**, *105*, 10007.

(15) Hara, K.; Kuwabara, H.; Kajimoto, O., *J. Phys. Chem. A*, **2001**, *105*, 7174.

(16) Chuang, T. J.; Eisenthal, K. B., *Journal of Chemical Physics*, **1972**, *57*, 5094.

(17) Mandal, D.; Sen, S.; Bhattacharyya, K.; Tahara, T., *Chem. Phys. Lett.*, **2002**, *359*, 77.

(18) Dutt, G. B.; Doraiswamy; Periasamy, N., *Journal of Chemical Physics,* **1991**, *94*, 5360.

(19) Gebicki, J. M.; Hicks, M., *Nature (London, United Kingdom),* **1973**, *243*, 232.

(20) Hargreaves, W. R.; Deamer, D. W., *Biochemistry,* **1978**, *17*, 3759.

(21) Sacerdote, M. G.; Szostak, J. W., *Proceedings of the National Academy of Sciences of the United States of America,* **2005**, *102*, 6004.

(22) Chen, I. A.; Szostak, J. W., *Biophysical Journal,* **2004**, *87*, 988.

(23) Morigaki, K.; Walde, P.; Misran, M.; Robinson, B. H., *Colloids and Surfaces, A: Physicochemical and Engineering Aspects,* **2003**, *213*, 37.

(24) Chen, I. A.; Szostak, J. W., *Proceedings of the National Academy of Sciences of the United States of America,* **2004**, *101*, 7965.

(25) Monnard, P.-A.; Deamer, D. W., *Methods in Enzymology,* **2003**, *372*, 133.

(26) Cistola, D. P.; Hamilton, J. A.; Jackson, D.; Small, D. M., *Biochemistry,* **1988**, *27*, 1881.

(27) Walde, P.; Wick, R.; Fresta, M.; Mangone, A.; Luisi, P. L., *Journal of the American Chemical Society,* **1994**, *116*, 11649.

(28) Namani, T.; Walde, P., *Langmuir,* **2005**, *21*, 6210.

(29) Kamp, F.; Zakim, D.; Zhang, F.; Noy, N.; Hamilton, J. A., *Biochemistry,* **1995**, *34*, 11928.

(30) Zhang, F.; Kamp, F.; Hamilton, J. A., *Biochemistry,* **1996**, *35*, 16055.

(31) Kleinfeld, A. M.; Chu, P.; Romero, C., *Biochemistry,* **1997**, *36*, 14146.

(32) Hanczyc, M. M.; Fujikawa, S. M.; Szostak, J. W., *Science (Washington, DC, United States),* **2003**, *302*, 618.

(33) Oberholzer, T.; Wick, R.; Luisi, P. L.; Biebricher, C. K., *Biochemical and Biophysical Research Communications,* **1995**, *207*, 250.

(34) Ekwall, P.; Mandell, L.; Fontell, K., *Acta Chemica Scandinavica (1947-1973),* **1968**, *22*, 697.

(35) Haines, T. H., *Proceedings of the National Academy of Sciences of the United States of America,* **1983**, *80*, 160.

(36) Hope, M. J.; Bally, M. B.; Webb, G.; Cullis, P. R., *Biochimica et Biophysica Acta, Biomembranes,* **1985**, *812*, 55.

(37) Goldie, S. N.; Blanchard, G. J., *Journal of Physical Chemistry A,* **2001**, *105*, 6785.

(38) Jiang, Y.; Blanchard, G. J., *Journal of Physical Chemistry,* **1994**, *98*, 6436.

(39) Jiang, Y.; Blanchard, G. J., *Journal of Physical Chemistry,* **1994**, *98*, 9411.

(40) Stevenson, S. A.; Blanchard, G. J., *Langmuir,* **2006**, *in review.*

(41) McBain, J. W.; Salmon, C. S., *Journal of the American Chemical Society,* **1920**, *42*, 426.

(42) MacDonald, R. C.; MacDonald, R. I.; Menco, B. P.; Takeshita, K.; Subbarao, N. K.; Hu, L. R., *Biochimica et biophysica acta,* **1991**, *1061*, 297.

(43) DeWitt, L.; Blanchard, G. J.; LeGoff, E.; Benz, M. E.; Liao, J. H.; Kanatzidis, M. G., *Journal of the American Chemical Society,* **1993**, *115*, 12158.

(44) Lide, D. R. *CRC Handbook of Chemistry and Physics*; CRC Press: Boca Raton, FL, 1990-1991; Vol. 71st Edition.

(45) Cistola, D. P.; Atkinson, D.; Hamilton, J. A.; Small, D. M., *Biochemistry,* **1986**, *25*, 2804.

(46) Apel, C. L.; Deamer, D. W.; Mautner, M. N., *Biochimica et Biophysica Acta, Biomembranes,* **2002**, *1559*, 1.

(47) Karpovich, D. S.; Blanchard, G. J., *Journal of Physical Chemistry,* **1995**, *99*, 3951.

(48) Drexhage, K. H., *Journal of Luminescence,* **1970**, *1,2*, 693.

(49) Girard, C.; Martin, O. J. F.; Dereux, A., *Physical Review Letters,* **1995**, *75*, 3098.

(50) Lukosz, W.; Kunz, R. E., *Optics Communications,* **1977**, *20*, 195.

(51) Lukosz, W.; Kunz, R. E., *Journal of the Optical Society of America,* **1978**, *67*, 1607.

(52) Blanchard, G. J., *Journal of Physical Chemistry,* **1988**, *92*, 6303.

(53) Dela Cruz, J. L.; Blanchard, G. J., *Journal of Physical Chemistry A,* **2001**, *105*, 9328.

(54) Goldie, S. N.; Blanchard, G. J., *Book of Abstracts, 213th ACS National Meeting, San Francisco, April 13-17,* **1997**, ANYL.

(55) Kelepouris, L.; Blanchard, G. J., *Journal of Physical Chemistry B,* **2003**, *107*, 1079.

(56) Debye, P. Polar Molecules. In *Chemical Catalog Co.* New York, 1929.

(57) Hu, C.-M.; Zwanzig, R., *Journal of Chemical Physics,* **1974**, *60*, 4354.

(58) Perrin, F., *Journal de Physique et le Radium,* **1936**, *7*, 1.

(59) Zwanzig, R.; Harrison, A. K., *Journal of Chemical Physics,* **1985**, *83*, 5861.

(60) Edward, J. T., *Journal of Chemical Education,* **1970**, *47*, 261.

(61) Goldie, S. N.; Blanchard, G. J., *Journal of Physical Chemistry A,* **1999**, *103*, 999.

(62) Jiang, Y.; Blanchard, G. J., *Journal of Physical Chemistry,* **1995**, *99*, 7904.

(63) Piston, D. W.; Bilash, T.; Gratton, E., *Journal of Physical Chemistry,* **1989**, *93*, 3963.

(64) Povich, M. J.; Mann, J. A.; Kawamoto, A., *Journal of Colloid and Interface Science,* **1972**, *41*, 145.

(65) Shinitzky, M.; Dianoux, A. C.; Gitler, C.; Weber, G., *Biochemistry,* **1971**, *10*, 2106.

(66) Menger, F. M.; Jerkunica, J. M., *Journal of the American Chemical Society,* **1978**, *100*, 688.

(67) Cone, R. A., *Nature: New biology,* **1972**, *236*, 39.

(68) Poo, M.; Cone, R. A., *Nature,* **1974**, *247*, 438.

(69) Koan, M. M.; Blanchard, G. J., *Journal of Physical Chemistry B,* **2006**, *in review.*

Chapter 5

INVESTIGATING THE HYDROPHOBIC REGION OF MICELLES AND UNILAMELLAR VESICLES USING FLUORESCENCE RESONANCE ENERGY TRANSFER

Introduction

Micelles have attracted considerable interest for a number of years due to their many interesting properties, such as their size, shape, and permeability. In addition, micelles have been shown to act as biomimetic and encapsulating systems. Many studies of micelles have utilized time domain optical spectroscopy to observe the dynamics of a probe molecule associated within the micellar environment and to correlate the dynamics of the probe molecule with that of the micelle as a function of viscosity, pressure, and probe solubility.[1-18] Micelles and bilayer vesicle structures share many properties, such as the amphiphilic nature of their constituents, but differ fundamentally in the details of their structure. Unilamellar vesicles have also found use as biomimetic and encapsulating systems and have been used in drug delivery as well as immunological studies. Unlike micelles, which are typically composed of surfactant molecules, unilamellar vesicles are usually formed from phospholipids. Since the molecules used to construct these structures are different, differences in their molecular organization are difficult to compare directly.

Alkanoate amphiphiles, such as octanoate, oleate and decanoate, are capable of forming micelles or vesicles depending on solution parameters, such as pH.[19-27] Sodium decanoate solutions will form micelles at alkaline pH,

provided the concentration is above the CMC, and will form bilayers (vesicular) structures at intermediate pH, provided the concentration is above the critical formation concentration,[28] analogous to the phase transition reported in the more extensively studied octanoic acid [20,23,27,29] or oleic acid[20,26,27,30] systems. The pH range for vesicle formation has been reported as 6.8 – 7.8 for decanoic acid/decanoate, with solutions of higher pH existing in the micellar phase and solutions of lower pH resulting in precipitation.[23,28] If the spontaneously-assembled vesicles are extruded through a small-pore (100 nm) filter, stable vesicles of comparatively well defined size can be generated.[19,31,32] Since the same molecular constituents can form either micelles or vesicles, we can make relatively direct comparisons between the two structures.

For interrogating heterogeneous systems, it is possible to use fluorescent compounds that will either partition selectively into a given phase or reside at the interface between two phases. This environmental selectivity, when combined with fluorescence resonance energy transfer (FRET) measurements, has been used in the study of heterogeneous systems such as micelles, vesicles, and lipid bilayers. [33-55] The topology of these systems can significantly influence the efficiency of energy transfer since the dipolar coupling process that mediates energy transfer depends on both the average distance and relative orientation of the molecules involved. Chromophore reorientation measurements can provide information on the microenvironment(s) that exist within a heterogeneous system. Micellar and vesicular systems are ideal candidates for energy transfer experiments, and previous work in this area has examined energy transfer

between molecules in micelles and vesicles [44,48,51,56] We are particularly interested in the nonpolar region of micelles and vesicles, and understanding the differences between these two structures that are comprised of the same molecules.

We have sequestered perylene inside decanoate/decanoic acid micelles and vesicles and have used the time-resolved fluorescence of this chromophore to obtain information on how acceptor chromophores in the aqueous phase interact with the donor. Perylene is a hydrophobic chromophore that has been studied extensively, making it an appropriate choice for a probe to be sequestered within the nonpolar region of micelles and vesicles. The ionic acceptor chromophore, disodium fluorescein (DSF) has spectroscopic properties well suited to its role as an optical acceptor.

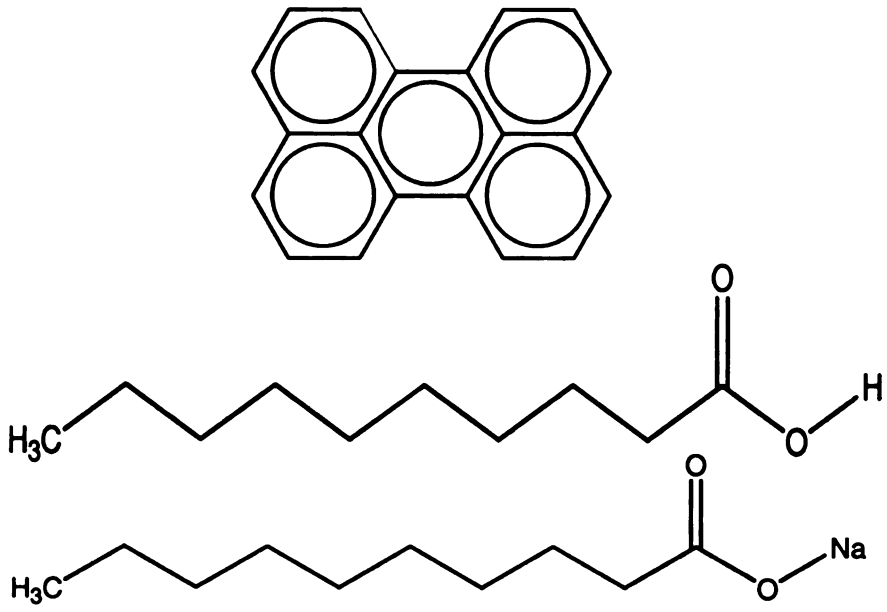

Figure 5.1 – The structures of perylene, sodium decanoate, and decanoic acid

Experimental Section

Materials. Decanoic acid sodium salt (sodium decanoate, 98%) was purchased from Fluka and used as received. Perylene and disodium fluorescein were obtained from Sigma-Aldrich, Inc and used as received. Structures for these chemicals can be seen in Figure 5.1. Sodium phosphate, ethanol, and hydrochloric acid were purchased from Fisher. For all solutions, perylene was first dissolved in a 95% ethanol solution, (10^{-4} M) then added to the decanoate solutions for solubility reasons. The resulting solutions were ca. 10% ethanol, 90% aqueous micelle solution. For all time-resolved fluorescence measurements, the solution temperatures were maintained at 298 ±0.5 K (Neslab EX100-DD). Micelle solutions were maintained at a pH of ca. 9.3 (Orion Research digital ionanalyzer/501) using 150 mM phosphate buffer, while vesicle solutions were lowered to a pH of ca. 7.0 by adding 0.1 M HCl. All solutions were 100 mM sodium decanoate, approximately twice the critical micelle[28,57] and twice the critical bilayer[23,25,28] formation concentration.

Time-Correlated Single Photon Counting Measurements. Fluorescence lifetime and anisotropy measurements of perylene in decanoic acid/decanoate micelle or vesicle containing solutions were made using a time-correlated single photon counting (TCSPC) instrument that has been described in detail previously,[58] and a more complete description is available in Chapter 1. The excitation wavelength was 420 nm and the sample emission was collected at 470 nm.

Vesicle Formation. Vesicles were formed using the extrusion method.[42] First, the solutions containing decanoate (100 mM) at pH 7.0 were subjected to five freeze-thaw-vortex cycles, with each cycle consisting of freezing the sample in liquid nitrogen for five minutes, then heating the sample in a hot water bath (ca. 60° C) for five minutes, followed by vortexing the sample for two minutes. The resulting solution was then passed through polycarbonate filters with 100 nm diameter pores eleven times using a Mini-Extruder system (Avanti Polar Lipids). The resulting unilamellar vesicles were used within two days of extrusion.

TEM Imaging. Unilamellar vesicle samples were stained with uranyl acetate. A 5 µL drop was placed on formvar and carbon coated grids, allowed to sit for several minutes, and the excess was removed with a filter paper. The microscope was a JEOL 100CX (Japan) operated at an accelerating voltage of 100 kV. A representative image of decanoate vesicles is shown in Figure 5.2a.

Cryo-TEM imaging. Cryogenic TEM images were acquired on our micelle samples by Dow-Corning Analytical Solutions, Auburn Hills, MI. To prepare the samples, ca. 2.3 mL of the micelle-containing solution was loaded on a holey carbon film coated Cu TEM grid using a micropipette. The excess fluid on the grid surface was removed by blotting the surface with a filter paper make an aqueous thin film for the TEM. The grid was immersed in liquid ethane contained in a small vessel that itself was housed in a larger liquid nitrogen vessel. The water film on the grid was vitrified to avoid water crystallization. The sample was loaded into the TEM (JEOL JEM 2100F) and the morphology was observed below 104 K. The digital images were acquired using a Gatan CCD camera

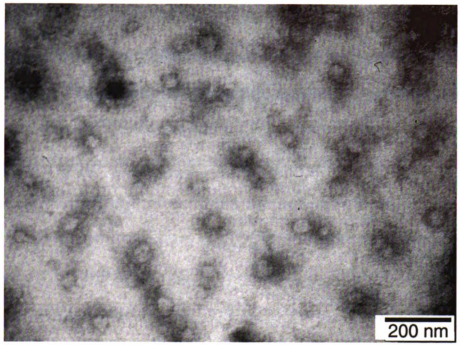

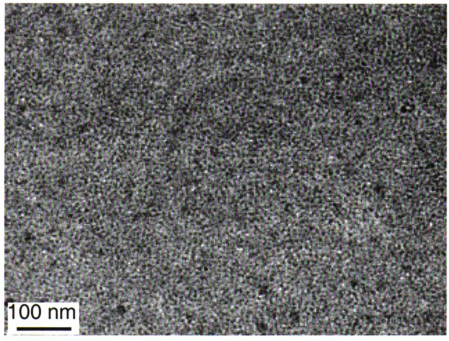

Figure 5.2 - (a) TEM image of decanoic acid/decanoate unilamellar vesicles. The average size is ca. 100 nm diameter. (b) Cryo-TEM image of decanoate micelles (dark features) indicating a characteristic diameter of ca. 10 nm.

attached at the bottom of the TEM column and Digital Micrograph software. A representative cryo-TEM image of the decanoate micelle is shown in Figure 5.2b.

Results and Discussion

The objective of this work is to better understand the differences between the hydrophobic regions of micelles and vesicles. Micelles and vesicles bear some structural similarity, but there are differences in the curvature and characteristic length scale of any organization within these structures. To this point, our ability to address these differences has been limited by the number of systems that are capable of forming both micelle and vesicle structures. A recent report by Namani and Walde has shown the decanoic acid/sodium decanoate system to be capable of forming either micelles or vesicles, depending on the solution pH.[28] They have reported that the pH range for vesicle formation is between 6.4 and 7.8. The bilayer-forming phase is stable when the pH of the system is similar to the pK_a of the acid (the pK_a for decanoic acid is 4.83),[59] due to hydrogen bonding interactions between the protonated and deprotonated acid head groups.[22,24,27,30] The difference between the pK_a of the acid and the actual pH at which bilyer formation occurs has been studied before,[19,26,28,30,60,61] with a significant focus on the deviation between the pH of the bulk solution and the pH of a polyanionic surface. Because both the micelle and vesicle systems are composed of the same alkanoic acid, we can compare the dynamics of the perylene molecule sequestered within each of these structural entities directly. Differences in fluorescence lifetime and reorientation time for perylene sequestered in micelles and vesicles provides insight into the structural differences in the aliphatic regions of these two structural forms. We first consider the fluorescence lifetime data to provide a qualitative comparison of the

local environment(s) characteristic of these two structures, then consider the fluorescence anisotropy data for each to gain further insight.

Fluorescence lifetime data. Fluorescence lifetime measurements of perylene are useful in providing a qualitative picture of the local environment. The concentration of optical donor in the micelles is such that we estimate there to be a single perylene chromophore in approximately 0.5% of the micelles, while for vesicles, the chromophore:vesicle ratio is close to unity. The optical acceptor concentrations we use are such that in a homogeneous solution, the average distance between donor and acceptor would be 150 Å or more. Under these experimental conditions, very little donor-acceptor excitation transfer will be seen, and we will observe acceptor concentration-dependent changes in the donor fluorescence lifetime only if the optical acceptor interacts preferentially with the micelles or vesicles.

The transfer of energy between molecules can occur by a number of mechanisms, ranging from dipolar coupling to collisional quenching. We are concerned in this work with the former phenomenon because of the characteristic length scale over which it operates. The transfer of energy by dipolar coupling has been described by Förster, [62]

$$k_{DA} = \frac{\kappa^2 k_r^D}{n^4 R^6} \cdot 8.8 x 10^{17} \int \frac{\varepsilon_A(\bar{\nu}) f_D(\bar{\nu})}{\bar{\nu}^4} d\bar{\nu} = \frac{\kappa^2 k_r^D}{n^4} \left(\frac{R_0}{R} \right)^6 \qquad 5.1$$

where k_{DA} is the rate constant for energy transfer between donor and acceptor. The κ term is a function of the relative orientation of the donor and acceptor transition dipole moments and, for our experimental conditions $\langle\kappa^2\rangle = 2/3$. The

term k_r^D is the donor radiative decay rate constant in the absence of optical acceptor, *n* is the refractive index and R is the intermolecular donor-acceptor distance. The integral term is a measure of the spectral overlap between the emission spectrum of the optical donor and the absorption spectrum of the acceptor. The spectral overlap term, combined with the several constants on the right hand side of Eq. 5.1 is typically referred to as the critical radius, R_0, a quantity which serves as an effective gauge of the operating distance of this dipolar coupling process. While the term R_0 will vary for each donor-acceptor pair, for most organic chromophore pairs, $R_0 \sim 50$ Å. [54,55,62,63] Based on the spectral profiles of perylene emission and DSF absorption, and the extinction and fluorescence quantum yield data on these molecules, we estimate $R_0 \sim 54$ Å for the perylene/DSF pair. We excite perylene at 420 nm and measure its fluorescence lifetime at ca. 470 nm, without interference from acceptor emission. The measurement of donor lifetime as a function of acceptor concentration is a direct means of evaluating variations in k_{DA}, since this rate constant will operate in an additive manner with the intramolecular decay rate constant(s) that govern the depopulation of the donor excited state. Since the concentration of perylene is held constant at 10^{-5} M, energy transfer between two donor molecules should be negligible because of the small fraction of micelles that contain a perylene molecule. Even if this process were significant, it would appear as a depolarization of the perylene fluorescence, but not a diminution of its lifetime. [64]

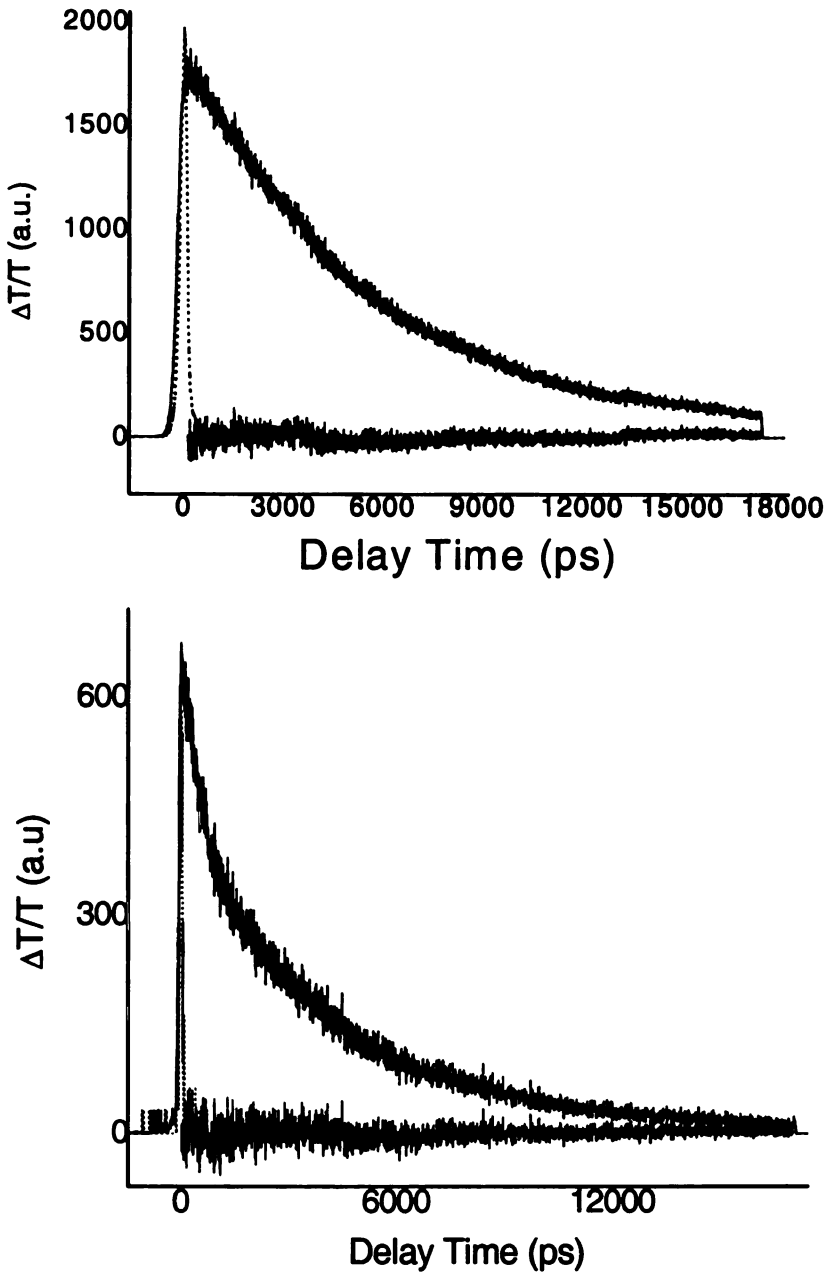

Figure 5.3 - (a) Experimental scans for perylene in decanoate vesicles, along with the instrumental response function. (b) Experimental scans for perylene in decanoate vesicles and 10^{-3} M DSF present. These data are typical of those obtained for lifetime measurements.

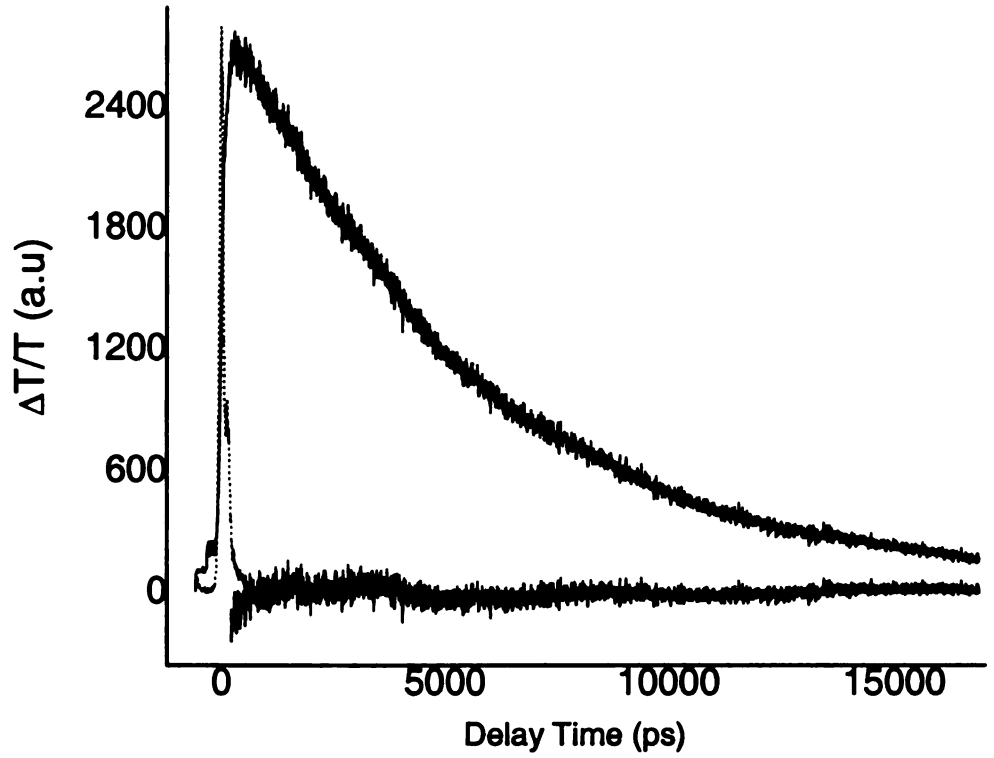

Figure 5.4 - Experimental scans for perylene in decanoate micelles, along with the instrumental response function.

a

Acceptor Concentration (M)	τ_{fl1} (ps)	τ_{fl1} (ps)
0	5942 ± 10	-
10^{-5}	5977 ± 19	-
10^{-4}	5806 ± 9	-
10^{-3}	4723 ± 12	659 ± 16

b

Acceptor Concentration (M)	τ_{fl1} (ps)
0	5815 ± 10
10^{-5}	5681 ± 18
10^{-4}	5530 ± 19
10^{-3}	4196 ± 12

Table 5.1 - (a) Fluorescence lifetime data for perylene sequestered in decanoate vesicles. (b) Fluorescence lifetime data for perylene sequestered in decanoate/decanoic acid micelles. The data reported here are the averages of 6 independent determinations, and the uncertainties reported are ± 1σ.

We first consider the interactions between perylene and DSF in decanoic acid/decanoate unilamellar vesicles. As shown in Table 5.1a, the fluorescence lifetime of perylene decreases as the DSF concentration increases. In addition to the decrease in fluorescence lifetime, the increasing acceptor concentration also affects the functionality of the perylene decay. For 10^{-3} M DSF, we observe a two-component perylene fluorescence lifetime. Representative experimental scans for the vesicle system can be seen in Figure 5.3, while micelle scans are presented in Figure 5.4. The data for both systems is shown in Table 5.1. We understand this behavior in the context of interactions between the acceptor chromophore and the vesicle, and will return to this discussion after considering the micelle data.

We compare the vesicle data to those that we have obtained for perylene and DSF in decanoate micelles. As the concentration of acceptor increases, we observe a decrease in the fluorescence lifetime of perylene. For 10^{-3} M DSF concentration, however, we do not observe a change in the functionality of the perylene population decay. The fact that we observe a change functionality of the decay for perylene in vesicles but not in micelles is interesting and points to the difference between the surface charge of the two structures. Also of interest are the exponential prefactors for the perylene double exponential decay in vesicles. For 10^{-3} M DSF in the vesicle-containing solution, the fast lifetime component (τ = 659 ps) represents 38% of the total, with the longer decay (τ= 4723 ps) accounting for 62% of the total decay intensity. The weighted average

of these lifetimes, the value that we get is somewhat faster than the perylene lifetime found for the micelle system with 10^{-3} M acceptor present. The finding of the two-component donor decay for vesicle systems at high acceptor concentration and the one component donor decay in micelle systems could be the result of the different relative abundances of the micelles and vesicles.

In addition to qualitative insight into excitation transport between the interior and exterior region of micelles and vesicles, the lifetime data can also provide somewhat more quantitative insight into the properties of the interfacial region. We consider that acceptors form a complex with the micelle. In this picture, the acceptors are either in very close spatial proximity to the donor when interacting with the micelle, or too far distant to transfer excitation efficiently when not interacting with the micelle. This model is clearly an oversimplification, but it allows for the ready use of the Förster equation in the estimation of association constants for these systems.

It is first important to consider the approximate stoichiometry of the donor, acceptor and micelles in our solutions. As noted above, the perylene donor concentration is such that there is one donor per ~200 micelles. As we increase the acceptor concentration from 10^{-5} M to 10^{-3} M, the acceptor-to-micelle stoichiometry changes from one acceptor per ~ 200 micelles to one acceptor for ~2 micelles. Because of the perylene:micelle ratio of 1:200, for a 10^{-5} M acceptor concentration, there is one acceptor per ~200 micelles, so only 0.0025% of the micelles will have both a donor sequestered within and an acceptor complexed to them. Under these conditions, there will be essentially no donor-containing

micelles that are complexed to more than one acceptor. We can thus approximate safely that for low acceptor concentrations, the equilibrium process we monitor with our donor lifetime measurements corresponds to interactions between single donors and single acceptors.

Before considering the information content of these data, we need to evaluate the sizes of the micelles under investigation. The cryo-TEM data on our micelles (Figure 5.2b) indicate that the micelles are in the sub-10 nm range, but we are not able to extract precise average diameters. It is important to consider that these micelles have experienced vitrification, so it is not unreasonable to expect that there has been some structural perturbation prior to acquisition of the images. The larger point of these images is that we do indeed have nanoscale micelles present in our solutions, and with their existence established, we will use the more precise estimates of micelle size that have been reported elsewhere. Specifically, the radius of a sodium decanoate micelle is taken to be 23 Å.[65]

The lifetimes we measure are treated as weighted averages of the fluorescence lifetime of perylene in micelles complexed with one acceptor and the lifetime of perylene in an uncomplexed micelle. We take the experimentally determined fluorescence lifetime as the weighted average of the free form $\tau_{free} = (k_r^D)^{-1}$ and the complexed form, where $\tau_{cplx} = (k_r^D + k_{DA})^{-1}$, with k_{DA} being calculated for R =23 Å and R_0 as given above.

$$\tau_{obs} = n_{free}\tau_{free} + n_{cplx}\tau_{cplx}$$
$$n_{free} = \frac{[M]}{[M]+[MA]}, \qquad n_{cplx} = \frac{[MA]}{[M]+[MA]} \qquad 5.2$$

From these calculations, we recover the fractional contributions from the free and complexed forms of the perylene-containing micelles. For the acceptor association with the micelles, the relevant equilibrium process is:

$$M + A \underset{}{\overset{K}{\rightleftharpoons}} MA \qquad K = \frac{[MA]}{[M][A]} = \frac{n_{cplx}}{n_{free}[A]} \qquad 5.3$$

We know [M] and [A] from solution composition, and determine the ratio of [MA]/[M] experimentally from the lifetime measurements. We determine the quantities n_{free} and n_{cplx} (Eq. 5.2), and use them to calculate K. We find that for DSF present at 10^{-5} M in decanoate vesicles, K is not measurable. If we increase the DSF concentration to 10^{-4} M, we recover K ~ 230 M^{-1}. For DSF present at 10^{-5} M in micelles, we find that K ~ 2300 M^{-1}. If we increase the DSF concentration to 10^{-4} M and 10^{-3} M, we recover ~ 519 M^{-1} and ~ 389 M^{-1} respectively. It is possible that the formation constant for the 10^{-4} M and 10-3 M system is not markedly different from that of the 10^{-5} M solution, but rather the difference between the values it due to more than one acceptor molecule complexing to the micelle. For a multiple equilibrium process,

$$M + A \underset{}{\overset{K_1}{\rightleftharpoons}} MA + A \underset{}{\overset{K_2}{\rightleftharpoons}} MA_2 \qquad K = K_1 K_2 \qquad 5.4$$

From the micelle experiment with 10^{-5} M acceptor, K_1 ~ 2000, and for the 10^{-4} M acceptor solution, K_1K_2 ~ 500 with the 10^{-3} M DSF solution, K_1K_2 ~400. This leads to K_2 values of ~ 0.25 and ~ 0.2, respectively. While it is normal for the equilibrium constants to diminish monotonically with the addition of complexing species, the difference between K_1 and K_2 for acceptor/micelle complexation is substantial. It is possible that the facile translational motion of the acceptor on

the micelle or vesicle "surface" as well as the size of the acceptor molecules give rise to a significant contribution from steric effects for the association of multiple acceptors with a given micelle or vesicle.

Rotational diffusion within the micelles. We have studied the rotational diffusion dynamics of perylene within the micelles and vesicles as a function of acceptor concentration in order to understand the influence of the acceptor molecules on the motional freedom of the sequestered donor. Rotational diffusion has been used extensively to interrogate local organization in solutions, because of the well developed theoretical framework for interpretation of the data and the relatively high information content of the experimental signals. [16,42,66-68] Our data indicate that the acceptor molecules influence donor motion differently in micelles and vesicles.

We obtain fluorescence depolarization data by exciting perylene with a vertically polarized light pulse and collecting the emission decay transients polarized parallel and perpendicular to the excitation polarization. These data are combined to produce the induced orientational anisotropy function, R(t), which is discussed in Chapter 1, equation 1.2. The chemical information contained in the data lies in the decay time constant(s) of R(t), and its zero-time value. We note that donor-donor excitation transport can give rise to fluorescence depolarization, the same physical phenomenon that we use to characterize the molecular motion of perylene sequestered within micelles. The D-A excitation transport data (*vide supra*) point to modest donor-acceptor excitation transport, and given the low perylene concentrations used (~1 perylene

per 200 micelles), we believe that fluorescence depolarization resulting from donor-donor transport does not contribute measurably to our data. Experimental scans for perylene in decanoate vesicles as well as decanoate micelles can be seen in Figures 5.5 and 5.6, respectively.

Because we are studying heterogeneous systems, it is fair to consider which model is most appropriate for the treatment of the anisotropy data. For chromophores tethered to a substantially larger entity, such as a protein, or imbedded in a mono- or bilayer structure, the hindered rotor model is appropriate.[35,69] In this model the chromophore is bound at one point within the system and its motion is considered in the context of the conic volume it sweeps out. For the micellar systems we are concerned with here, the hindered rotor model is not appropriate because the chromophore is not bound to a specific point in or on the micelle. Rather, perylene is free to diffuse within the micelle, and we treat this system in the context of perylene reorienting in a quasi-bulk solvent. The model most appropriate for this type of system is the modified Debye-Stokes-Einstein (DSE) equation, [70] which is explained in Chapter 1. For perylene the hydrodynamic volume is 225 $Å^3$, T = 300 K, S = 0.69 (prolate rotor based on single exponential decay). [71,72] Our experimental anisotropy data are all single exponential decays, consistent with perylene reorienting as a prolate rotor within the micelles. Perylene has been shown previously to reorient either as a prolate rotor (single exponential anisotropy decay) or as an oblate rotor (double

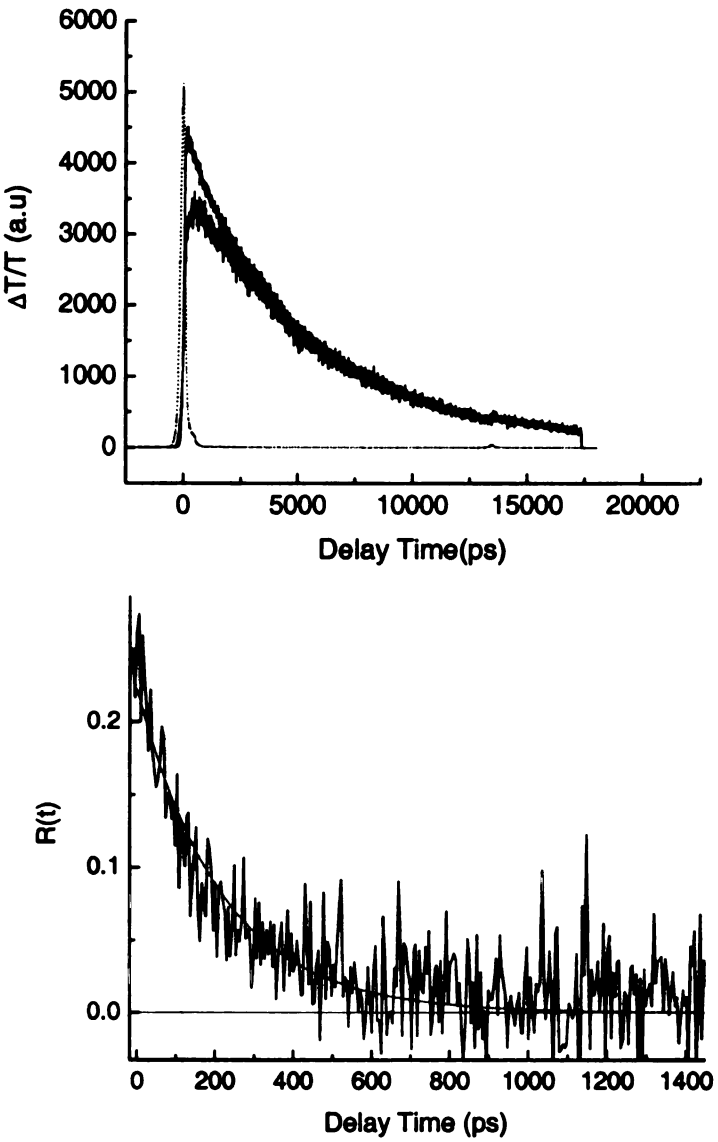

Figure 5.5 - (a) Experimental $I_{\parallel}(t)$ and $I_{\perp}(t)$ scans for perylene in decanoate vesicles, along with the instrumental response funcation. These data are typical of those obtained for reorientation measurements. (b) Anisotropy function, R(t), generated from the data shown in (a). The decay is single exponential and is fit to the function $R(t) = R(0) \exp(-t/\tau)$.

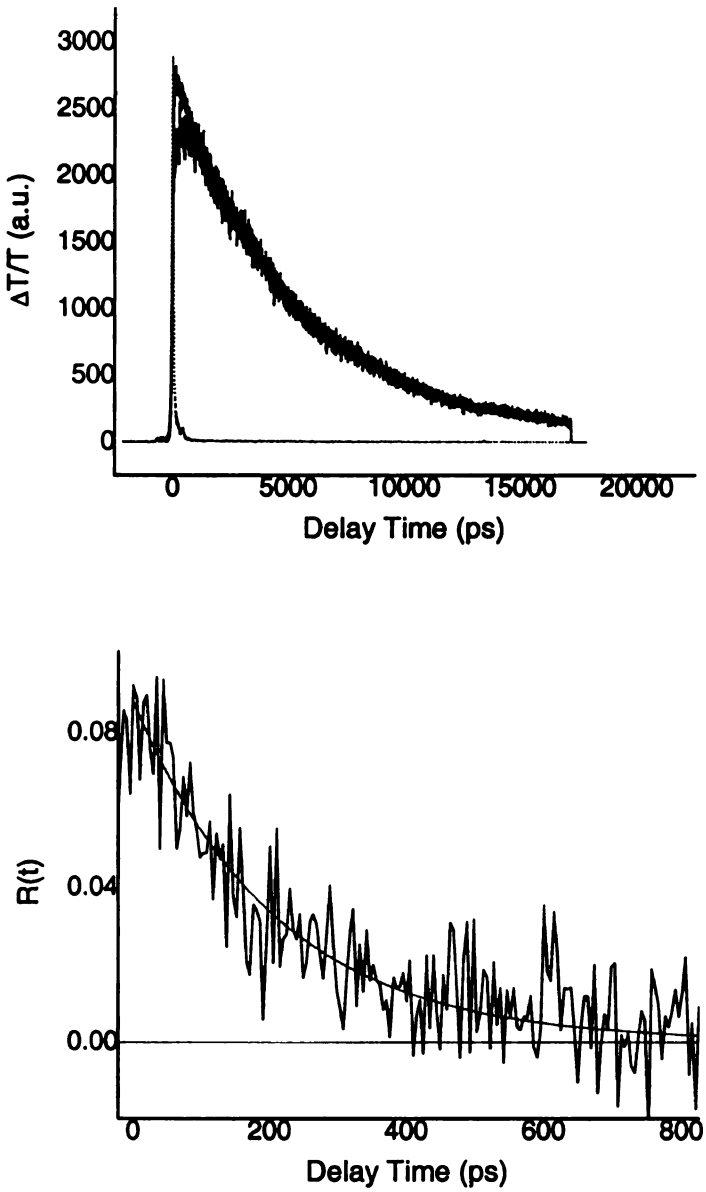

Figure 5.6 - (a) Experimental $I_{\parallel}(t)$ and $I_{\perp}(t)$ scans for perylene in decanoate micelles, along with the instrumental response funcation. These data are typical of those obtained for reorientation measurements. (b) Anisotropy function, R(t), generated from the data shown in (a). The decay is single exponential and is fit to the function $R(t) = R(0) \exp(-t/\tau)$.

conditions, experimental data for perylene in *n*-alkanes are consistent with behavior intermediate between the stick and slip limits. From the modified DSE model, in the stick limit we calculate the quantity τ_{or}/η = 78 ps/cP, and in the slip limit we calculate τ_{or}/η = 5.8 ps/cP. Experimentally we know from earlier work on perylene in *n*-alkanes longer than C_8, τ_{or}/η = 12.7 ± 1.5 ps/cP, intermediate between the stick and slip limit, and we use this experimental value to estimate the viscosity of the micellar media.[13,71-74] For perylene in the sodium decanoate/decanoic acid micelles in the absence of acceptor molecules, the effective viscosity is 21 cP and with the addition of anionic DSF acceptor, the effective viscosity of the interior of the micelle decreases to 10 cP for 10^{-3} M DSF (see Table 5.2a). The decrease in apparent viscosity with the addition of acceptor indicates that the solution phase ionic species interact with the micelle in such a way at to make the interior of the micelle more fluid. It is interesting that the largest decrease in the effective viscosity of the micelle interior occurs upon the initial addition of acceptor molecules. This indicates that the presence of DSF in the decanoate/decanoic acid micelles is somehow perturbing the micellar system, an effect which might result from the properties of the acceptor molecule.

For sodium decanoate/decanoic acid vesicles, we do not observe analogous monotonic trends with increasing acceptor concentration (see Table 5.2b). For the native vesicle, in the absence of any optical acceptor, we recover a viscosity of 15 cP for the hydrophobic region. As anionic DSF acceptor is

Acceptor Concentration (M)	τ_{OR} (ps)	η (cP)
0	194 ± 10	15
10^{-5}	141.7 ± 3	11
10^{-4}	142.4 ± 11	11
10^{-3}	186.8 ± 3	14

Acceptor Concentration (M)	τ_{OR}	η (cP)
0	268 ± 6	21
10^{-5}	175 ± 4	14
10^{-4}	144.3 ± 7	11
10^{-3}	132.2 ± 8	10

Table 5.2 - (a) Rotational diffusion time constants of perylene sequestered in the nonpolar region of decanoic acid/decanoate vesicles (b) Rotational diffusion time constants of perylene sequestered inside decanoate micelles. The data reported here are the averages of 6 independent determinations, and the uncertainties reported are ± 1σ.

added to the vesicle-containing solution, the viscosity of the nonpolar region ranges from 11.0 cP to 14.0 cP, but there is no clear trend in these data. From these effective viscosity data, we can infer the mobility of perylene sequestered within the vesicle walls. The model used to relate the translational diffusion coefficient to solution parameters such as viscosity is the Stokes-Einstein equation[75]

$$D = \frac{k_B T}{6\pi\eta r} \tag{4}$$

where D is the translational diffusion coefficient of perylene and r is the radius of a sphere of volume 225 $Å^3$. For the vesicle solution without any DSF present, the viscosity was 15 cP, we recover a translational diffusion coefficient of 4.2×10^{-7} $cm^2 s^{-1}$. This value is an order of magnitude larger than the diffusion coefficients typically observed for lipid systems.[5] The difference between our value and those observed for lipid systems is most likely due to the size of our vesicles, as well as radius of curvature of our systems. We also need to consider the validity of the Stokes-Einstein equation. The Stokes-Einstein equation is valid under ideal conditions for homogenous solutions. It also assumes that the diffusing molecule is a sphere. The solutions that we are examining are obviously not homogenous, and perylene is not a perfect sphere.

Conclusions

We have examined the fluorescence lifetime and reorientation dynamics of perylene sequestered in micelle and vesicle structures formed from sodium decanoate/decanoic acid solutions in the presence of varying concentrations of the ionic optical acceptor DSF. The decrease in perylene lifetime in the presence of DSF is consistent with dipolar excitation transport. We use anisotropy decay data to compare the viscosities of the hydrophobic regions of micelles and vesicles in the presence of acceptor molecules and find that the rigidity of the micellar structures decreases with the increase in ionic strength, while no change is noted in the vesicle structures.

Literature Cited

(1) Jarzeba, W.; Walker, G. C.; Johnson, A. E.; Kahlow, M. A.; Barbara, P. F. *J. Phys. Chem.* **1988**, *92*, 7039.

(2) Visser, A. J. W. G.; Vos, K.; van Hoek, A.; Santema, J. S. *J. Phys. Chem.* **1988**, *92*, 759.

(3) Marcus, A. H.; Dichun, N. A.; Fayer, M. D. *J. Phys. Chem.* **1992**, *96*, 8930.

(4) Templeton, E. F. G.; Quitevis, E. L.; Kenney-Wallace, G. A. *Journal of Physical Chemistry* **1985**, *89*, 3238.

(5) Vaz, W. L. C.; Criado, M.; Madeira, V. M. C.; Schoellmann, G.; Jovin, T. M. *Biochemistry* **1982**, *21*, 5608.

(6) Streletzky, K.; Phillies, G. D. J. *Langmuir* **1995**, *11*, 42.

(7) Nandi, N.; Bagchi, B. *J. Phys. Chem.* **1996**, *100*, 13914.

(8) Maiti, N. C.; Krishna, M. M. G.; Britto, P. J.; Periasamy, N. *J. Phys. Chem. B* **1997**, *101*, 11051.

(9) Matzinger, S.; Hussey, D. H.; Fayer, M. D. *J. Phys. Chem. B* **1998**, *102*, 7216.

(10) Riter, R. E.; Willard, D. M.; Levinger, N. E. *J. Phys. Chem. B* **1998**, *102*, 2705.

(11) Willard, D. M.; Riter, R. E.; Levinger, N. E. *J. Am. Chem. Soc.* **1998**, *120*, 4151.

(12) Palma, S.; Manzo, R. H.; Allemandi, D.; Fratoni, L.; Lo Nostro, P. *Colloids and Surfaces, A: Physicochemical and Engineering Aspects* **2003**, *212*, 163.

(13) Pal, S. K.; Mandal, D.; Sukul, D.; Bhattacharyya, K. *Chemical Physics* **1999**, *249*, 63.

(14) Cang, H.; Brace, D. D.; Fayer, M. D. *Journal of Physical Chemistry B* **2001**, *105*, 10007.

(15) Hara, K.; Kuwabara, H.; Kajimoto, O. *J. Phys. Chem. A* **2001**, *105*, 7174.

(16) Chuang, T. J.; Eisenthal, K. B. *Journal of Chemical Physics* **1972**, *57*, 5094.

(17) Mandal, D.; Sen, S.; Bhattacharyya, K.; Tahara, T. *Chem. Phys. Lett.* **2002**, *359*, 77.

(18) Dutt, G. B.; Doraiswamy; Periasamy, N. *Journal of Chemical Physics* **1991**, *94*, 5360.

(19) Gebicki, J. M.; Hicks, M. *Nature (London, United Kingdom)* **1973**, *243*, 232.

(20) Hargreaves, W. R.; Deamer, D. W. *Biochemistry* **1978**, *17*, 3759.

(21) Sacerdote, M. G.; Szostak, J. W. *Proceedings of the National Academy of Sciences of the United States of America* **2005**, *102*, 6004.

(22) Chen, I. A.; Szostak, J. W. *Biophysical Journal* **2004**, *87*, 988.

(23) Morigaki, K.; Walde, P.; Misran, M.; Robinson, B. H. *Colloids and Surfaces, A: Physicochemical and Engineering Aspects* **2003**, *213*, 37.

(24) Chen, I. A.; Szostak, J. W. *Proceedings of the National Academy of Sciences of the United States of America* **2004**, *101*, 7965.

(25) Monnard, P.-A.; Deamer, D. W. *Methods in Enzymology* **2003**, *372*, 133.

(26) Cistola, D. P.; Hamilton, J. A.; Jackson, D.; Small, D. M. *Biochemistry* **1988**, *27*, 1881.

(27) Walde, P.; Wick, R.; Fresta, M.; Mangone, A.; Luisi, P. L. *Journal of the American Chemical Society* **1994**, *116*, 11649.

(28) Namani, T.; Walde, P. *Langmuir* **2005**, *21*, 6210.

(29) Ekwall, P.; Mandell, L.; Fontell, K. *Acta Chemica Scandinavica (1947-1973)* **1968**, *22*, 697.

(30) Haines, T. H. *Proceedings of the National Academy of Sciences of the United States of America* **1983**, *80*, 160.

(31) Hanczyc, M. M.; Fujikawa, S. M.; Szostak, J. W. *Science (Washington, DC, United States)* **2003**, *302*, 618.

(32) Hope, M. J.; Bally, M. B.; Webb, G.; Cullis, P. R. *Biochimica et Biophysica Acta, Biomembranes* **1985**, *812*, 55.

(33) DelaCruz, J. L.; Blanchard, G. J. *Journal of Physical Chemistry B* **2003**, *107*, 7102.

(34) Dutt, G. B. *Journal of Physical Chemistry B* **2002**, *106*, 7398.

(35) Kelepouris, L.; Blanchard, G. J. *Journal of Physical Chemistry B* **2002**, *106*, 6600.

(36) Kelepouris, L.; Blanchard, G. J. *Journal of Physical Chemistry B* **2003**, *107*, 1079.

(37) Klein, U. K. A.; Haar, H. P. *Chemical Physics Letters* **1978**, *58*, 531.

(38) Maiti, N. C.; Krishna, M. M. G.; Britto, P. J.; Periasamy, N. *Journal of Physical Chemistry B* **1997**, *101*, 11051.

(39) Maiti, N. C.; Mazumdar, S.; Periasamy, N. *Journal of Physical Chemistry* **1995**, *99*, 10708.

(40) Menger, F. M. *Accounts of Chemical Research* **1979**, *12*, 111.

(41) Quitevis, E. L.; Marcus, A. H.; Fayer, M. D. *Journal of Physical Chemistry* **1993**, *97*, 5762.

(42) MacDonald, R. C.; MacDonald, R. I.; Menco, B. P.; Takeshita, K.; Subbarao, N. K.; Hu, L. R. *Biochimica et biophysica acta* **1991**, *1061*, 297.

(43) Barzykin, A. V.; Tachiya, M. *Journal of Chemical Physics* **1995**, *102*, 3146.

(44) Choi, K. J.; Turkevich, L. A.; Loza, R. *Journal of Physical Chemistry* **1988**, *92*, 2248.

(45) de Oliveira, H. P. M.; Gehlen, M. H. *Chemical Physics* **2003**, *290*, 85.

(46) De, S.; Girigoswami, A.; Mandal, A. K. *Spectrochimica Acta, Part A: Molecular and Biomolecular Spectroscopy* **2003**, *59A*, 2487.

(47) Ediger, M. D.; Domingue, R. P.; Fayer, M. D. *Journal of Chemical Physics* **1984**, *80*, 1246.

(48) Kenney-Wallace, G. A.; Flint, J. H.; Wallace, S. C. *Chemical Physics Letters* **1975**, *32*, 71.

(49) Saha, D. C.; Ray, K.; Misra, T. N. *Spectrochimica Acta, Part A: Molecular and Biomolecular Spectroscopy* **2000**, *56A*, 797.

(50) Wistrom, C. A.; Jones, G. M.; Tobias, P. S.; Sklar, L. A. *Biophysical Journal* **1996**, *70*, 988.

(51) Johansson, L. B. A.; Niemi, A. *Journal of Physical Chemistry* **1987**, *91*, 3020.

(52) Mattjus, P.; Molotkovsky, J. G.; Smaby, J. M.; Brown, R. E. *Analytical Biochemistry* **1999**, *268*, 297.

(53) Stryer, L. *Annual Review of Biochemistry* **1978**, *47*, 819.

(54) Birch, D. J. S.; Suhling, K.; Holmes, A. S.; Salthammer, T.; Imhof, R. E. *Pure and Applied Chemistry* **1993**, *65*, 1687.

(55) Ediger, M. D.; Fayer, M. D. *Journal of Chemical Physics* **1983**, *78*, 2518.

(56) Marcus, A. H.; Diachun, N. A.; Fayer, M. D. *Journal of Physical Chemistry* **1992**, *96*, 8930.

(57) McBain, J. W.; Salmon, C. S. *Journal of the American Chemical Society* **1920**, *42*, 426.

(58) DeWitt, L.; Blanchard, G. J.; LeGoff, E.; Benz, M. E.; Liao, J. H.; Kanatzidis, M. G. *Journal of the American Chemical Society* **1993**, *115*, 12158.

(59) Lide, D. R. *CRC Handbook of Chemistry and Physics*; CRC Press: Boca Raton, FL, 1990-1991; Vol. 71st Edition.

(60) Cistola, D. P.; Atkinson, D.; Hamilton, J. A.; Small, D. M. *Biochemistry* **1986**, *25*, 2804.

(61) Apel, C. L.; Deamer, D. W.; Mautner, M. N. *Biochimica et Biophysica Acta, Biomembranes* **2002**, *1559*, 1.

(62) Forster, T. *Ann. Physik.* **1948**, *2*, 55.

(63) Jones, G. M.; Wofsy, C.; Aurell, C.; Sklar, L. A. *Biophysical Journal* **1999**, *76*, 517.

(64) Keller, L.; Hussey, D. M.; Fayer, M. D. *Journal of Physical Chemistry* **1996**, *100*, 10257.

(65) Merta, J.; Garamus, V. M.; Kuklin, A. I.; Willumeit, R.; Stenius, P. *Langmuir* **2000**, *16*, 10061.

(66) Klein, U. K. A.; Haar, H. P. *Chemical Physics Letters* **1979**, *63*, 40.

(67) Labhart, H.; Pantke, E. R. *Chemical Physics Letters* **1973**, *23*, 482.

(68) Youngren, G. K.; Acrivos, A. *Journal of Chemical Physics* **1975**, *63*, 3846.

(69) Lipari, G.; Szabo, A. *Biophysical Journal* **1980**, *30*, 489.

(70) Debye, P. Polar Molecules. In *Chemical Catalog Co.* New York, 1929.

(71) Goldie, S. N.; Blanchard, G. J. *Journal of Physical Chemistry A* **1999**, *103*, 999.

(72) Jiang, Y.; Blanchard, G. J. *Journal of Physical Chemistry* **1994**, *98*, 6436.

(73) Jiang, Y.; Blanchard, G. J. *Journal of Physical Chemistry* **1995**, *99*, 7904.

(74) Zinsli, P. E. *Chemical Physics* **1977**, *20*, 299.

(75) Einstein, A. *Annalen der Physik (Weinheim, Germany)* **1905**, *17*, 549.

Chapter 6

CONCLUSIONS AND FUTURE WORK

In this dissertation, we have studied the fluorescence lifetime and rotation diffusion dynamics of perylene in micellar and vesicular environments. For the micellar systems, we have concluded that the electric double layer plays a substantial role in mediating interfacial interactions. For the micelle and vesicle systems, we have concluded that there are differences in the structures. To better understand the micellar and vesicular interfacial region, more studies regarding the specific differences between the two structures are needed.

The work performed in chapter 2 of this dissertation shows that the counterions present in the micellar solutions do indeed effect the environment of the micellar interior. The reason for the non-monotonic variations in the microviscosities of the micellar interiors was inconclusive with the available data. In chapter 3, we attempt to explain the non-monotonic variations by the presence of a cosolvent in the micelle solutions. The data we present there collectively point to the existence of microscopic heterogeneity in these binary solvent systems. Altering the counterions of the anionic and cationic micellar systems or performing similar experiments on a nonionic surfactant system would provide additional insight into the role of the double layer in mediating solvation.

In chapters 4 and 5 of this dissertation, the differences between micelle and vesicle systems were examined and we determined that the organization of the two structures was notably different. More specifically, the micelle systems

were found to have a more rigid structure than their bilayer or vesicle counterparts. We believe that this is due to the difference in the size and the radii of curvature of the two structures. We also found that increasing the acceptor concentration allows multiple acceptors to form complexes with the vesicle surface but not with the micelle surface, a fact which we contribute to the different charges present on the micelle and vesicle surfaces. Future work with this research would entail using the information gained here about micellar and vesicular structures and applying similar studies to phospholipid vesicular systems. Another avenue for scientific exploration would be trying similar studies on langmuir-blodgett films, to probe the differences between curved and flat structures.